8-28-2015 12:00 AM

Examination of the Non-linear V̇O2p Response to Exercise: Non-invasive Evidence of Linear Systems Control Using V̇O2p Kinetic Analyses

Daniel A. Keir
The University of Western Ontario

Supervisor
John M. Kowalchuk
The University of Western Ontario

Graduate Program in Kinesiology
A thesis submitted in partial fulfillment of the requirements for the degree in Doctor of Philosophy

Examination of the Non-linear $\dot{V}O_{2p}$ Response to Exercise: Non-invasive Evidence of Linear Systems Control Using $\dot{V}O_{2p}$ Kinetic Analyses

(Thesis format: Integrated-Article)

by

Daniel A. Keir

Graduate Program in Kinesiology

A thesis submitted in partial fulfillment
of the requirements for the degree of
Doctor of Philosophy

The School of Graduate and Postdoctoral Studies
The University of Western Ontario
London, Ontario, Canada

ABSTRACT

The pulmonary O_2 uptake ($\dot{V}O_{2p}$) response to exercise has been characterized by exponential kinetics that remain constant regardless of the exercise protocol used to force the change in $\dot{V}O_{2p}$ (kinetics are invariant). A system that responds in this way is classified as "dynamically linear", implying that a first-order rate reaction controls $\dot{V}O_2$ at the muscle level ($\dot{V}O_{2m}$). However, slowed $\dot{V}O_{2p}$ kinetics when initiating exercise from raised baseline intensities challenges this notion. The purpose of this thesis was to characterize the rate ($\tau\dot{V}O_{2p}$) and magnitude (gain) of adjustment of $\dot{V}O_{2p}$ in response to step-transitions initiated from a wide range of exercise intensities to examine whether $\dot{V}O_2$ kinetics at the muscle level function as a dynamically linear system. *In silico* experiments were included to corroborate responses measured *in vivo*. Using breath-by-breath $\dot{V}O_{2p}$ during step- and ramp-incremental exercise it was demonstrated that: 1) $\dot{V}O_{2p}$ kinetics were invariant and fast ($\tau\dot{V}O_{2p}$ ~20s) when transitions of varying ΔWR were initiated from a common WR (Chapter III); and 2) the $\dot{V}O_{2p}$ response to ramp exercise was linearly related to WR and well described by a mono-exponential (Chapter IV) – consistent with dynamically linear control. However, it was also demonstrated in the same groups of participants that $\tau\dot{V}O_{2p}$ and gain increased as a function of baseline intensity (Chapters III and IV) – refuting this notion. Modelling the summed influence of muscle compartments based on *in vivo* measurements in Chapter III revealed that $\tau\dot{V}O_{2p}$ could appear fast (20 s) despite being derived from $\tau\dot{V}O_{2m}$ values ranging 15-40 s and $\tau\dot{Q}_m$ ranging 20-45 s. Additionally, it was demonstrated that the $\dot{V}O_{2p}$ response to ramp exercise in Chapter IV could also be characterized by an exponential function with $\tau\dot{V}O_{2p}$ and gain parameters that vary as a

function of WR. Collectively, these data suggest that $\dot{V}O_{2p}$ kinetics are slowed dependent on WR and may be strongly influenced by muscle metabolic and circulatory heterogeneity. Therefore, it is proposed that at the muscle level $\dot{V}O_2$ kinetics operate as a linear system and that non-linear $\dot{V}O_{2p}$ responses to exercise may reflect a "heterogeneity of linear responses" within the range of muscle fibres recruited to address the exercise challenge.

Keywords: breath-by-breath pulmonary O_2 uptake, kinetics, gas exchange, computational modelling, dynamic linearity, first-order response, fibre type heterogeneity, metabolic rate, $\dot{V}O_2$ slow component, on-transient**,** skeletal muscle metabolism, mono-exponential, ramp-incremental exercise

CO-AUTHORSHIP

This thesis includes versions of the following manuscripts that were submitted and accepted for publication or are in preparation to be submitted for publication:

1. **Keir, D.A.**, Murias, J.M., Paterson, D.H., & Kowalchuk, J.M. Breath-by-breath $\dot{V}O_{2p}$ kinetics: effect of data processing on confidence in estimating model parameters. (Experimental Physiology. 99(11): 1511-22; 2014).

2. **Keir, D.A.,** Robertson, T.C., Benson, A.P., Rossiter, H.B., & Kowalchuk, J.M. The influence of metabolic and circulatory heterogeneity on the expression of pulmonary $\dot{V}O_2$ kinetics in humans. (Experimental Physiology. In revision)

3. **Keir, D.A.,** Benson, A.P., Love, L.K., Robertson, T.C., Rossiter, H.B., & Kowalchuk, J.M. Influence of muscle metabolic heterogeneity in determining the $\dot{V}O_{2p}$ response to ramp-incremental exercise.

Both D.A. Keir and J. M. Kowalchuk contributed to the design of all studies with helpful input from D.H. Paterson. The design of studies 1, 2, and 3 were also largely contributed to by J.M. Murias (study 1) and H.B. Rossiter (studies 2 and 3). All data were collected and analyzed by D.A. Keir with collection assistance provided by T.C. Robertson, A.P. Benson, and L.K. Love. The original manuscripts comprising this thesis were written by D.A. Keir with feedback provided by the co-authors.

ACKNOWLEDGEMENTS

I would like to extend appreciation to my supervisor, Dr. John Kowalchuk. Thank you for taking a chance on me as a doctoral student when no one else would. Your guidance and advice throughout my tenure have been invaluable and your approach to "the research process" has molded me to become even more fastidious than you! Thank you for your mentorship.

To Dr. Juan Murias, I attribute much of my early successes as a researcher to you. Thank you for seeing in me what I did not see in myself. Your relentless encouragement, praise, and willingness to include me in your work have been instrumental in my development. I would also like to acknowledge: Dr. Don Paterson, Dr. Silvia Pogliaghi, Dr. Matt Spencer, Dr. Glen Belfry and Dr. Olivier Serresse – for being constant and reliable sources of encouragement, positivity and counsel; as well as my fellow graduate students, Josh Nederveen, Federico Fontana, and Kait McLay – for their immense support and assistance over the past four years.

An integral part in the coming together of this thesis stemmed from the insightful contributions of Dr. Harry Rossiter and Dr. Al Benson and I would also like to acknowledge both Taylor Robertson and Lorenzo Love for their participation and involvement in data collection. Importantly, it would not have been possible to collect any data at all if not for the services and technical support provided by Mr. Brad Hansen and the financial support provided by the Natural Sciences and Engineering Research Council of Canada and the Ontario Ministry of Training, Colleges and Universities.

Finally, none of my accomplishments would be possible or worth celebrating without the love and support of my parents and Dana – you are my inspiration, my confidence, and my pride.

TABLE OF CONTENTS

LIST OF TABLES

LIST OF FIGURES

CHAPTER IV: Influence of muscle metabolic heterogeneity in determining the $\dot{V}O_{2p}$ response to ramp-incremental exercise

LIST OF ABBREVIATIONS

$A\text{-}\bar{v}O_{2diff}$	arterio-venous oxygen difference
AIC	Akaike information criterion
A_p	amplitude of pulmonary oxygen increase
ADP	adenosine diphosphate
ATP	adenosine triphosphate
ANOVA	analysis of variance
bpm	beats per minute
BSL	baseline
χ^2	chi-squared
Ca^{2+}	calcium
C_aO_2	arterial O_2 content
$C_{\bar{v}}O_2$	mixed venous O_2 content
CI_{95}	95% confidence interval
CK	creatine kinase
CO_2	carbon dioxide
CP	critical power
Cr	creatine
ΔG_{ATP}	Gibbs free energy of ATP hydrolysis
EMG	electromyography
ETC	electron transport chain
$FADH_2$	flavin adenine dinucleotide
G	gain
G_P	primary gain
G_{tot}	total gain
GET	gas exchange threshold
H^+	hydrogen
H_2O	water
HbO_2	oxygenated hemoglobin
HHb	deoxygenated hemoglobin

HR	heart rate
$[La^-]_b$	blood lactate concentration
LBF	leg blood flow
LS	lower step
LT	lactate threshold
MCM	multi-compartment model
MLSS	maximal lactate steady-state
MR	metabolic rate
MRT	mean response time
NADH	nicotinamide adenine dinucleotide
NIRS	near-infrared spectroscopy
O_2	oxygen
PCO_2	partial pressure of carbon dioxide
PCr	phosphocreatine
PDH	pyruvate dehydrogenase
$P_{ET}CO_2$	end-tidal partial pressure of carbon dioxide
$P_{ET}CO_2$	end-tidal partial pressure of oxygen
P_i	inorganic phosphate
PO	power output
PO_{peak}	peak power output
PO_2	partial pressure of oxygen
$\hat{\theta}_L$	estimated lactate threshold
$\dot{Q}$	blood flow
$\dot{Q}_b$	blood flow from body excluding active muscle
$\dot{Q}_m$	muscle blood flow
$\dot{Q}_{tot}$	cardiac output
RCP	respiratory compensation point
RI	ramp incremental
SD	standard deviation
SI	step incremental
SS	steady-state

τ	time constant
τ’	mean response time for the oxygen uptake response to ramp exercise
TCA	tricarboxylic acid
TD	time delay
US	upper step
$\dot{V}CO_{2p}$	rate of carbon dioxide production
$\dot{V}_E$	ventilation rate
$\dot{V}O_{2E}$	end-expiratory oxygen uptake
$\dot{V}O_{2I}$	end-inspiratory oxygen uptake
$\dot{V}O_{2p}$	pulmonary oxygen uptake
$\dot{V}O_{2b}$	oxygen uptake of the body excluding active muscle
$\dot{V}O_{2pBSL}$	baseline of pulmonary oxygen uptake
$\dot{V}O_{2m}$	muscle oxygen uptake
$\dot{V}O_{2max}$	maximal oxygen uptake
$\dot{V}O_{2pBSL}$	baseline of pulmonary oxygen uptake
$\tau\dot{V}O_{2p}$	time constant for adjustment of phase II pulmonary oxygen uptake
$\dot{V}O_{2peak}$	peak pulmonary oxygen uptake
$\dot{V}O_{2pSS}$	steady-state pulmonary oxygen uptake
W	watts
WR	work rate
WR_{peak}	peak work rate
μ_s	absorption coefficient
μ_a	scattering coefficient

CHAPTER I: Introduction

Basic Principles of $\dot{V}O_2$ Measurement and $\dot{V}O_2$ Responses to Exercise

With every breath we take, atmospheric air is drawn into our lungs so that oxygen (O_2) may be transferred into the blood and delivered to the tissues where it is used to produce the energy necessary for our bodies to function. At the cellular level, this process is known as oxidative phosphorylation which is the primary metabolic process by which humans resynthesize energy. As the energetic demands of our cells increase, so too does the demand for O_2 supply to their mitochondria and through the coordination of multiple physiological systems our bodies increase the uptake, transport, and delivery of O_2 to our cells; of which the largest consumers of O_2 are skeletal muscle.

Gas Exchange, O_2 uptake and Exercise

Exercise can impose an enormous challenge on the body as the demand to increase the intake of O_2 and removal of carbon dioxide (CO_2) (i.e., gas exchange) may increase more then 15-fold during high intensities of dynamic muscle movement. The process by which gas exchange increases is facilitated by simultaneous adjustments between the respiratory, cardiovascular, neurological and muscle metabolic systems to: i) draw O_2 from the atmosphere into the lungs so that it can be delivered to active tissue mitochondria where it is utilized to synthesize energy in the form of adenosine triphosphate (ATP); and ii) to remove CO_2 produced as a by-product of oxidative metabolism and the buffering of hydrogen ions (H^+).

Although oxidative metabolism is efficient at providing the free energy to drive contractile processes within skeletal muscle, it does not increase immediately with sudden

increases in energetic demand. Rather, oxidative phosphorylation, and subsequently the collective profile of muscle O_2 utilization ($\dot{V}O_{2m}$), displays an "exponential" projection towards a new "steady-state" (Whipp *et al.* 1982; Rossiter *et al.* 1999; Bangsbo *et al.* 2000). This implies that on transition to higher metabolic requirements (i.e., greater intensities of exercise and thus ATP requirements) there is a transient mismatch between the rate of ATP hydrolysis required to sustain the level of muscle metabolic activity and the actual rate of mitochondrial oxidative ATP supply. This mismatch necessitates the utilization of supplementary ATP-resynthesis pathways (substrate-level phosphorylation in the form of phosphocreatine (PCr) hydrolysis and glycolysis/glycolgenolysis) that are rapidly responsive but limited in capacity. A consequence of reliance on these non-oxidative and low capacitance pathways is that they are associated with metabolic by-products that are directly related to muscle fatigue (Fitts, 1994) and so, slower increases in the rate of O_2 utilization (and greater reliance on these non-oxidative pathways) for a given change in ATP demand may contribute to exercise intolerance. Therefore, quantification of the rate at which $\dot{V}O_{2m}$ adjusts to changes in metabolic demand, or its *kinetics*, is of interest because it provides insight into: i) the body's ability to coordinate the transport of O_2 from atmosphere to mitochondria; ii) the skeletal muscle's ability to maintain metabolic stability in order to delay fatigue and tolerate exercise; and iii) the intracellular factors that regulate oxidative phosphorylation.

Measuring $\dot{V}O_2$

Direct measurements of $\dot{V}O_{2m}$ at the level of the exercising muscle may be ascertained by resolving the Fick equation which dictates that the rate of muscle O_2 utilization ($\dot{V}O_{2m}$) is equal to the product of muscle blood flow ($\dot{Q}_m$) and the amount of O_2

extracted from the blood as it transits the muscle vasculature (i.e., the difference in arterial (C_aO_2) and venous muscle O_2 content (C_vO_2); $\dot{V}O_{2m} = \dot{Q}_m \cdot [C_aO_2 - C_vO_2]$). Unfortunately, measurement of arterial-venous O_2 difference (a-vO_{2diff}) during exercise in humans is difficult as it necessitates the use of invasive blood sampling techniques. To circumvent these challenges, measurement of breath-by-breath pulmonary O_2 uptake ($\dot{V}O_{2p}$) is used as an alternative and non-invasive method by which oxidative metabolism may be quantified and studied in humans under a broad range of physiological and exercise conditions. Through the use of fast-gas analysis systems, the rate at which O_2 is taken up at the mouth in a single breath may be obtained by measuring the volume of air, fractional concentration of O_2, and time associated with inspiration-expiration pairs over a single breath cycle and computing the difference between the rate by which O_2 is inspired ($\dot{V}O_{2I}$) and expired ($\dot{V}O_{2E}$). A shortcoming of this approach is that it does not account for breath-to-breath changes in alveolar O_2 stores (e.g., unequal end-inspired *versus* end-expired lung volumes) which can lead to distortions in the kinetic profile of gas exchange (Capelli *et al.* 2011). For this reason, algorithms have been developed (e.g., Swanson, 1980; Beaver *et al.* 1981) to adjust for breath-to-breath changes in alveolar O_2 stores and correctly estimate alveolar-to-capillary O_2 transfer (i.e., breath-by-breath $\dot{V}O_{2p}$) from data collected at the mouth.

Provided that the time required for deoxygenated blood from the active tissue to transit venous circulation towards the lung is accounted for, the profile of $\dot{V}O_{2p}$ closely resembles that of $\dot{V}O_{2m}$ during exercise (Barstow *et al.* 1990; Grassi *et al.* 1996; Rossiter *et al.* 1999; Krustrup *et al.* 2009). In response to a step-change in exercise work rate, $\dot{V}O_{2p}$ exponentially projects towards a new steady-state O_2 requirement in a manner characterized by three identifiable phases (Whipp *et al.* 1982; Barstow *et al.* 1990); for

reference see Figure 1.1A). The first phase (Phase I, or the cardiodynamic component) occurs as a result of an increase in the magnitude of pulmonary blood flow and is not reflective of active muscle metabolism (Barstow *et al.* 1990). Phase II (or the fundamental component) reflects the non-steady-state portion of the $\dot{V}O_{2p}$ response representing a decrease in venous O_2 content (widening of the a-vO_{2diff}) arising from increased O_2 extraction and tissue O_2 utilization. This phase resembles a single exponential projecting towards a new steady-state (Whipp *et al.* 1981). Attainment of the new steady-state marks the beginning of phase III which is characterized by a plateau as long as the exercise intensity remains below an individual's lactate threshold (i.e., within the *moderate* intensity domain; discussed later). Importantly, the kinetics of phase II $\dot{V}O_{2p}$ closely resemble those of $\dot{V}O_{2m}$ measured *in vivo* (Rossiter *et al.* 1999; Krustrup *et al.* 2009; Wüst *et al.* 2013) and thus provide a useful method by which the regulation of oxidative metabolism may be studied, non-invasively, in humans during whole-body exercise.

$\dot{V}O_{2p}$ Kinetics

Quantification of the magnitude and rate at which phase II $\dot{V}O_{2p}$, adjusts to a given change in WR describes $\dot{V}O_{2p}$ kinetic analyses. The kinetics of the phase II $\dot{V}O_{2p}$ response are typically characterized by a first-order four parameter exponential model (i.e., 'mono'-exponential, see Figure 1.1B) of which two parameters are related to $\dot{V}O_{2p}$ (dependent variables) and two to time (independent variables). The first two terms of the model include: $\dot{V}O_{2p}$ baseline ($\dot{V}O_{2pbsl}$) which is a fixed parameter representing the pre-transition

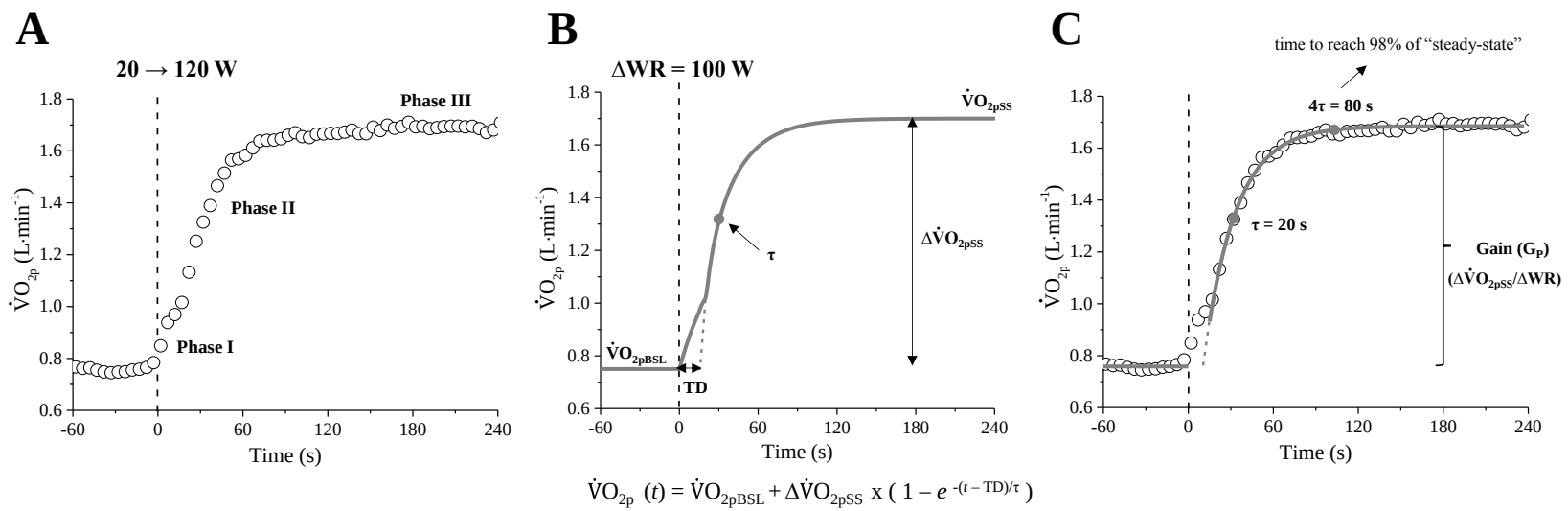

Figure 1.1. ***A***) A typical $\dot{V}O_{2p}$ profile across the transient in response to a step-change in work rate from a low intensity (20 W) to a moderate, sub-lactate threshold, intensity (120 W) performed during cycling exercise. The vertical dashed line denotes the onset of exercise. Note the three phases of the response (phase I: "cardiodynamic", ~0 – 15 s; phase II: "fundamental", ~15 – 95 s; and phase III: "steady-state", ~95 – 240 s) each corresponding to distinct physiological events (see text for detailed description of each phase). ***B***) Schematic illustration of the modelled response profile for the data from "*A*". The mono-exponential function describing the phase II $\dot{V}O_{2p}$ response is displayed below the *x*-axis, with model parameters of the function indicated on the profile. ***C***) The $\dot{V}O_{2p}$ response from "*A*" with the phase II model profile from "*B*" superimposed. Note that one time constant (τ) represents the time it takes for the adjustment of $\dot{V}O_{2p}$ to reach within 37% of the new "steady-state" ($\dot{V}O_{2pSS}$). It follows that $\dot{V}O_{2p}$ is within 14% of $\dot{V}O_{2pSS}$ at 2τ (1.0 - [(0.37 x 0.63) + 0.63] = 0.14), 5% at 3τ (1.0 – [(0.14 x 0.63) + 0.86] = 5%), 2% at 4τ (1.0 - [(0.05 x 0.63) + 0.95] = 0.02), and <1% at 5τ. Therefore, for a τ equal to 20 s, the $\dot{V}O_{2p}$ response reaches 63% of $\Delta\dot{V}O_{2pSS}$ after 20 s (or 1τ), and 98% after 80 s (or 4τ). The primary gain of the response (G_P) is quantified as the change in $\dot{V}O_{2p}$ for a given change in WR, conveying information regarding the efficiency of the muscle to utilize O_2 to sustain contraction/ATP resynthesis requirements.

steady-state $\dot{V}O_{2p}$ (e.g. $\dot{V}O_{2p}$ at 20 W cycling) and the $\dot{V}O_{2p}$ amplitude (A_p) which describes the change in $\dot{V}O_{2p}$ from $\dot{V}O_{2pbsl}$ to the new steady-state $\dot{V}O_{2p}$ ($\dot{V}O_{2pss}$) ($A_p = \Delta\dot{V}O_{2p} = \dot{V}O_{2pss} - \dot{V}O_{2pbsl}$). The other two model parameters reflect the time components of the $\dot{V}O_{2p}$ response. The time delay (TD) term represents the time at which the exponential asymptote crosses (or meets) the pre-transition steady-state value ($y = \dot{V}O_{2pbsl}$; x = TD) and is not used for physiological interpretation and the time constant for $\dot{V}O_{2p}$ ($\tau\dot{V}O_{2p}$) describes the curved portion of the phase II exponential response. The time constant parameter represents the rate at which $\dot{V}O_{2p}$ changes and is quantified as the time required for $\dot{V}O_{2p}$ to reach 63% of the $\Delta\dot{V}O_{2pss}$. Hence, given real breath-by-breath fluctuations in gas exchange, approximately four time constants ($4 \times \tau\dot{V}O_{2p}$ = 98.1%) represents the duration of the phase II $\dot{V}O_{2p}$ adjustment period and the time to the beginning of phase III (see Figure 1.1C).

Oxidative Phosphorylation and Limitations to $\dot{V}O_2$ kinetics

That $\dot{V}O_{2m}$, and thus muscle oxidative phosphorylation, do not instantaneously increase with sudden increases in metabolic demand has been the focus of (and impetus for) a large body of work striving to uncover the mechanisms that contribute to the finite kinetic adjustment of mitochondrial oxidative phosphorylation. The oxidative phosphorylation reaction in skeletal muscle during exercise can be depicted and simplified as follows:

$$5ADP + 5P_i + 2NADH + 2H^+ + O_2 \rightarrow 5ATP + 2NAD^+ + 2H_2O \quad (1.1)$$

Within the mitochondria, reducing equivalents in the form of nicotinamide adenine dinucleotide (NADH) and flavin adenine dinucleotide ($FADH_2$) (derived from the oxidation of fat and carbohydrate within the tricarboxylic acid (TCA) cycle and glycolysis

and beta oxidation) are oxidized and deliver electron pairs to the inner mitochondrial membrane. The transferred electrons participate in a sequence of oxidation-reduction reactions through a number of protein complexes embedded in the membrane (electron transport chain; ETC) towards the cytochrome *c* oxidase protein where they reduce O_2 to water. The movement of electrons through the ETC causes protons to be transferred out of the mitochondrial matrix creating an electrochemical gradient across the inner membrane. The free energy associated with this gradient drives the ATP synthase enzyme complex to resynthesize ATP from adenosine diphosphate (ADP) and inorganic phosphate (P_i). Since O_2 is requisite to provide the necessary energy to phosphorylate ADP, this process is collectively referred to as "oxidative phosphorylation". It is generally believed that the kinetic control of oxidative phosphorylation depends on adequate phosphate delivery (ADP and P_i) and the relative concentrations of its substrates (i.e., NADH and O_2) (Wüst *et al.* 2013). Therefore, oxidative phosphorylation would be affected primarily by a reduction in "phosphorylation potential" (increase [ADP] and [P_i]), in addition to changes in "redox potential" (increased [NADH] relative to [NAD^+]) and [O_2] (Wilson, 1994). However, the control mechanisms that determine $\dot{V}O_2$ kinetics in skeletal muscle cells remains controversial.

In isolated mitochondria, control of $\dot{V}O_2$ has been closely linked to [ADP] (Chance & Williams 1955) suggesting that $\dot{V}O_{2m}$ kinetics are consequent to a first-order rate reaction (specifically the unimolecular reaction of ADP feedback to a given mitochondrial pool) (Rossiter, 2011). Based on this theory, a major factor purported to mediate the increase in [ADP], and thus the dynamic adjustment of $\dot{V}O_{2m}$, resides in the mitochondrial transfer of high-energy phosphates, particularly via PCr. At exercise onset, [PCr] stores are

reduced exponentially with a temporal profile similar to that of $\dot{V}O_{2m}$ and phase II $\dot{V}O_{2p}$ (Rossiter *et al.* 1999; Rossiter *et al.* 2001) in humans and during contractions in rat muscle *in situ* (Meyer, 1988). The functional coupling between the kinetics of [PCr] breakdown and $\dot{V}O_{2m}$ increase (i.e., similar τ values) suggests that the increase in [ADP] required to drive the adjustment of oxidative phosphorylation during changes in metabolic rate may be modulated by the rate of PCr hydrolysis during the on-transient phase. According to this hypothesis, at exercise onset, increases in mitochondrial [ADP] and [P_i], are initially delayed by the creatine kinase (CK)-catalyzed hydrolysis of PCr (Mahler, 1985). Since the outer mitochondrial membrane is permeable to PCr and Cr, these substrates are effectively "shuttled" in and out of the mitochondria so that [PCr] remains high in the cytosol (near the myosin ATPase where it can rephosphorylate ADP: $PCr + H^+ + ADP \rightarrow ATP + Cr$) and [Cr] remains high in the mitochondrial intermembrane space (near the ADP-ATP translocase protein where it can be phosphorylated at the expense of ATP: $Cr + ATP \rightarrow PCr + H^+ + ADP$). In this system, only once cytosolic [PCr] stores begin to deplete would mitochondrial [ADP] and [P_i] delivery sufficiently increase to drive oxidative phosphorylation towards a new steady-state. This control mechanism has been supported by experiments that have reported "faster than normal" (i.e., $\tau < 15$ s) $\dot{V}O_{2m}$ kinetics following acute CK inhibition in both isolated myocyte (Kindig *et al.* 2005) and *in situ* dog models (Grassi *et al.* 2011b) and following removal of the CK via genetic mutation in mice (Roman *et al.* 2002). Thus, evidence exists to suggest that at exercise onset, CK-mediated phosphate buffering acts to temporally diminish increases in [ADP] and fundamentally limit the adjustment of $\dot{V}O_{2m}$.

It is important to note however, that the model of PCr-mediated control of $\dot{V}O_{2m}$ kinetics largely ignores the contributions of NADH and O_2 provision. Indeed there are many circumstances where changes in convective and diffusive O_2 delivery to muscle have altered $\dot{V}O_{2p}$ kinetics. Relative to control conditions (normoxic upright cycling), reductions in: heart rate via beta-blockade (Hughson & Kowalchuk 1991); arterial O_2 content and pressure via hypoxic gas breathing (Hughson & Kowalchuk 1995; Engelen *et al.* 1996; Spencer *et al.* 2012; Bowen *et al.* 2013), and perfusion (driving) pressure for blood flow via supine exercise (MacDonald *et al.* 1998) have all led to a relative slowing of $\dot{V}O_{2p}$ kinetics. However, a significant argument against the role of O_2 provision in limiting the $\dot{V}O_{2p}$ response has been that increases in O_2 delivery via elevations in blood flow, C_aO_2, or increases in the diffusion gradient for O_2 at the capillary-muscle interface have been ineffective at speeding the response (Grassi *et al.* 1998a; Grassi *et al.* 1998b). Furthermore, microvascular PO_2 has been shown to remain unchanged for ~20 s following the onset of exercise in an *in situ* rat model (Behnke *et al.* 2001) implying that intracellular PO_2 and (thus O_2 availability) is in "excess" at exercise onset or conversely that O_2 delivery is increasing at a greater rate than oxidative metabolism. Based on a series of studies showing that $\dot{V}O_{2p}$ kinetics could be speeded by improvements in the matching of O_2 delivery (and its distribution) to O_2 utilization in healthy young and older individuals (Murias *et al.* 2010a; Murias *et al.* 2010b; Murias *et al.* 2011; Murias *et al.* 2012), Murias *et al.* (2014) proposed a model suggesting that for $\tau\dot{V}O_{2p}$ values > ~ 20 s, O_2 delivery to the tissues can play a critical role in determining the speed of $\dot{V}O_{2p}$ kinetics. Collectively, this body of research suggests that the fundamental limitation to the $\dot{V}O_{2p}$ (and thus oxidative phosphorylation) response at exercise onset resides in intracellular control mechanisms,

however situations do/can exist where O_2 provision contributes to alterations in the kinetic component of $\dot{V}O_2$.

In addition to limitations related to the delivery of phosphates to and from the mitochondria, activation of rate-limiting enzymes and provision of oxidative substrates to the mitochondrial TCA cycle and ETC have been implicated as possible regulatory or limiting sites for $\dot{V}O_2$ on transition to higher metabolic rates. For example, pyruvate dehydrogenase (PDH) could be viewed as a rate-limiting enzyme important for oxidative metabolism. PDH governs the conversion of carbohydrate-derived pyruvate to acetyl-coA; which enters the TCA cycle in the mitochondria yielding NADH and $FADH_2$. Thus, delayed activation of PDH at exercise onset could slow the delivery of oxidisable substrate to the TCA cycle and slow the adjustment of oxidative phosphorylation (Timmons *et al.* 1998; Howlett *et al.* 1999). In addition to PDH, there are several other rate-limiting reactions within the oxidative pathway whose enzyme activity at exercise onset (via inhibition or deactivation) could impact the substrates contributing to the overall flux in equation 1.1 and exert an influence on $\dot{V}O_{2m}$ kinetics.

Taken together, it is evident that the mechanism(s) responsible for controlling the rate of muscle O_2 uptake during the transition to greater metabolic rates are complex. At the single fibre level, control likely resides in the ability to provide adequate substrate (O_2, NADH, $FADH_2$, ADP, P_i, Cr) to the intramyocellular mitochondria primarily via a phosphate-linked regulatory control system that is functionally related to PCr hydrolysis and the level of its metabolites. Secondary to this fundamental limitation, further slowing of $\dot{V}O_2$ is likely dependent on the provision of O_2 and other oxidative substrates (e.g., NADH, acetyl coA, etc.) to the mitochondrial TCA cycle and ETC.

Up until this point, much of the information provided has operated under the assumption that $\dot{V}O_2$ adjusts to changes in metabolic demand by a kinetic process that is linear and first-order (i.e., mono-exponential). However, in many circumstances, the profile of $\dot{V}O_{2p}$ on transition to higher metabolic rates displays both time- and amplitude-based non-linearities that challenge traditional views of $\dot{V}O_2$ dynamics and reveal greater complexity of the mechanisms governing the regulation of oxidative metabolism. The following section, and this thesis, will focus on the "non-linear" behaviour of $\dot{V}O_{2p}$ and provide perspective on what this behaviour conveys in terms of respiratory control.

Control of $\dot{V}O_{2p}$ Kinetics

First-Order Responses

A linear, first-order system is one whose output variable values change proportionally with input variable values based on a single critical rate modulator. For example, it has been suggested that muscle O_2 utilization ($\dot{V}O_2$) increases in proportion to metabolic demand as controlled by the creatine kinase reaction (Meyer, 1988).

A system that operates with first-order kinetics has predictable output response patterns to a given input stimulus. For example, if an output variable, y, is forced to increase (by an input stimulus) to a given magnitude, Δy, the rate (dy/dt) at which it will increase at any instant of time (t) will be proportional to how far it is from its target (i.e., the error signal). The proportionality of this may described by the rate constant, k, ($(dy/dt) \cdot y(t) = k$) or the inverse of the rate constant, τ ($(dy/dt) \cdot \tau = y(t)$). Thus, if $\dot{V}O_2$, is forced to increase by a given $\Delta\dot{V}O_2$ (for e.g., by an instantaneous increase in ATP demand) the rate of increase at any time will be proportional to how far it is from its required target $\dot{V}O_2$ "steady-state"

(i.e., the $\dot{V}O_2$ at which it started plus $\Delta\dot{V}O_2$) as described by τ. This exemplifies how a first-order system necessitates exponential response kinetics. Importantly, this type of system is described by a first-order differential equation with constant coefficients (e.g., τ) which mandates that the rate of increase in $\dot{V}O_2$ at any time should always be proportional to its target value (as dictated by the error signal) and this should hold regardless of the initial $\dot{V}O_2$ or whether the target value is constant (as it would be during step-exercise) or changing (as it would be during ramp exercise) (Dillon, 2012). Stated differently, a dynamically linear, first-order system must respond with the same rate of adjustment (τ) and efficiency (gain) irrespective of the function that forced the response.

Dynamic System Linearity and $\dot{V}O_{2p}$ Kinetics

In the early 1900s it was observed that the rate at which O_2 is consumed is linearly related to exercise intensity or WR (Hill *et al.* 1924; Henry, 1951). This observation remains relevant today as the linear association between steady-state $\dot{V}O_{2p}$ and exercise intensity (and its implication of a linear relationship between the rate of oxidative phosphorylation and metabolic demand) forms the foundation from which the principles of exercise metabolism and prescription are taught. This relationship may be exemplified in ramp-incremental-type exercise protocols where it is common to observe $\dot{V}O_{2p}$ linearly increasing as a function of WR (Davis *et al.* 1982). A major implication of this observation is that $\dot{V}O_{2p}$ depends only on WR and thus the $\dot{V}O_{2p}$ response amplitude is directly proportional to the change in WR used to "force" the response (i.e., input pattern). Given this type of linear relationship, it also is appropriate to assume that the time parameters or the "dynamics" describing the $\dot{V}O_{2p}$ response are constant (or "linear") regardless of the input pattern or forcing function (e.g., impulse, step, ramp functions) (Lamarra, 1990).

From a systems control perspective, a process that abides by the aforementioned criteria is considered to be "dynamically linear", and may be characterized by a first-order differential equation (as previously described). Therefore, in response to a given change in stimulus (e.g., WR), a system under first-order, dynamically linear control would mandate: i) a kinetic output pattern that is independent of the input stimulus (i.e., time parameters are invariant regardless of whether the input pattern is derived, integrated, or summed) and; ii) amplitude-based changes that are proportional to the magnitude of a singular input and/or summed magnitudes of multiple inputs (principle of superposition) (Cautero *et al.* 2005). The expected $\dot{V}O_{2p}$ response (output) profile to various forcing (input) functions are displayed in Figure 1.2. Note that regardless of the baseline or amplitude of the forcing function the rate at which $\dot{V}O_{2p}$ exponentially increases and the magnitude of the increases remain constant (i.e., τ and gain of each WR input pattern are the same). Furthermore, the net response of two or more inputs at a given time is the sum of the responses which would have been caused by both inputs if they were performed in series.

It is based on the observation of the linear relationship between steady-state $\dot{V}O_{2p}$ and WR (at least within the *moderate* intensity domain), and the assumptions associated with that relationship, that the mono-exponential transfer function relating the $\dot{V}O_{2p}$ response to changes in WR (and thus an approximation of the relationship between changes in oxidative phosphorylation to changes in metabolic demand) was established (Henry, 1951; Whipp, 1971; Cerretelli & Di Prampero 1987). This method of characterizing the dynamic response of $\dot{V}O_{2p}$ has provided the means by which to study the regulation of

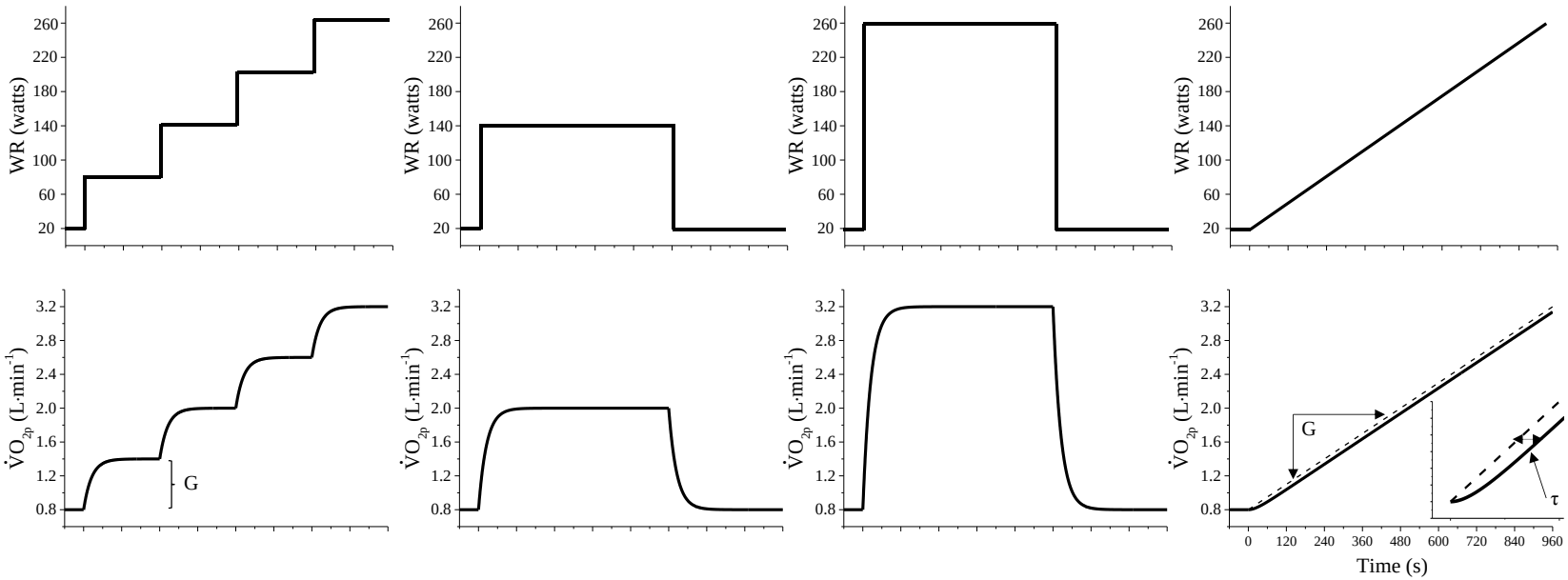

Figure 1.2. Dynamically linear, first order $\dot{V}O_{2p}$ kinetic responses to various forcing functions (including square-wave steps of varying amplitudes and from varying baselines and ramp function). Note that for a system having dynamically linear response dynamics, regardless of the forcing function, the rate of adjustment of $\dot{V}O_{2p}$ (as described by the time constant, τ) will be the same and that the change in $\dot{V}O_{2p}$ for a given change in work rate (as described by the Gain, G) will be invariant.

oxidative metabolism and elucidate the mechanisms of physiological control, however, it has gradually been demonstrated that the dynamics of $\dot{V}O_{2p}$ do not conform to the principles of a dynamically linear system but rather, $\dot{V}O_{2p}$ kinetics display intensity-dependent non-linear behaviours indicative of complex, higher-order control (Barstow & Mole 1991; Rossiter, 2011).

Challenges to Dynamic Linearity

As early as the 1970s, it was demonstrated that the profile of $\dot{V}O_{2p}$ does not always conform to the principles of a dynamically linear system in that it displays amplitude-based irregularities when transitioning to exercise intensities above the intensity that elicits net lactate productions (i.e., above the lactate threshold) (Whipp & Wasserman 1972; Whipp & Mahler 1980; Roston *et al.* 1987; Barstow & Mole 1991; Paterson & Whipp 1991; Whipp, 1994; Özyener *et al.* 2001). These "irregularities" are marked by a greater $\dot{V}O_{2p}$ gain (G: $\Delta\dot{V}O_{2p}/\Delta WR$), implying that there is a larger or 'excess' O_2 requirement beyond that which would be predicted from a linear $\dot{V}O_{2p}$ – WR relationship. Furthermore, this 'extra' $\dot{V}O_{2p}$ is considered to be of delayed onset (Barstow & Mole 1991; Paterson & Whipp 1991; Özyener *et al.* 2001) indicating more complex dynamics of the adjustment in $\dot{V}O_{2p}$ to changes in exercise WR; refuting a purely mono-exponential response. This 'additional' component of the $\dot{V}O_{2p}$ response, commonly referred to as the "slow component of $\dot{V}O_{2p}$" (Whipp, 1994; Gaesser & Poole 1996) has been shown to originate within the active muscle (Poole *et al.* 1988) and has been mechanistically linked to: 1) a fatigue-associated and progressive reduction in the efficiency of both skeletal muscle contraction (increased ATP cost of force production; P/W) and mitochondrial energy production (increased O_2 cost of ATP resynthesis; P/O) (Cannon *et al.* 2014; Korzeniewski

& Zoladz 2015); 2) a delayed recruitment of less oxidatively efficient, higher-order, muscle fibres, to supplement (or replace) any already recruited muscle fibres whose force generating capacities become attenuated (Gaesser & Poole 1996; Jones *et al.* 2011); 3) a simultaneous activation and recruitment of metabolically diverse muscle fibre pools (comprising an extremely wide range of $\dot{V}O_2$ time constants and gains) whose homogenized exponential responses are featured and expressed in different proportions throughout the on-transient (Brittain *et al.* 2001; Whipp *et al.* 2005; Wilkerson & Jones 2006; Wilkerson & Jones 2007; DiMenna & Jones 2009).

Within an individual, relative exercise intensity may be stratified, based on the absence or presence of a $\dot{V}O_{2p}$ slow component and its behaviour on transition from low- to higher- intensities of exercise. This is accomplished by identifying a range of constant-load WRs that elicit similar $\dot{V}O_{2p}$ response profiles and arranging them into clusters or exercise intensity "domains" (Whipp *et al.* 2005). In the exercise intensity domain schema outlined by Whipp *et al.* (2005), the spectrum of work intensities ranging from rest to supra-maximal include: the *moderate*, *heavy*, *very heavy* and *severe* intensity domains which are demarcated by the lactate threshold (LT), "critical power" (CP) or "maximal lactate steady-state" (MLSS), and $\dot{V}O_{2max}$ (although alternative classifications exists; (Poole *et al.* 2008)). The *moderate* intensity domain represents a range of WRs where $\dot{V}O_{2p}$ reaches a steady-state without a sustained metabolic acidosis, i.e., below LT (Roston *et al.* 1987). At all WRs above the LT, a $\dot{V}O_{2p}$ slow component is manifest. In the *heavy* intensity domain, i.e., WRs between LT and CP/MLSS, exercise is characterized by a delayed stabilization in $\dot{V}O_{2p}$ accompanied by an elevated but stable arterial lactate ($[La^-]$) and acidosis (Keir *et al.* 2015). In the *very heavy* intensity domain (i.e., >CP/MLSS), $\dot{V}O_{2p}$,

arterial (and muscle) [La^-] and [H^+], and PCr breakdown can no longer stabilize (Poole *et al.* 1988; Jones *et al.* 2008) and exhaustion ensues at the attainment of $\dot{V}O_{2max}$ (Gaesser & Poole 1996). *Severe* intensity exercise marks all WRs where exhaustion occurs prior to the achievement of $\dot{V}O_{2max}$. By virtue of their existence, the exercise intensity domains (at least those above *moderate*, i.e., >LT) indicate a complexity of muscle metabolic response dynamics that cannot be explained by a linear model of $\dot{V}O_2$ control.

That a $\dot{V}O_{2p}$ slow component is not evident at all exercise intensities within the *moderate* intensity domain, suggests that the kinetics of $\dot{V}O_{2p}$ conform to the principles of a dynamically linear system so long as the exercise intensity is below the LT (Whipp & Wasserman 1972; Whipp *et al.* 1982; Roston *et al.* 1987; Barstow *et al.* 1990; Özyener *et al.* 2001). While the $\dot{V}O_{2p}$ response to step-changes in WR within this domain are indeed well described by a single exponential function that attains a steady-state $\dot{V}O_{2p}$ (Rossiter *et al.* 1999), the kinetic parameters of phase II $\dot{V}O_{2p}$ associated with transitions performed within different regions of the domain have been shown to violate the principle of superposition which defines dynamic linearity. This principle dictates that the $\dot{V}O_{2p}$ response must exhibit both amplitude- and temporal-based invariance regardless of the magnitude and pattern of the change in WR used to drive the $\dot{V}O_{2p}$ response. Yet, it has consistently been shown that for the same WR increment (i.e., ΔWR), $\tau\dot{V}O_{2p}$ and functional gain (G_P: $\Delta\dot{V}O_{2pSS}/\Delta$WR) are increased when exercise is initiated from an elevated compared to lower baseline WR within the *moderate* domain (Brittain *et al.* 2001; MacPhee *et al.* 2005; Bowen *et al.* 2011; Spencer *et al.* 2011; Williams *et al.* 2013; Keir *et al.* 2014). For example, using a constant-load "double-step" exercise model whereby the *moderate* intensity domain was bisected into two identical step-WR increments (between 20 W and

90% LT), Brittain *et al.* (2001) observed an ~ 15 s greater $\tau\dot{V}O_{2p}$ during transitions initiated from a raised (upper step, US; ~ 40 s) compared to a lower (lower step, LS; ~ 25 s) baseline WR, as well as a greater G_p (11.9 vs. 10.6 $ml \cdot min^{-1} \cdot W^{-1}$). Additional evidence refuting dynamically linear behaviour within this domain is the absence of symmetry between on-transient and off-transient $\dot{V}O_{2p}$ kinetics (Rossiter *et al.* 1999; Özyener *et al.* 2001; Cautero *et al.* 2005). Thus, despite the absence of a $\dot{V}O_{2p}$ slow component, sub-LT exercise has also been shown to demonstrate non-linear behaviour.

Together, these findings clearly argue against a 'true' linear relationship between $\dot{V}O_{2p}$ and WR, even though $\dot{V}O_{2p}$ is typically observed to increase proportionately with WR during ramp incremental exercise to exhaustion (Davis *et al.* 1982; Whipp *et al.* 1982; Rossiter *et al.* 2006; Murgatroyd *et al.* 2014) and during sub-LT, step incremental exercise (Zoladz *et al.* 1995). Due to challenges surrounding adequate and accurate characterization of the $\dot{V}O_{2p}$ kinetic response during *heavy* and *very heavy* exercise (where $\dot{V}O_{2p}$ reaches [or fails to reach] a delayed steady-state due to the influence of the $\dot{V}O_{2p}$ slow component), it becomes increasingly difficult to utilize $\dot{V}O_{2p}$ kinetic analyses for studying the factors that control and regulate oxidative metabolism. However, given that responses to various forcing functions within the *moderate* intensity domain are less complex in that they are well described by a mono-exponential function, this domain offers a less confounded and more controllable 'environment' by which the regulation of $\dot{V}O_{2p}$, and thus oxidative phosphorylation and its controlling mechanism(s), may be studied. For this reason, in recent years, our laboratory has focused on investigating the mechanisms associated with the 'non-linear' response dynamics of $\dot{V}O_{2p}$ within the confines of the *moderate* intensity

domain. Of particular interest, is the highly reproducible phenomena that $\dot{V}O_{2p}$ kinetics are slower when initiated from elevated baseline intensities.

Transitions from elevated moderate baseline intensities

Within the *moderate* intensity domain, phase II $\tau\dot{V}O_{2p}$ and G_P are greater when step-transitions with a common WR increment are initiated from a lighter- compared to a higher-intensity baseline WR (Hughson & Morrissey 1982; Brittain *et al.* 2001; MacPhee *et al.* 2005; Bowen *et al.* 2011; Spencer *et al.* 2011; Williams *et al.* 2013). Within the context of this 'double-step' model, several mechanisms have been proposed to explain the slower $\dot{V}O_{2p}$ kinetics in the US.

Among the first to report this phenomenon were Hughson and Morrissey (1982) who suggested that the slower $\dot{V}O_{2p}$ kinetics in US compared to LS was related to limitations in convective O_2 delivery/transport consequent to a shift from parasympathetic to sympathetically-mediated control of heart rate dynamics. An insufficiency in convective O_2 delivery was later supported by MacPhee *et al*. (2005) who reported a slower rate of adjustment in conduit (bulk) femoral artery blood flow concomitant with slower $\dot{V}O_{2p}$ kinetics in US. However, the influence of O_2 provision in this regard, has been largely refuted as the dynamics of the NIRS-derived [HHb] signal (reflective of the balance between local muscle O_2 delivery and O_2 utilization) have been shown to adjust at a slower rate (concomitant with the dynamic adjustments of $\dot{V}O_{2p}$) in the US compared to the LS in healthy young (MacPhee *et al.* 2005; Williams *et al.* 2013) and older men (Spencer *et al.* 2011) implying that the underlying blood flow response (indicative of O_2 delivery) is responding at a rate similar to that of O_2 utilization. This notion has recently been supported by Wüst *et al*. (Wüst *et al.* 2014), who were unable to reduce $\tau\dot{V}O_{2p}$ in the US (towards the

$\tau\dot{V}O_{2p}$ value associated with LS) even after increasing pre-transition O_2 delivery (via pump-perfusion) to the highest level achieved during a spontaneous control in an *in situ* dog model during evoked isometric tetanic contractions. Thus, it appears unlikely that blood flow and O_2 delivery to and within the microvasculature are responsible for the slower $\dot{V}O_{2p}$ dynamics associated with transitions from elevated baselines.

An alternative explanatory mechanism related to muscle recruitment pattern may be derived from the size principle outlined by Henneman & Mendell (1981). Using this principle, it is postulated that at lower baseline WRs (e.g., LS), lower-order fibres that are kinetically-efficient, (higher oxidative fibres with greater metabolic "efficiency") might be preferentially recruited to contribute to the ATP requirements for force production, whereas transitions initiated from higher WRs (e.g., US) would recruit a greater proportion of higher-order muscle fibres which are kinetically, less-efficient and slower (with intrinsically less metabolic "efficiency") (Brittain *et al.* 2001). Therefore, the resultant $\dot{V}O_{2p}$ dynamics to step-changes involving a greater proportion of the latter should produce a kinetic adjustment that is slower. Such a notion of disparities in O_2 requirement per unit increase in WR between fibre populations (e.g., type I vs type II) are substantiated (Crow & Kushmerick 1982; Barstow *et al.* 1996; Pringle *et al.* 2003; Krustrup *et al.* 2008), offering validity to a fibre recruitment-mediated mechanism governing the rate of adjustment of $\dot{V}O_{2p}$ during work-to-work transitions. In support of this hypothesis, DiMenna *et al.* (2010a) reported slower $\dot{V}O_{2p}$ kinetics with *heavy* intensity exercise transitions made from a baseline of *moderate* compared to light intensity ($\tau\dot{V}O_{2p}$ = 48 s versus 28 s, respectively). Furthermore, no differences in $\tau\dot{V}O_{2p}$ were observed between the first ($\tau\dot{V}O_{2p}$ = 28 s) and second ($\tau\dot{V}O_{2p}$ = 27 s) of two consecutive bouts of *heavy*

intensity exercise transitions initiated from the same light intensity baseline (i.e., same muscle recruitment); where baseline $\dot{V}O_{2p}$ in the second bout was elevated (relative to the first) due to incomplete $\dot{V}O_{2p}$ recovery time between bouts (i.e., elevated metabolic rate). These data implicated a role of the elevated pre-transition work rate and its effect on muscle fibre recruitment (rather than an effect of an elevated metabolic rate) as the primary mechanism by which $\dot{V}O_{2p}$ kinetics are slowed when transitions are initiated from elevated baseline intensities. However, it should be emphasized that this study examined $\dot{V}O_{2p}$ kinetics in transitions to *heavy* intensity exercise where muscle fibre recruitment and metabolic responses to exercise are clearly different from those associated with the *moderate* intensity domain. Interpretation of the data is further confounded by the fact that a prior bout of *heavy* intensity exercise has occasionally been shown to speed $\dot{V}O_{2p}$ kinetics ("priming" effect) in a subsequent exercise transition (Gurd *et al.* 2005; DeLorey *et al.* 2007). Regardless, a hypothesis of a progressive muscle fibre recruitment-related mechanism remains plausible.

It is also possible that oxidative phosphorylation may adjust more slowly in muscle that is already active due to a reduced intramuscular energy state (or reduced "metabolic stability") consequent to the elevated pre-transition work and/or metabolic rate (Bowen *et al.* 2011; Grassi *et al.* 2011a). Though speculative, this hypothesis suggests that local disruptions to the intracellular metabolic state consequent to a raised metabolic rate, i.e., higher [ADP_{free}] and [Pi], and lower [ATP], would reduce the Gibbs free energy (ΔG_{ATP} related to [ADP_{free}] x [Pi] x $[ATP]^{-1}$) associated with ATP hydrolysis (i.e., less negative ΔG_{ATP}) thereby increasing the ATP requirement for the WR increment (greater $\Delta ATP/\Delta WR$) resulting in a greater G_P ($\Delta \dot{V}O_{2pSS}/\Delta WR$) and a longer time to achieve a

$\dot{V}O_{2pSS}$ (greater $\tau\dot{V}O_{2p}$) (Jeneson *et al.* 1995; Meyer & Foley 1996). While this hypothesis remains to be directly tested in humans, Wüst *et al.* (2014) observed a slowing of $\dot{V}O_{2p}$ kinetics on transition when tetanic contractions were initiated from a raised metabolic rate despite uniform stimulation and increased O_2 delivery in dog muscle *in situ*. Additionally, Bowen *et al.* (2011) attempted to resolve the influences of muscle recruitment (i.e., effect of raised WR) and muscle metabolic stability (i.e., effect of elevated metabolic rate) in humans using both the double-step exercise model and two separate single-step transitions from 20 W to 90%LT separated by either 30 s (i.e., partial recovery) or 12 min (i.e., complete recovery) baseline cycling. In contrast to DiMenna *et al.* (2010a), despite exercise transitions being initiated from a common baseline WR for both single-step transitions, $\dot{V}O_{2p}$ kinetics were slower after partial compared to complete recovery (i.e., with an elevated baseline metabolic rate), and the $\tau\dot{V}O_{2p}$ (and baseline $\dot{V}O_{2p}$) was not different from that observed in the US of the double-step protocol (Bowen *et al.* 2011). These data suggested that the raised metabolic rate, rather than fibre recruitment, contributed to the slower $\dot{V}O_{2p}$ response when exercise transitions are initiated from the upper regions of the *moderate* intensity domain.

Transitions from elevated baseline intensities beyond the moderate intensity domain

In addition to DiMenna *et al.* (2010a), many other studies have reported progressively slower adjustments in phase II $\dot{V}O_{2p}$ and increases in gain in response to 'work-to-work' exercise transitions from progressively elevated baseline intensities beyond the *moderate* domain (Wilkerson & Jones 2006; Wilkerson & Jones 2007; DiMenna *et al.* 2009; DiMenna *et al.* 2010b; DiMenna *et al.* 2010). Based on the assumption that human skeletal muscle is comprised of fibers with a spectrum of distinct

biochemical characteristics (Bottinelli & Reggiani 2000; Bottinelli, 2001) and that fibres are recruited in a hierarchical manner depending on the intensity of contractile activity (Henneman & Mendell 1981) these authors reasoned that manipulating pre-transition baseline WR would isolate and unveil response characteristics of the motor units located at different positions within the recruitment hierarchy (DiMenna & Jones 2009). Collectively, these data suggest that $\dot{V}O_{2p}$ kinetics become progressively slower as a function of baseline WR (or as a function of higher-order fibre recruitment); and since contractile intensity (or WR) is the stimulus that drives motor unit recruitment, this hypothesis may be justifiable. However, it cannot be discounted that the intensity-dependent changes in the dynamics of the homogenized $\dot{V}O_{2p}$ signal reflect differences in kinetic modulation within the range of recruited fibres and within single fibres themselves.

Summary

The slower $\dot{V}O_{2p}$ kinetics accompanying transitions from elevated baseline intensities and the appearance of a $\dot{V}O_{2p}$ slow component provide evidence to suggest that oxidative phosphorylation does not conform to a dynamically linear system, controlled by a first-order rate reaction. A summary of the evidence refuting the control of $\dot{V}O_2$ by a process that is dynamically linear and first-order are presented in Figure 1.3 (note the deviations in the $\dot{V}O_{2p}$ output profile compared to those in Figure 1.2). These non-linear behaviours belie the foundations from which $\dot{V}O_{2p}$ kinetic analyses were established and imply a great complexity to the control of oxidative metabolism on transition to greater levels of metabolic demand (i.e., one that is beyond first-order). The overall purpose of this thesis is to examine the "non-linearity" of $\dot{V}O_{2p}$ and provide perspective on what this behaviour conveys in terms of the control of muscle O_2 utilization.

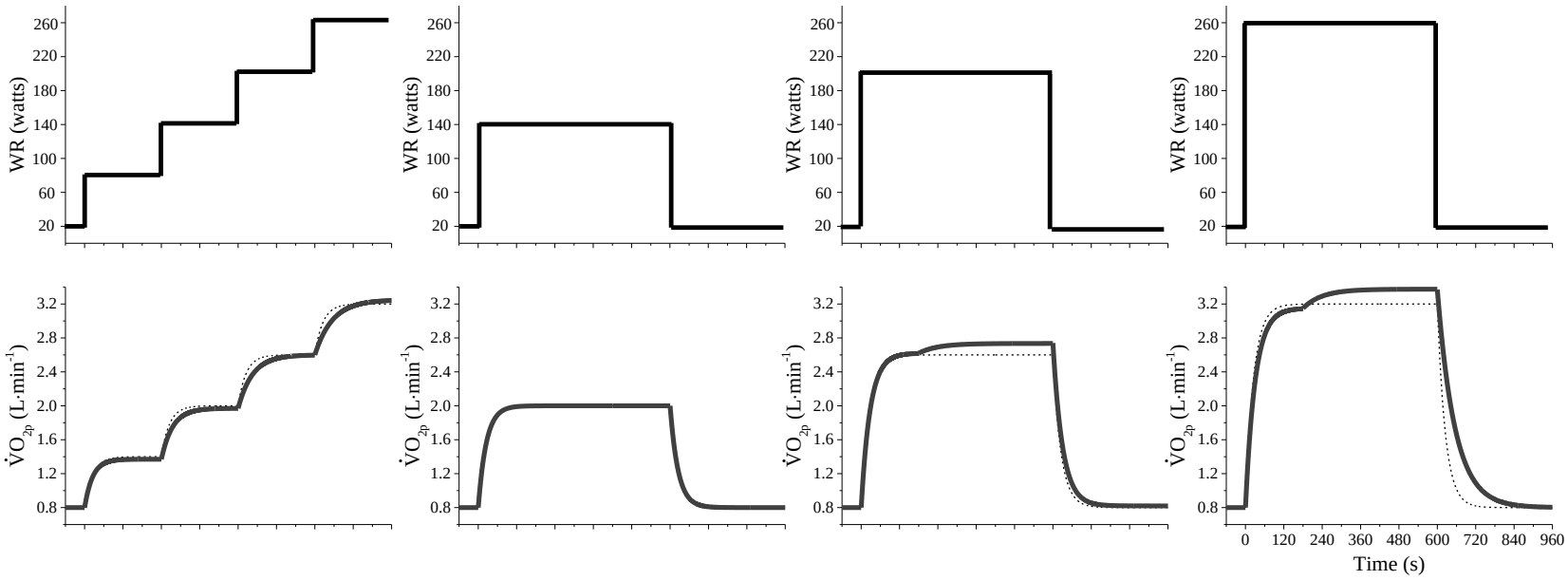

Figure 1.3. Typical $\dot{V}O_{2p}$ kinetic responses to the same forcing function as Figure 1.2 except with inclusion of an intermediate square-wave change from a low baseline in the place of ramp-incremental changes. Note the "non-linearity" in the $\dot{V}O_{2p}$ response profiles. Depending on the forcing function, the rate of adjustment of $\dot{V}O_{2p}$ (as described by the time constant, τ) and the change in $\dot{V}O_{2p}$ for a given change in work rate (as described by the Gain, G) will differ depending on forcing function baseline and amplitude (deviations from the "dynamically linear" system in Figure 1.2. can be seen by comparing the *dashed* profiles (from 1.2) to the *grey line* profiles here). Also note the intensity-dependent appearance of an additional component of $\dot{V}O_{2p}$ challenging the assumption of first-order control of $\dot{V}O_2$.

Overview of Studies

Since the collection of breath-by-breath $\dot{V}O_{2p}$ and kinetic analyses of those data form an integral part of the methodology in this thesis, Chapter II will critically examine some of the fundamental aspects of $\dot{V}O_{2p}$ kinetic analyses including: assessing the characteristic of breath-by-breath $\dot{V}O_{2p}$ data, breath-by-breath $\dot{V}O_{2p}$ data processing, and model fitting. However, the primary focus of the studies that comprise this thesis will be on investigating the mechanisms associated with the "non-linear" response dynamics of $\dot{V}O_{2p}$ within the confines of the *moderate* intensity domain and beyond with particular regard to the phenomena of slower $\dot{V}O_{2p}$ kinetics with transitions initiated from elevated baseline intensities (Chapters III-IV). The specific purposes of this thesis are:

1. To investigate the effect of different breath-by-breath $\dot{V}O_{2p}$ data processing techniques on parameter estimation and confidence of phase II $\dot{V}O_{2p}$ kinetics.
2. To quantify the magnitude and variability of breath-by-breath $\dot{V}O_{2p}$ "noise" both within (between test-repetitions), between individuals and at various intensities.
3. To determine in the same participants: i) the relationship between baseline metabolic rate and $\dot{V}O_{2p}$ kinetics for a constant WR increment; and ii) the $\dot{V}O_{2p}$ kinetics over a range of WR increments initiated from a constant baseline metabolic rate; exclusively within the *moderate*-intensity domain.
4. To determine the extent by which circulatory dynamics may contribute to the slowed $\dot{V}O_{2p}$ kinetics from progressively increasing baseline metabolic rates or from transitions with progressively increasing WR increments with constant, low baseline intensities.

5. To determine, in a single group of participants, the relationship between baseline intensity and phase II $\tau\dot{V}O_{2p}$ and gain over a range of baseline WRs spanning the *moderate, heavy,* and *very heavy*-intensity domains.
6. To use the relationships established in #5 to determine whether they may explain the "linear" $\dot{V}O_{2p}$vs WR response to ramp-incremental exercise.
7. To investigate whether the relationships established in #5 could be used to simulate and predict "non-linear" behaviours of $\dot{V}O_{2p}$ in response to step-transitions of varying intensity and ramp-incremental exercise of varying WR slopes.

Hypotheses

This thesis will specifically address the following hypotheses:

1. That $\dot{V}O_{2p}$ kinetic parameter estimates would not be affected by the procedure used to process the data.
2. That the characteristics of breath-by-breath $\dot{V}O_{2p}$ "noise" would vary within individuals (between test-repeats) and between individuals.
3. That the characteristics of breath-by-breath $\dot{V}O_{2p}$ "noise" would conform to a predictable Gaussian distribution independent of age group or steady-state exercise intensity.
4. That $\tau\dot{V}O_{2p}$ and G_P would increase as a function of *moderate* intensity baseline $\dot{V}O_{2p}$ when ΔWR was held constant but would be unchanged with increasing ΔWR step-changes from a constant baseline $\dot{V}O_{2p}$ condition.

5. That the slowed $\dot{V}O_{2p}$ kinetics observed with transitions from elevated baseline intensities would not be consequent to altered circulatory dynamics.
6. That both phase II $\tau\dot{V}O_{2p}$ and G_P would increase as a function baseline intensity baseline across a spectrum baseline WRs spanning the *moderate*, *heavy*, and *very heavy*-intensity domains.
7. That the time constant versus WR and gain versus WR relationships could be used to explain the linearity observed between $\dot{V}O_{2p}$ and WR during ramp-incremental exercise.

References

Bangsbo J, Krustrup P, Gonzalez-Alonso J, Boushel R & Saltin B (2000). Muscle oxygen kinetics at onset of intense dynamic exercise in humans. *Am J Physiol Regul Integr Comp Physiol* **279**, R899-906.

Barstow TJ, Jones AM, Nguyen PH & Casaburi R (1996). Influence of muscle fiber type and pedal frequency on oxygen uptake kinetics of heavy exercise. *J Appl Physiol* **81**, 1642-1650.

Barstow TJ, Lamarra N & Whipp BJ (1990). Modulation of muscle and pulmonary O2 uptakes by circulatory dynamics during exercise. *J Appl Physiol* **68**, 979-989.

Barstow TJ & Mole PA (1991). Linear and nonlinear characteristics of oxygen uptake kinetics during heavy exercise. *J Appl Physiol* **71**, 2099-2106.

Beaver WL, Lamarra N & Wasserman K (1981). Breath-by-breath measurement of true alveolar gas exchange. *J Appl Physiol* **51**, 1662-1675.

Behnke BJ, Kindig CA, Musch TI, Koga S & Poole DC (2001). Dynamics of microvascular oxygen pressure across the rest-exercise transition in rat skeletal muscle. *Respir Physiol* **126**, 53-63.

Bottinelli R (2001). Functional heterogeneity of mammalian single muscle fibres: do myosin isoforms tell the whole story? *Pflugers Arch* **443**, 6-17.

Bottinelli R & Reggiani C (2000). Human skeletal muscle fibres: molecular and functional diversity. *Prog Biophys Mol Biol* **73**, 195-262.

Bowen TS, Murgatroyd SR, Cannon DT, et al. (2011). A raised metabolic rate slows pulmonary O_2 uptake kinetics on transition to moderate-intensity exercise in humans independently of work rate. *Exp Physiol* **96**, 1049-1061.

Bowen TS, Rossiter HB, Benson AP, et al. (2013). Slowed oxygen uptake kinetics in hypoxia correlate with the transient peak and reduced spatial distribution of absolute skeletal muscle deoxygenation. *Exp Physiol* **98**, 1585-1596.

Brittain CJ, Rossiter HB, Kowalchuk JM & Whipp BJ (2001). Effect of prior metabolic rate on the kinetics of oxygen uptake during moderate-intensity exercise. *Eur J Appl Physiol* **86**, 125-134.

Cannon DT, Bimson WE, Hampson SA, et al. (2014). Skeletal muscle ATP turnover by ^{31}P magnetic resonance spectroscopy during moderate and heavy bilateral knee extension. *J Physiol* **592**, 5287-5300.

Capelli C, Cautero M & Pogliaghi S (2011). Algorithms, modelling and VO_2 kinetics. *Eur J Appl Physiol* **111**, 331-342.

Cautero M, di Prampero PE, Tam E & Capelli C (2005). Alveolar oxygen uptake kinetics with step, impulse and ramp exercise in humans. *Eur J Appl Physiol* **95**, 474-485.

Cerretelli P & Di Prampero PE (1987). Gas Exchange in Exercise. In Handbook of Physiology, Section 3, The Respiratory System, vol. IV, ed. Farhi LE &Tenney SM, pp. 297-339. American Physiological Society, Bethesda, MD.

Chance B & Williams GR (1955). Respiratory enzymes in oxidative phosphorylation. I. Kinetics of oxygen utilization. *J Biol Chem* **217**, 383-393.

Crow MT & Kushmerick MJ (1982). Chemical energetics of slow- and fast-twitch muscles of the mouse. *J Gen Physiol* **79**, 147-166.

Davis JA, Whipp BJ, Lamarra N, Huntsman DJ, Frank MH & Wasserman K (1982). Effect of ramp slope on determination of aerobic parameters from the ramp exercise test. *Med Sci Sports Exerc* **14**, 339-343.

DeLorey DS, Kowalchuk JM, Heenan AP, Dumanoir GR & Paterson DH (2007). Prior exercise speeds pulmonary O_2 uptake kinetics by increases in both local muscle O_2 availability and O_2 utilization. *J Appl Physiol* **103**, 771-778.

Dillon PF (2012). Stability, complexity and non-linear systems. In Biophysics: A physiological approach, 1st edn, pp. 257-260. Cambridge University Press, New York.

DiMenna F & Jones AM (2009). "Linear" versus "nonlinear" VO2 responses to exercise: reshaping traditional beliefs **7**, 67-84.

DiMenna FJ, Bailey SJ, Vanhatalo A, Chidnok W & Jones AM (2010a). Elevated baseline VO_2 per se does not slow O_2 uptake kinetics during work-to-work exercise transitions. *J Appl Physiol (1985)* **109**, 1148-1154.

DiMenna FJ, Fulford J, Bailey SJ, Vanhatalo A, Wilkerson DP & Jones AM (2010b). Influence of priming exercise on muscle [PCr] and pulmonary O_2 uptake dynamics during 'work-to-work' knee-extension exercise. *Respir Physiol Neurobiol* **172**, 15-23.

DiMenna FJ, Wilkerson DP, Burnley M, Bailey SJ & Jones AM (2009). Influence of extreme pedal rates on pulmonary O_2 uptake kinetics during transitions to high-intensity exercise from an elevated baseline. *Respir Physiol Neurobiol* **169**, 16-23.

DiMenna FJ, Wilkerson DP, Burnley M, Bailey SJ & Jones AM (2010). Priming exercise speeds pulmonary O_2 uptake kinetics during supine "work-to-work" high-intensity cycle exercise. *J Appl Physiol* **108**, 283-292.

Engelen M, Porszasz J, Riley M, Wasserman K, Maehara K & Barstow TJ (1996). Effects of hypoxic hypoxia on O2 uptake and heart rate kinetics during heavy exercise. *J Appl Physiol* **81**, 2500-2508.

Fitts RH (1994). Cellular mechanisms of muscle fatigue. *Physiol Rev* **74**, 49-94.

Gaesser GA & Poole DC (1996). The slow component of oxygen uptake kinetics in humans. *Exerc Sport Sci Rev* **24**, 35-71.

Grassi B, Gladden LB, Samaja M, Stary CM & Hogan MC (1998a). Faster adjustment of O_2 delivery does not affect VO_2 on-kinetics in isolated in situ canine muscle. *J Appl Physiol* **85**, 1394-1403.

Grassi B, Gladden LB, Stary CM, Wagner PD & Hogan MC (1998b). Peripheral O_2 diffusion does not affect VO_2 on-kinetics in isolated insitu canine muscle. *J Appl Physiol* **85**, 1404-1412.

Grassi B, Poole DC, Richardson RS, Knight DR, Erickson BK & Wagner PD (1996). Muscle O_2 uptake kinetics in humans: implications for metabolic control. *J Appl Physiol* **80**, 988-998.

Grassi B, Porcelli S, Salvadego D & Zoladz JA (2011a). Slow VO_2 kinetics during moderate-intensity exercise as markers of lower metabolic stability and lower exercise tolerance. *Eur J Appl Physiol* **111**, 345-355.

Grassi B, Rossiter HB, Hogan MC, et al. (2011b). Faster O_2 uptake kinetics in canine skeletal muscle in situ after acute creatine kinase inhibition. *J Physiol* **589**, 221-233.

Gurd BJ, Scheuermann BW, Paterson DH & Kowalchuk JM (2005). Prior heavy-intensity exercise speeds VO_2 kinetics during moderate-intensity exercise in young adults. *J Appl Physiol* **98**, 1371-1378.

Henneman E & Mendell LM (1981). Functional organization of motorneuron pool and its inputs. In Handbook of Physiology, The Nervous System, ed. Brooks V, pp. 423-507. Am. Physiol. Soc., Bethesda, MD.

Henry FM (1951). Aerobic oxygen consumption and alactic debt in muscular work. *J Appl Physiol* **3**, 427-438.

Hill AV, Long CNH & Lupton H (1924). Muscular exercise, lactic acid and supply and utilization of oxygen: VI. The oxygen debt at the end of exercise. **97**, 127-137.

Howlett RA, Heigenhauser GJ, Hultman E, Hollidge-Horvat MG & Spriet LL (1999). Effects of dichloroacetate infusion on human skeletal muscle metabolism at the onset of exercise. *Am J Physiol* **277**, E18-25.

Hughson RL & Kowalchuk JM (1991). Beta-blockade and oxygen delivery to muscle during exercise. *Can J Physiol Pharmacol* **69**, 285-289.

Hughson RL & Kowalchuk JM (1995). Kinetics of oxygen uptake for submaximal exercise in hyperoxia, normoxia, and hypoxia. *Can J Appl Physiol* **20**, 198-210.

Hughson RL & Morrissey M (1982). Delayed kinetics of respiratory gas exchange in the transition from prior exercise. *J Appl Physiol* **52**, 921-929.

Jeneson JA, Westerhoff HV, Brown TR, Van Echteld CJ & Berger R (1995). Quasi-linear relationship between Gibbs free energy of ATP hydrolysis and power output in human forearm muscle. *Am J Physiol* **268**, C1474-84.

Jones AM, Grassi B, Christensen PM, Krustrup P, Bangsbo J & Poole DC (2011). Slow component of VO_2 kinetics: mechanistic bases and practical applications. *Med Sci Sports Exerc* **43**, 2046-2062.

Jones AM, Wilkerson DP, DiMenna F, Fulford J & Poole DC (2008). Muscle metabolic responses to exercise above and below the "critical power" assessed using 31P-MRS. *Am J Physiol Regul Integr Comp Physiol* **294**, R585-93.

Keir DA, Fontana FY, Robertson TC, et al. (2015). Exercise Intensity Thresholds: Identifying the Boundaries of Sustainable Performance. *Med Sci Sports Exerc*.

Keir DA, Nederveen JP, Paterson DH & Kowalchuk JM (2014). Pulmonary O_2 uptake kinetics during moderate-intensity exercise transitions initiated from low versus elevated metabolic rates: insights from manipulations in cadence. *Eur J Appl Physiol* **114**, 2655-2665.

Kindig CA, Howlett RA, Stary CM, Walsh B & Hogan MC (2005). Effects of acute creatine kinase inhibition on metabolism and tension development in isolated single myocytes. *J Appl Physiol* **98**, 541-549.

Korzeniewski B & Zoladz JA (2015). Possible mechanisms underlying slow component of VO_2 on-kinetics in skeletal muscle. *J Appl Physiol* **118**, 1240-1249.

Krustrup P, Jones AM, Wilkerson DP, Calbet JA & Bangsbo J (2009). Muscular and pulmonary O_2 uptake kinetics during moderate- and high-intensity sub-maximal knee-extensor exercise in humans. *J Physiol* **587**, 1843-1856.

Krustrup P, Secher NH, Relu MU, Hellsten Y, Soderlund K & Bangsbo J (2008). Neuromuscular blockade of slow twitch muscle fibres elevates muscle oxygen uptake and energy turnover during submaximal exercise in humans. *J Physiol* **586**, 6037-6048.

Lamarra N (1990). Variables, constants, and parameters: clarifying the system structure. *Med Sci Sports Exerc* **22**, 88-95.

MacDonald MJ, Shoemaker JK, Tschakovsky ME & Hughson RL (1998). Alveolar oxygen uptake and femoral artery blood flow dynamics in upright and supine leg exercise in humans. *J Appl Physiol* **85**, 1622-1628.

MacPhee SL, Shoemaker JK, Paterson DH & Kowalchuk JM (2005). Kinetics of O_2 uptake, leg blood flow, and muscle deoxygenation are slowed in the upper compared with lower region of the moderate-intensity exercise domain. *J Appl Physiol* **99**, 1822-1834.

Mahler M (1985). First-order kinetics of muscle oxygen consumption, and an equivalent proportionality between QO_2 and phosphorylcreatine level. Implications for the control of respiration. *J Gen Physiol* **86**, 135-165.

Meyer RA & Foley JM (1996). Cellular Processes integrating the metabolic response to exercise. In Handbook of Physiology. Exercise: Regulation and Integration of Multiple Systems, ed. Rowell LB & Shepherd JT, pp. 841-869. Am. Physiol. Soc., Bethesda, MD.

Meyer RA (1988). A linear model of muscle respiration explains monoexponential phosphocreatine changes. *Am J Physiol* **254**, C548-53.

Murgatroyd SR, Wylde LA, Cannon DT, Ward SA & Rossiter HB (2014). A 'ramp-sprint' protocol to characterise indices of aerobic function and exercise intensity domains in a single laboratory test. *Eur J Appl Physiol*.

Murias JM, Kowalchuk JM & Paterson DH (2011). Speeding of VO_2 kinetics in response to endurance-training in older and young women. *Eur J Appl Physiol* **111**, 235-243.

Murias JM, Kowalchuk JM & Paterson DH (2010a). Speeding of VO_2 kinetics with endurance training in old and young men is associated with improved matching of local O_2 delivery to muscle O_2 utilization. *J Appl Physiol* **108**, 913-922.

Murias JM, Kowalchuk JM & Paterson DH (2010b). Time course and mechanisms of adaptations in cardiorespiratory fitness with endurance training in older and young men. *J Appl Physiol* **108**, 621-627.

Murias JM, Spencer MD & Paterson DH (2014). The critical role of O_2 provision in the dynamic adjustment of oxidative phosphorylation. *Exerc Sport Sci Rev* **42**, 4-11.

Murias JM, Spencer MD, Pogliaghi S & Paterson DH (2012). Non-invasive estimation of microvascular O_2 provision during exercise on-transients in healthy young males. *Am J Physiol Regul Integr Comp Physiol* **303**, R815-823.

Özyener F, Rossiter HB, Ward SA & Whipp BJ (2001). Influence of exercise intensity on the on- and off-transient kinetics of pulmonary oxygen uptake in humans. *J Physiol* **533**, 891-902.

Paterson DH & Whipp BJ (1991). Asymmetries of oxygen uptake transients at the on- and offset of heavy exercise in humans. *J Physiol* **443**, 575-586.

Poole DC, Barstow TJ, McDonough P & Jones AM (2008). Control of oxygen uptake during exercise. *Med Sci Sports Exerc* **40**, 462-474.

Poole DC, Ward SA, Gardner GW & Whipp BJ (1988). Metabolic and respiratory profile of the upper limit for prolonged exercise in man. *Ergonomics* **31**, 1265-1279.

Pringle JS, Doust JH, Carter H, et al. (2003). Oxygen uptake kinetics during moderate, heavy and severe intensity "submaximal" exercise in humans: the influence of muscle fibre type and capillarisation. *Eur J Appl Physiol* **89**, 289-300.

Roman BB, Meyer RA & Wiseman RW (2002). Phosphocreatine kinetics at the onset of contractions in skeletal muscle of MM creatine kinase knockout mice. *Am J Physiol Cell Physiol* **283**, C1776-83.

Rossiter H (2011). Exercise: Kinetic Considerations for Gas Exchange. *Comp Physiol* **1**, 203-244.

Rossiter HB, Kowalchuk JM & Whipp BJ, (2006). A test to establish maximum O_2 uptake despite no plateau in the O_2 uptake response to ramp incremental exercise. *J Appl Physiol* **100**, 764-770.

Rossiter HB, Ward SA, Doyle VL, Howe FA, Griffiths JR & Whipp BJ (1999). Inferences from pulmonary O_2 uptake with respect to intramuscular [phosphocreatine] kinetics during moderate exercise in humans. *J Physiol* **518**, 921-932.

Rossiter HB, Ward SA, Kowalchuk JM, Howe FA, Griffiths JR & Whipp BJ (2001). Effects of prior exercise on oxygen uptake and phosphocreatine kinetics during high-intensity knee-extension exercise in humans. *J Physiol* **537**, 291-303.

Roston WL, Whipp BJ, Davis JA, Cunningham DA, Effros RM & Wasserman K (1987). Oxygen uptake kinetics and lactate concentration during exercise in humans. *Am Rev Respir Dis* **135**, 1080-1084.

Spencer MD, Murias JM, Grey TM & Paterson DH (2012). Regulation of VO_2 kinetics by O_2 delivery: insights from acute hypoxia and heavy-intensity priming exercise in young men. *J Appl Physiol* **112**, 1023-1032.

Spencer MD, Murias JM, Kowalchuk JM & Paterson DH (2011). Pulmonary O_2 uptake and muscle deoxygenation kinetics are slowed in the upper compared with lower region of the moderate-intensity exercise domain in older men. *Eur J Appl Physiol* **111**, 2139-2148.

Swanson GD (1980). Breath-to-breath considerations for gas exchange kinetics. In Exercise Bioenergetics and Gas Exchange, ed. Cerretelli P & Whipp BJ, pp. 211-222. Elsevier, Amsterdam.

Timmons JA, Gustafsson T, Sundberg CJ, Jansson E & Greenhaff PL (1998). Muscle acetyl group availability is a major determinant of oxygen deficit in humans during submaximal exercise. *Am J Physiol* **274**, E377-80.

Whipp BJ (1971). Rate constant for the kinetics of oxygen uptake during light exercise. *J Appl Physiol* **30**, 261-263.

Whipp BJ (1994). The slow component of O2 uptake kinetics during heavy exercise. *Med Sci Sports Exerc* **26**, 1319-1326.

Whipp BJ, Davis JA, Torres F & Wasserman K (1981). A test to determine parameters of aerobic function during exercise. *J Appl Physiol Respir Environ Exerc Physiol* **50**, 217-221.

Whipp BJ & Mahler M (1980). Dynamics of pulmonary gas exchange during exercise. In Pulmonary Gas Exchange, Vol II, Organism and Environment, ed. West JB, pp. 33-96. Academic Press, New York.

Whipp BJ, Ward SA, Lamarra N, Davis JA & Wasserman K (1982). Parameters of ventilatory and gas exchange dynamics during exercise. *J Appl Physiol Respir Environ Exerc Physiol* **52**, 1506-1513.

Whipp BJ, Ward SA & Rossiter HB (2005). Pulmonary O_2 uptake during exercise: conflating muscular and cardiovascular responses. *Med Sci Sports Exerc* **37**, 1574-1585.

Whipp BJ & Wasserman K (1972). Oxygen uptake kinetics for various intensities of constant-load work. *J Appl Physiol* **33**, 351-356.

Wilkerson DP & Jones AM (2007). Effects of baseline metabolic rate on pulmonary O_2 uptake on-kinetics during heavy-intensity exercise in humans. *Respir Physiol Neurobiol* **156**, 203-211.

Wilkerson DP & Jones AM (2006). Influence of initial metabolic rate on pulmonary O_2 uptake on-kinetics during severe intensity exercise. *Respir Physiol Neurobiol* **152**, 204-219.

Williams AM, Paterson DH & Kowalchuk JM (2013). High-intensity interval training speeds the adjustment of pulmonary O_2 uptake, but not muscle deoxygenation, during moderate-intensity exercise transitions initiated from low and elevated baseline metabolic rates. *J Appl Physiol* **114**, 1550-1562.

Wilson DF (1994). Factors affecting the rate and energetics of mitochondrial oxidative phosphorylation. *Med Sci Sports Exerc* **26**, 37-43.

Wüst RC, McDonald JR, Sun Y, et al. (2014). Slowed muscle oxygen uptake kinetics with raised metabolism are not dependent on blood flow or recruitment dynamics. *J Physiol* **592**, 1857-71.

Wüst RC, van der Laarse WJ & Rossiter HB (2013). On-off asymmetries in oxygen consumption kinetics of single Xenopus laevis skeletal muscle fibres suggest higher-order control. *J Physiol* **591**, 731-744.

Zoladz JA, Rademaker AC & Sargeant AJ (1995). Non-linear relationship between O_2 uptake and power output at high intensities of exercise in humans. *J Physiol* **488**, 211-217.

CHAPTER II: Breath-by-breath $\dot{V}O_{2p}$ kinetics: effect of data processing on confidence in estimating model parameters

Introduction

Pulmonary oxygen uptake ($\dot{V}O_{2p}$) kinetics describe the rapidity by which muscle O_2 uptake (and mitochondrial oxidative phosphorylation) adjusts to a change in metabolic demand (Grassi *et al*. 1996; Krustrup *et al*. 2009). Measurement of breath-by-breath $\dot{V}O_{2p}$ consequent to step increases in work rate (WR) combined with kinetic modelling of the $\dot{V}O_{2p}$ profile provide a useful method by which the adjustment of muscle oxidative metabolism and the factors along the O_2 transport/utilization pathway that modulate "activation" of muscle oxidative metabolism can be studied, non-invasively, in humans during exercise. In response to a step-increase in WR performed within the moderate-intensity domain (i.e., below the lactate threshold), the profile of the fundamental $\dot{V}O_{2p}$ response, following a brief delay (phase I), increases exponentially (phase II) towards new steady-state (phase III) (Whipp *et al*. 1982). The phase II $\dot{V}O_{2p}$ response is typically characterized by a first-order four parameter model which can easily be applied to any breath-by-breath dataset using the iterative non-linear least squares regression technique.

Inherent in breath-by-breath measurements are non-uniformities in breathing pattern which result in variability (or "noise") around the mean $\dot{V}O_{2p}$ response. The $\dot{V}O_{2p}$ signal-to-noise ratio can vary considerably both within (between repeat trials) and between individuals (Lamarra *et al*. 1987) and therefore, characterization of a phase II $\dot{V}O_{2p}$ profile requires multiple repetitions of a given input signal and averaging of the output responses, which results in a "cleaner", more representative response as the number of repetitions increases (for specific detail see Lamarra *et al*. 1987; Spencer *et al*. 2013b). A mono-

exponential model can be fit to the representative response using a non-linear least squares regression technique from which the phase II parameter estimates are derived. The goodness of fit is most often reported as the 95% confidence interval (CI_{95}) for $\tau\dot{V}O_{2p}$ where a narrower CI_{95} reflects a greater confidence in the model fit and the estimation of the model parameters describing this fit.

In order to combine multiple repetitions various data processing techniques can be used. Typically, after individual trials are time-aligned (such that the onset of the transition begins at a common "start" point – e.g., t = 0 s) data are processed using a number of strategies which may include: linear interpolation to 1-s time intervals, ensemble averaging across trials, and further averaging into larger time bins (e.g., 5-s bins). While different data processing approaches are described in the literature, comparison of these different approaches using a common data set and their effect on the estimation of the model parameters have not been examined in detail. Therefore, it is not clear how results from studies using different data processing strategies can be compared. Furthermore, the influence of using linear interpolation techniques to create second-by-second data from the breath data, especially in the early period of the exercise transition, and thus allow ensemble-averaging of multiple trials, has not been established adequately. For instance, it could be argued that combining and sorting data from different transitions (without any interpolation) could be the most physiological and thus meaningful way of averaging multiple step-transitions; however, this idea has not been tested.

Recent work has investigated the effect of various data treatment methods on optimizing confidence intervals for $\dot{V}O_{2p}$ kinetic parameters (Francescato *et al*. 2014), however these analyses used data that were simulated based on a single theoretical on-

transient $\dot{V}O_{2p}$ response (i.e., fixed model parameter estimates). Furthermore, data were simulated while incorporating a fixed standard deviation of normally distributed $\dot{V}O_{2p}$ noise (100 ml·min^{-1}). While Francescato and colleagues provide some interesting findings with respect to data processing treatment, their findings may not be applicable for $\dot{V}O_{2p}$ kinetic analyses in participants differing in age, fitness, or health status, who exhibit a wide dynamic range of $\dot{V}O_{2p}$ responses, varying degrees of signal-to-noise characteristics and breath-by-breath variability. Given these uncertainties, a systematic analysis examining the effect of data processing technique on parameter estimation and confidence of phase II $\dot{V}O_{2p}$ kinetics seemed warranted. To that aim, data previously collected and published in different studies from a heterogeneous group of young and older participants were re-examined using different data processing methods. Unprocessed data were chosen as the 'gold standard' by which to compare all other techniques because, in theory, it contains the truest physiological response signal. An additional aim was to examine the magnitude and variability of breath-by-breath $\dot{V}O_{2p}$ noise within individuals (between trial repetitions), within age groups (between subjects from a similar age cohort) and between young and older adults.

Methods

Ethical approval. The study was conducted according to the Declaration of Helsinki and all procedures were approved by The University of Western Ontario Research Ethics Board. All participants had volunteered previously and provided written consent to participate in research studies in our laboratory over the past several years.

Participants. Data from nine young (27 ± 7 years, mean ± SD) and nine older men (68 ± 7 years) which had been collected previously and published in different studies were considered for this analysis (Murias *et al*. 2010; Spencer *et al*. 2013a). For the present study, original, raw, and unprocessed data files were selected and re-analyzed using the methods described below. As reported previously, subjects were healthy, non-smokers with no known history of musculoskeletal, respiratory, cardiovascular, and metabolic conditions (see Table 2.1 for subject characteristics).

Exercise Protocol. Each subject reported to the laboratory to perform a fatigue-limited ramp incremental exercise test (with 4 min at 20 W and then a 20 or 25 $W \cdot min^{-1}$ ramp) on a cycle ergometer (model: Excalibur; Lode, Groningen, Netherlands) for determination of peak $\dot{V}O_{2p}$ ($\dot{V}O_{2peak}$), peak work rate (WR_{peak}) and estimated lactate threshold ($\hat{\theta}_L$) (also referred to as the gas exchange threshold). The $\dot{V}O_{2peak}$ was defined as the highest 20-s $\dot{V}O_{2p}$ computed from a rolling average, and WR_{peak} was defined as the final WR achieved at termination of the ramp incremental test. The $\hat{\theta}_L$ was determined by visual inspection using gas exchange and ventilatory indices as the $\dot{V}O_{2p}$ at which CO_2 output ($\dot{V}CO_{2p}$) began to increase out of proportion in relation to $\dot{V}O_{2p}$, with a systematic rise in the minute ventilation ($\dot{V}_E$)-to-$\dot{V}O_{2p}$ relationship and end-tidal PO_2, whereas the ventilatory equivalent of $\dot{V}CO_{2p}$ ($\dot{V}_E$ /$\dot{V}CO_{2p}$) and end-tidal PCO_2 were stable (Beaver *et al*. 1986).

Subjects returned to the laboratory on 4 separate occasions to perform a constant-load, step-transition in WR from a baseline of 20 W cycling to a WR selected to elicit a $\dot{V}O_{2p}$ equivalent to ~90% $\hat{\theta}_L$ for each individual subject; exercise at each WR was maintained for 6 min.

Data Collection. Breath-by-breath gas-exchange measurements similar to those described previously (Babcock *et al*. 1994) were made continuously during each exercise protocol. Briefly, inspired and expired flow rates were measured using a low dead space (90 mL) bidirectional turbine (Alpha Technologies VMM 110) which was calibrated before each test using a syringe of known volume. Inspired and expired gases were sampled continuously (50 Hz) at the mouth and analyzed for concentrations of O_2, CO_2, and N_2 by mass spectrometry (Perkin Elmer MGA-1100 and AMIS 2000) after calibration with precision-analyzed gas mixtures. Changes in gas concentrations were aligned with gas volumes by measuring the time delay for a square-wave bolus of gas passing the turbine to the resulting changes in fractional gas concentrations as measured by the mass spectrometer. Data were transferred to a computer, which aligned concentrations with volume information to build a profile of each breath. Breath-by-breath alveolar gas exchange was calculated by using algorithms of Beaver *et al*. (1981).

Data Processing. Data from individual trials were time-aligned such that the beginning of the on-transient corresponded to zero seconds. Trials were edited and aberrant data laying three standard deviations from the local mean were deleted (Lamarra *et al*. 1987; Rossiter *et al*. 2000). This was accomplished using the non-linear least squares regression method whereby the baseline (fitting window: ~-360 to 0 s) and on-transient (fitting window: ~0 to 360 s) were fit with a linear (slope equal to zero) and mono-exponential function (see below for details), respectively. The 99% prediction bands were used to identify any data points that lay 3 SD from the local mean. Care was taken not to delete data in the early portion of the transition where confidence limits were narrowest.

After individual trials within each subject were edited, like-repetitions were processed using the following techniques: *A*) all breaths from individual trials were combined into a single dataset and sorted by time (time of each breath was recorded to the nearest millisecond); *B*) all breaths from each individual trial were combined into a single dataset, sorted by time, and linearly interpolated on a second-by-second basis; *C*) all breaths from individual trials were combined into a single dataset, sorted by time, linearly interpolated on a second-by-second basis, and averaged into five second time bins; *D*) individual trials were linearly interpolated on a second-by-second basis (using interpolation technique 1: data points joined by straight line segments) and ensemble-averaged; *E*) individual trials were linearly interpolated on a second-by-second basis (interpolation technique 1), ensemble-averaged, and averaged into 5-s time bins; *F*) individual trials were linearly interpolated on a second-by-second basis (using interpolation technique 2: data points copied until next point appears) and ensemble-averaged; *G*) individual trials were linearly interpolated on a second-by-second basis (interpolation technique 2), ensemble-averaged, and averaged into 5-s time bins (see Figure 1 for details).

Data Fitting. The on-transient of each data processing treatment (*A*-*G*), for each individual subject was modelled with the following mono-exponential function:

$$\dot{V}O_{2p}(t) = \dot{V}O_{2pBSL} + A_p \cdot (1 - e^{-(t\text{-}TD)/\tau}) \qquad (2.1)$$

where, $\dot{V}O_{2p}(t)$ is the value of the dependent variable at any time during the transition, $\dot{V}O_{2pBSL}$ is the pre-transition baseline value, A_p is the steady-state increase in $\dot{V}O_{2p}$ (amplitude) above the baseline value, τ is the time constant of the response or the time for $\dot{V}O_{2p}$ to increase to 63% of the $\dot{V}O_{2pSS}$, and TD is the time delay. Phase I was excluded

from the fitting window by progressively moving the window (from ~35s) back towards time zero while examining the flatness of the residual profile and values of CI_{95} (where CI_{95} is equal to the SE [derived from the sum of squared residuals from the model parameter estimates] multiplied by the t-distribution value for the 2.5% two-tailed dimensions). The window that yielded the flattest residuals (visual inspection) and most reduced CI_{95} was considered as the mono-exponential region (Rossiter *et al*. 2001); note there are other methods by which the influence of phase I may be avoided (see Murias *et al.* 2011a). The end of the fitting window was set to ~240s. This value varied depending on visual inspection of the flatness of the residuals and the speed of the on-transient response in order to restrict the modeling to data lying within the transient phase (Bell *et al*. 2001). Once the optimal fitting window was established the non-linear least squares regression analysis was used. In order to improve the confidence in the $\tau\dot{V}O_{2p}$ parameter estimate, model convergence was established with the A_p and TD parameters first allowed to vary. Subsequently, the model was iterated again with fixed values for these parameters. All data editing, processing, and modeling were performed using OriginLab (OriginLab, Northampton, MA).

Noise Analysis. Breath-to-breath fluctuations (i.e., "noise") in the amplitude of $\dot{V}O_{2p}$ were determined for each individual trial so that the variability of breath-to-breath changes could be observed both with-in subjects (across all four trials) and between subjects (across individuals) and subject groups (young versus older). The steady-state $\dot{V}O_{2p}$ corresponding to the 20W cycling baseline (data from -180 to 0 s) and 90% $\hat{\theta}_L$ (data from $t = 4\tau$ + TD to 360 s) were considered for this portion of the analysis using individual edited trials.

"Noise" was estimated from the standard deviation (SD) of all data points within the steady-state window ($ml \cdot min^{-1}$). For each subject, the mean, standard deviation, and coefficient of variation (SD/mean) of the "noise" corresponding to baseline and 90% $\hat{\theta}_L$ steady-state values were calculated. For each group, amplitude histograms and probability-density scatter plots for inter-breath fluctuations in $\dot{V}O_{2p}$ during steady-state at 20 W and 90% $\hat{\theta}_L$ were also computed from values (obtained from each individual trial) corresponding to the instantaneous change in $\dot{V}O_{2p}$ from the mean $\dot{V}O_{2p}$ value normalized with respect to SD. Furthermore, quantile-quantile plots were constructed for each group at baseline and 90% $\hat{\theta}_L$ to inspect whether the $\dot{V}O_{2p}$ noise variability conformed to the characteristics of a standard normal distribution.

Statistical Analysis. Data are presented as means ± SD. A two-way (Age x Data Processing Technique) repeated measures analyses of variance (ANOVA) was used to determine statistical significance for the dependent variables. Bonferroni *post hoc* analyses were used when significant differences were found for the main effects of dependent variables. Pearson's product-moment correlation coefficients were computed in order to quantify the strength of relationships between variables. All statistical analyses were performed using SPSS Version 19.0, (SPSS Inc., Chicago, IL). Statistical significance was accepted at an alpha level less than 0.05.

Results

Subject characteristics, peak exercise, and moderate exercise values are presented in Table 2.1 (mean ± SD). Older adults had a lower ($p<0.05$) $\dot{V}O_{2peak}$, WR_{peak}, $\hat{\theta}_L$, and WR

at 90% $\hat{\theta}_L$ compared to young adults. There was a main effect of age on A_p and $\tau\dot{V}O_{2p}$ (0.56 vs 0.80 $L \cdot min^{-1}$ and 34 vs 21 s for old vs young, respectively, $p<0.05$), while the parameter estimates $\dot{V}O_{2pBSL}$, TD, and CI_{95} were not different between age groups ($p>0.05$).

There were no significant interactions between Age and Data Processing Technique for all dependent variables. Table 2.2 displays the group means (± SD) for all parameter estimates across all data processing techniques (*A*-*G*). There were no main effects of data processing technique on any of the parameter estimates ($p>0.05$), however there was a significant main effect of data processing technique on CI_{95} ($p<0.05$). Multiple comparisons testing yielded a number of significant differences between data processing condition and CI_{95}; these are denoted in Table 2.2. Data processing technique "*D*" yielded the narrowest confidence interval (group mean: 4 s; young: 3 s: older: 5 s) and this was different ($p<0.05$) from all other processing conditions (see Figure 2.2). Furthermore, when compared to condition "*A*" (unprocessed data), the mean CI_{95} for technique "*D*" was ~60% lower (group mean: 4 vs 10 s [see Figure 2.3]; young: 3 vs 8 s; older: 5 vs 11 s) despite displaying no difference in $\tau\dot{V}O_{2p}$ (group mean: 28 vs 27 s [see Figure 2.3]; young: 21 vs 20 s; older: 34 vs 35 s).

The absolute and relative frequency distributions representing the probability of occurrence for specific amplitude-based changes in the $\dot{V}O_{2p}$ noise data are displayed for the young group (Figure 2.4) and older group (Figure 2.5) for the $\dot{V}O_{2p}$ at baseline (panels A and B) and 90% $\hat{\theta}_L$ (panels C and D). The statistics of $\dot{V}O_{2p}$ noise for each subject as well as group means are presented in Table 2.3 (young) and Table 2.4 (older). Quantiles from the standard normal distribution (expected normal) are plotted as a function of the quantiles from the $\dot{V}O_{2p}$ noise distribution (observed value) for each group at baseline and

90% $\hat{\theta}_L$ (Figure 2.6). The linearity of each panel ($r^2 = 1.00$) suggests that each set of $\dot{V}O_{2p}$ noise data are approximately normally distributed.

Table 2.1. Subject characteristics and ramp incremental test results.

	Age (yr)	Mass (kg)	Height (m)	$\dot{V}O_{2peak}$ ($L \cdot min^{-1}$)	$\dot{V}O_{2peak}$ ($mL \cdot kg^{-1} \cdot min^{-1}$)	$\hat{\theta}_L$ ($L \cdot min^{-1}$)	Mod WR (W)
Young (n = 9)	27 ± 7	74 ± 9	1.77 ± 0.08	3.60 ± 0.52	48.4 ± 2.2	1.92 ± 0.29	97 ± 20
Older (n = 9)	68 ± 7*	81 ± 8	1.75 ± 0.06	2.33 ± 0.47*	28.9 ± 6.8*	1.50 ± 0.20*	70 ± 16*

Values are group mean ± SD. * Indicates difference from Young ($p<0.05$).

Table 2.2. Mean parameter estimates and confidence interval of mono-exponential fit for each data processing method (mean ± SD)

		A	B	C	D	E	F	G
Older (n=9)	$\dot{V}O_{2pbsl}$ ($L \cdot min^{-1}$)	0.89 ± 0.08	0.89 ± 0.08	0.89 ± 0.08	0.89 ± 0.08	0.89 ± 0.08	0.89 ± 0.08	0.89 ± 0.08
	A_p ($L \cdot min^{-1}$) †	0.56 ± 0.20	0.56 ± 0.20	0.56 ± 0.20	0.56 ± 0.20	0.56 ± 0.20	0.56 ± 0.20	0.56 ± 0.20
	TD (s)	13 ± 5	14 ± 4	13 ± 4	12 ± 6	12 ± 5	12 ± 6	11 ± 7
	$\tau\dot{V}O_{2p}$ (s) †	34 ± 10	33 ± 9	34 ± 9	35 ± 11	35 ± 10	35 ± 10	35 ± 11
	CI_{95} (s)*	11 ± 5^{d,e,f,g}	10 ± 5^{d,f}	12 ± 8^{d,f}	5 ± 2^{a,b,c,e,f,g}	8 ± 4^{a,d,f}	6 ± 3^{a,b,c,d,e,g}	9 ± 5^{a,d,f}
Young (n=9)	$\dot{V}O_{2pbsl}$ ($L \cdot min^{-1}$)	0.84 ± 0.10	0.84 ± 0.10	0.84 ± 0.10	0.84 ± 0.09	0.84 ± 0.09	0.84 ± 0.09	0.84 ± 0.09
	A_p ($L \cdot min^{-1}$) †	0.80 ± 0.25	0.80 ± 0.24	0.80 ± 0.24	0.80 ± 0.25	0.80 ± 0.25	0.80 ± 0.25	0.80 ± 0.25
	TD (s)	14 ± 3	16 ± 11	15 ± 12	14 ± 4	14 ± 3	13 ± 4	12 ± 4
	$\tau\dot{V}O_{2p}$ (s) †	20 ± 8	22 ± 9	23 ± 9	21 ± 8	21 ± 7	21 ± 8	21 ± 8
	CI_{95} (s)*	8 ± 7^{d,e,f,g}	7 ± 5^{d,f}	8 ± 7^{d,f}	3 ± 2^{a,b,c,e,f,g}	5 ± 3^{a,d,f}	4 ± 3^{a,b,c,d,e,g}	6 ± 4^{a,d,f}

* Indicates a main effect of Data Processing Technique ($p<0.05$). † Indicates main effect of Age ($p<0.05$). There were no significant Age x Data processing Technique interactions. For all model parameter estimates, no differences ($p>0.05$) were found amongst conditions. [a-g] indicate significant differences between data processing techniques for CI_{95} ($p<0.05$).

Table 2.3. Statistics of breath-to-breath fluctuations for $\dot{V}O_{2p}$ amplitude in young healthy subjects

	$\dot{V}O_{2p}$ ($ml \cdot min^{-1}$)	Noise ($ml \cdot min^{-1}$)		
Subject	mean	mean	SD	CV
1	803	87	17	0.20
2	814	101	21	0.21
3	809	121	22	0.18
4	861	149	64	0.43
5	766	99	27	0.27
6	802	96	28	0.29
7	892	118	11	0.09
8	969	179	59	0.33
9	751	123	40	0.33
Avg	**829**	**119**	**32**	**0.26**
Min	**751**	**87**	**11**	**0.09**
Max	**969**	**179**	**64**	**0.43**
	Steady-state at 90% $\hat{\theta}_L$			
1	1896	91	11	0.12
2	1713	136	52	0.38
3	1806	120	10	0.08
4	1409	133	47	0.35
5	1211	115	18	0.16
6	1873	94	24	0.25
7	1451	121	10	0.08
8	1765	314	139	0.44
9	1653	125	53	0.43
Avg	**1642**	**139**	**40**	**0.26**
Min	**1211**	**91**	**10**	**0.08**
Max	**1896**	**314**	**139**	**0.44**

$\dot{V}O_{2p}$ represents the mean steady-state $\dot{V}O_{2p}$ of all four trials during baseline (top) and at 90% $\hat{\theta}_L$ (bottom). "Noise" was calculated as the SD of all breaths during the steady-state of each trial. Statistics of breath-to-breath noise, both within-subject (across all four trials) and between-subjects (bolded font), are displayed. Steady-state $\dot{V}O_{2p}$ and breath-to-breath noise for baseline included data within the last three minutes of a 6-min bout of 20 W cycling. Mean $\dot{V}O_{2p}$ and breath-to-breath noise for 90% $\hat{\theta}_L$ included data within the steady-state only (i.e. 4τ + TD to the end of the 6 minute transition).

Table 2.4. Statistics of breath-to-breath fluctuations for $\dot{V}O_{2p}$ amplitude in healthy older subjects

Steady-state at Baseline

	$\dot{V}O_{2p}$ (ml·min^{-1})	Noise (ml·min^{-1})		
Subject	Mean	mean	SD	CV
1	613	175	144	0.82
2	921	179	11	0.06
3	855	96	11	0.12
4	842	104	24	0.23
5	869	85	10	0.11
6	1018	92	23	0.25
7	929	145	14	0.10
8	809	117	36	0.31
9	754	88	76	0.86
Avg	**846**	**120**	**39**	**0.32**
Min	**613**	**85**	**10**	**0.06**
Max	**1018**	**179**	**144**	**0.86**

Steady-state at 90% $\hat{\theta}_L$

1	1285	108	84	0.78
2	1349	172	24	0.14
3	1416	105	11	0.11
4	1355	102	11	0.11
5	1379	91	16	0.17
6	1374	101	21	0.21
7	1256	125	16	0.13
8	1608	149	37	0.25
9	1213	120	114	0.95
Avg	**1359**	**119**	**37**	**0.32**
Min	**1213**	**91**	**11**	**0.11**
Max	**1608**	**172**	**114**	**0.95**

$\dot{V}O_{2p}$ represents the mean steady-state $\dot{V}O_{2p}$ of all four trials during baseline (top) and at 90% $\hat{\theta}_L$ (bottom). "Noise" was calculated as the SD of all breaths during the steady-state of each trial. Statistics of breath-to-breath noise, both within-subject (across all four trials) and between-subjects (bolded font), are displayed. Steady-state $\dot{V}O_{2p}$ and breath-to-breath noise for baseline included data within the last three minutes of a 6-min bout of 20 W cycling. Mean $\dot{V}O_{2p}$ and breath-to-breath noise for 90% $\hat{\theta}_L$ included data within the steady-state only (i.e. 4τ + TD to the end of the 6 minute transition).

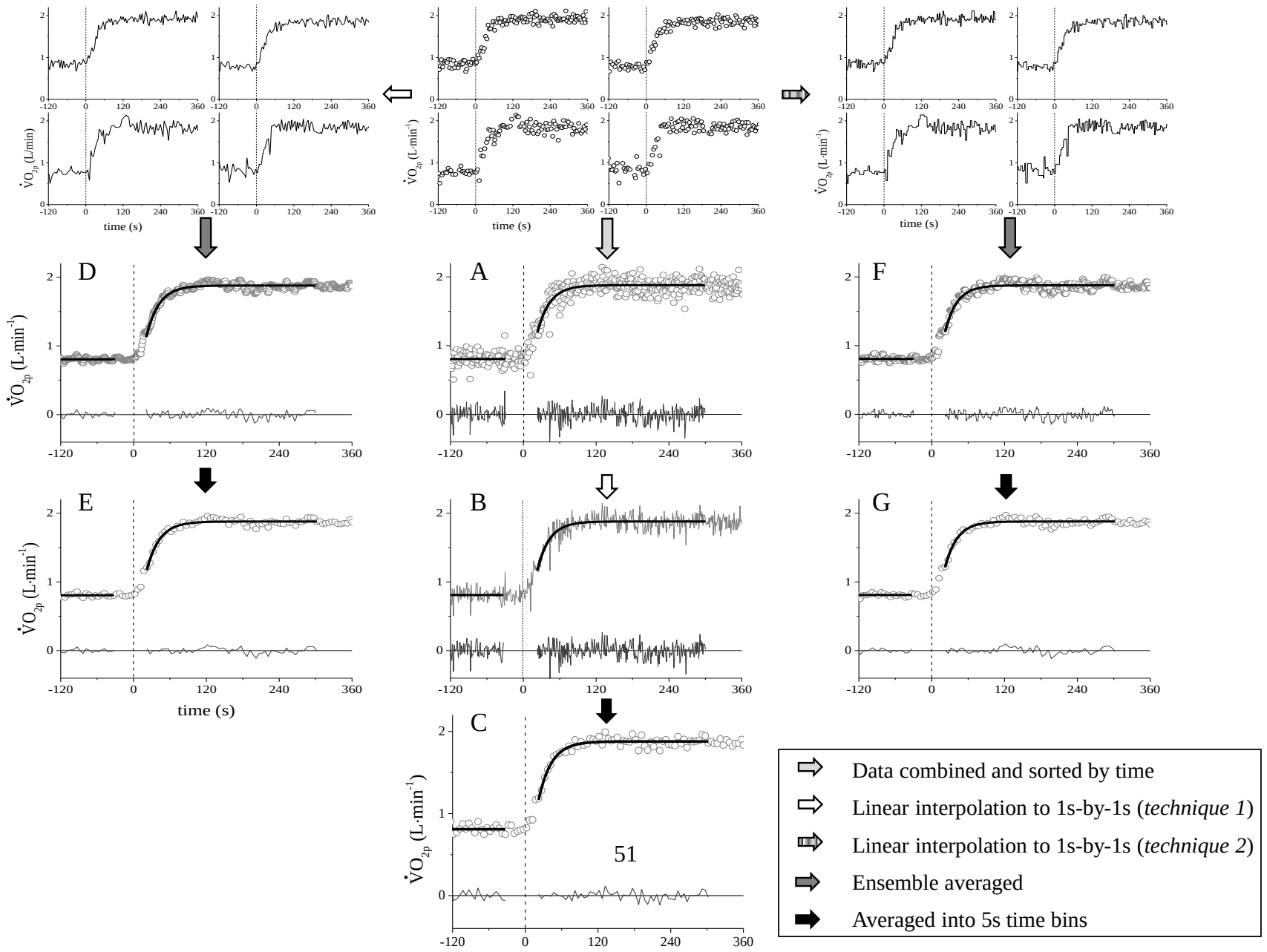
time (s)
D
A
F
E
B
G
C
51
Data combined and sorted by time
Linear interpolation to 1s-by-1s (*technique 1*)
Linear interpolation to 1s-by-1s (*technique 2*)
Ensemble averaged
Averaged into 5s time bins

Figure 2.1. Summary of data processing techniques. *Top middle* panel displays four raw data moderate-step transition trials for a representative individual. Black line represent model best-fits from non-linear least squares regression analyses; dark grey lines represent residuals from imposed fit; dashed line indicates onset of exercise transition; letters identify data processing "condition": **A**) raw data (trials time-aligned, breaths of all trials combined and sorted in time); **B**) raw data + interpolation (trials time-aligned, combined, sorted and linearly-interpolated to s-by-s); **C**) raw data+ interpolation + 5-s bin averaged; **D**) individual trial interpolation + ensemble-averaged (trials time-aligned, linearly-interpolated to s-by-s (technique 1: points joined by straight line segments), ensemble-averaged); **E**) 'D' + 5-sec bin averaged; **F**) individual trial interpolation + ensemble-averaged (trials time-aligned, linearly-interpolated to s-by-s (technique 2: points copied until subsequent point appears), ensemble-averaged); **G**) 'F' + 5-sec bin averaged.

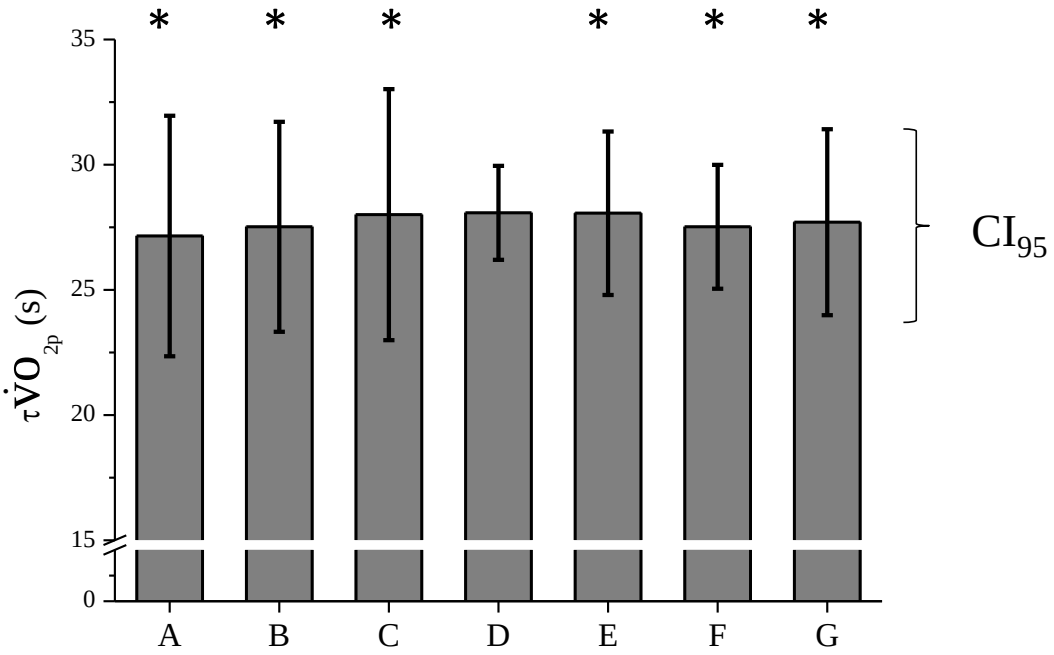

Figure 2.2. $\tau\dot{V}O_{2p}$ values for each data processing technique with 95% confidence interval bars. * denotes significant difference in CI_{95} from condition "*D*", $p<0.05$.

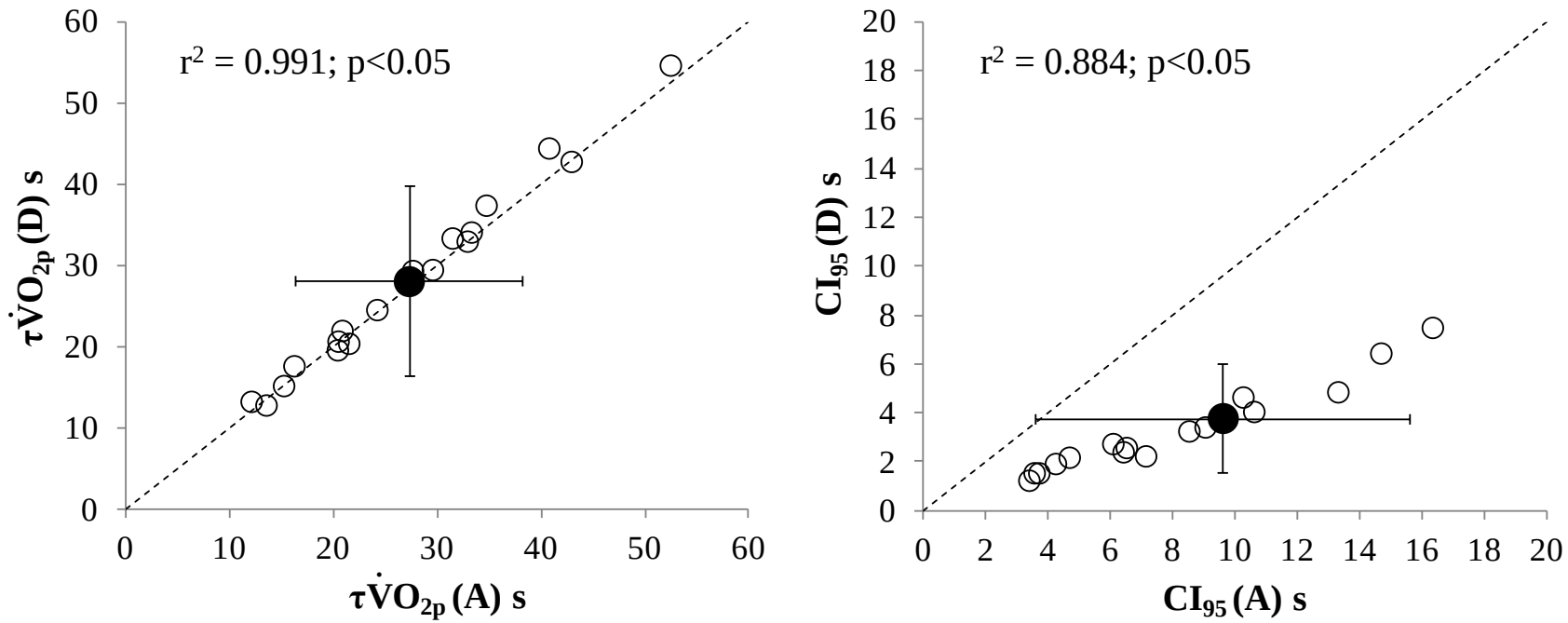

Figure 2.3. Individual $\tau\dot{V}O_{2p}$ and CI_{95} data for "pure" (condition "*A*") versus best "processed" (condition "*D*") data. White circles indicate individual data points; black circles indicate mean value ± SD; dashed diagonal line indicates line of identity (y=x).

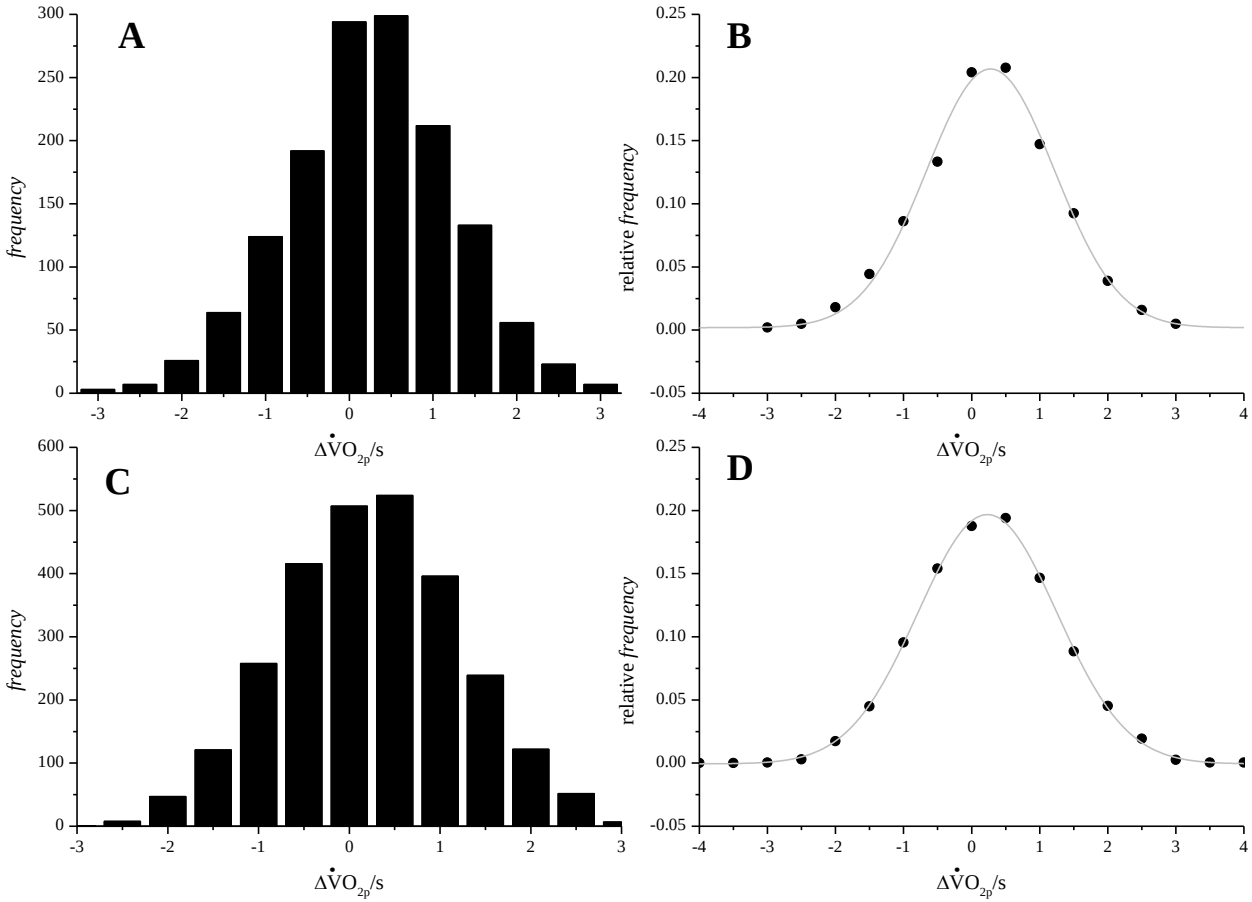
A
B
C
D
frequency
relative frequency
$\Delta\dot{V}O_{2p}$/s

Figure 2.4. Amplitude histogram and probability-density scatter plot for inter-breath fluctuations in $\dot{V}O_{2p}$ during steady-state at 20 W (panels *A* and *B*) and work rate corresponding to 90% of estimated lactate threshold ($\hat{\theta}_L$) (panels *C* and *D*) in young subjects. $\Delta\dot{V}O_{2p}$ represents instantaneous change in $\dot{V}O_{2p}$ from mean $\dot{V}O_{2p}$ value normalized with respect to SD (s). *Black circles* represent relative frequency of inter-breath fluctuations compiled from nine young subjects who each performed four step-transitions; *grey line* represents superimposed Gaussian best-fit model.

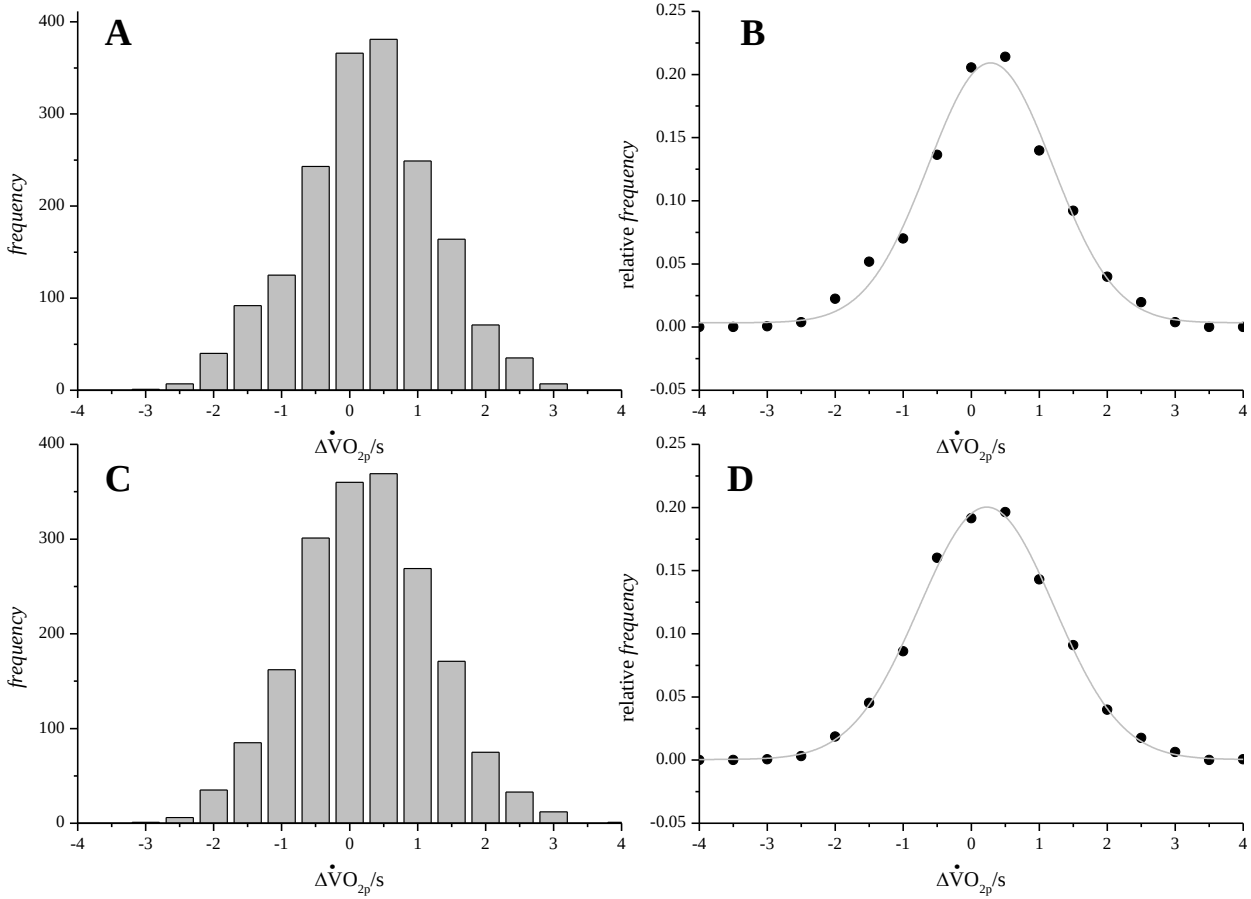
A
B
C
D
frequency
relative frequency
$\Delta\dot{V}O_{2p}$/s

Figure 2.5. Amplitude histogram and probability-density scatter plot for inter-breath fluctuations in $\dot{V}O_{2p}$ during steady-state at 20 W (panels *A* and *B*) and work rate corresponding to 90% of estimated lactate threshold ($\hat{\theta}_L$) (panels *C* and *D*) in older subjects. $\Delta\dot{V}O_{2p}$ represents instantaneous change in $\dot{V}O_{2p}$ from mean $\dot{V}O_{2p}$ value normalized with respect to SD (s). *Black circles* represent relative frequency of inter-breath fluctuations compiled from nine young subjects who each performed four step-transitions; *grey line* represents superimposed Gaussian best-fit model.

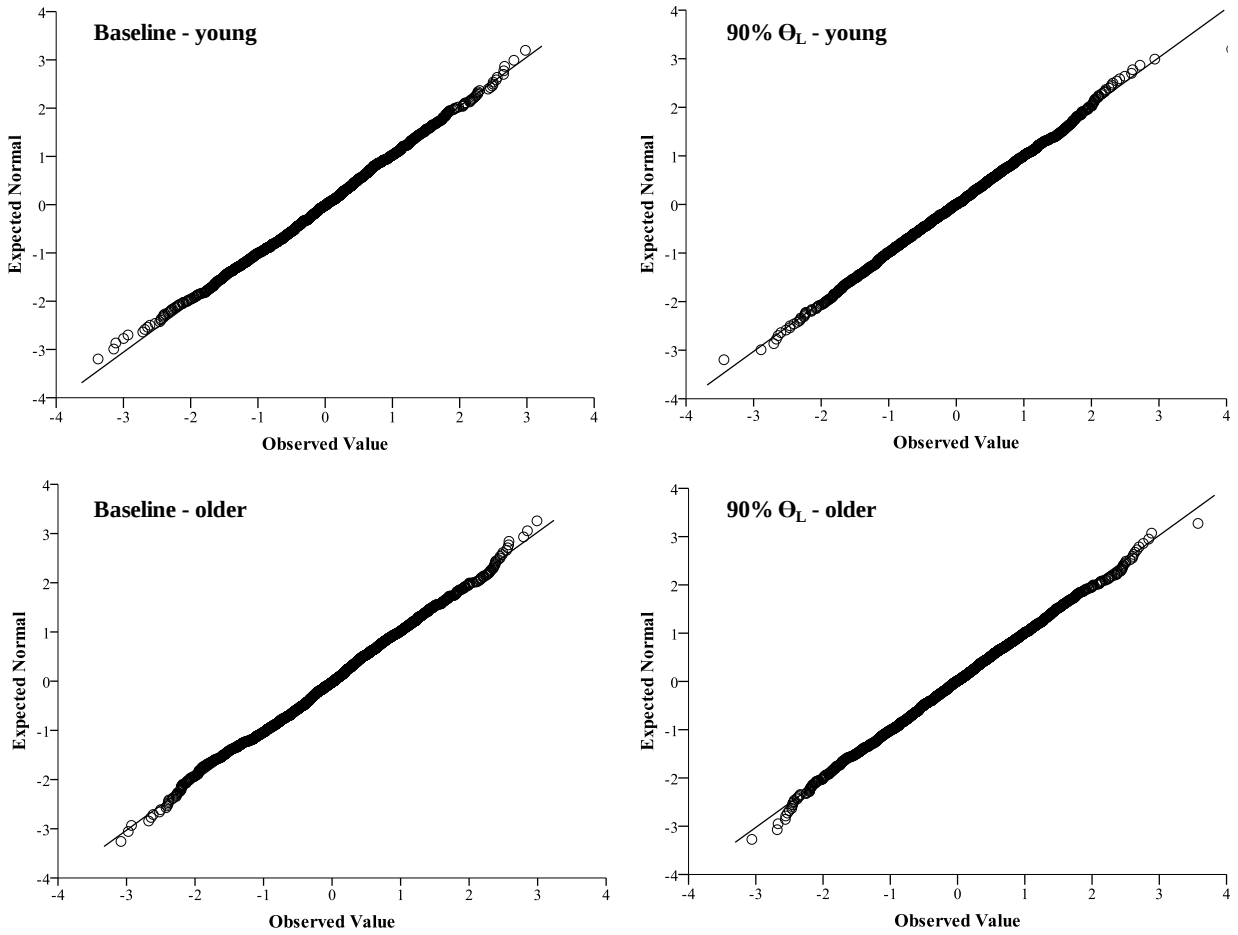
Baseline - young
90% Θ_L - young
Baseline - older
90% Θ_L - older
Expected Normal
Observed Value

Figure 2.6. Quantile – quantile plots of $\dot{V}O_{2p}$ noise distribution for steady-states at 20 W cycling baseline and 90% $\hat{\theta}_L$ for young (*top* panels) and older (*bottom* panels) subjects. Quantiles from the standard normal distribution (expected normal) are plotted as a function of the quantiles from the $\dot{V}O_{2p}$ noise distribution (observed value) for each group. Strong linear relationship for each panel ($r^2 = 1.00$) demonstrates that the data are well approximated by the standard normal distribution. Line indicates perfect matching of population distribution (i.e., standard normal) with sample (i.e., measured data).

Discussion

This study examined the effect of data processing techniques on phase II $\dot{V}O_{2p}$ model parameter estimates and goodness of fit using actual breath-by-breath data collected from a heterogeneous group of healthy young and older subjects. The major finding of this analysis was that data processing technique did not affect the estimation of model parameters but did affect confidence of their estimation such that the goodness of fit (as interpreted from the CI_{95} for $\tau\dot{V}O_{2p}$) could be markedly improved (i.e., a narrower 95% confidence limit) depending on the method by which data were processed prior to modelling. This finding was apparent for both young and older groups despite considerable with-in subject (between trials) and between subjects $\dot{V}O_{2p}$ amplitude noise variability (see noise statistics Table 2.4 and 2.5). Linearly interpolating the data from each individual trial to one-second intervals and ensemble-averaging the individual, interpolated, trials yielded the narrowest confidence interval, while the parameters estimates describing $\dot{V}O_{2p}$ kinetics with this technique did not differ from those estimated using "unprocessed" data (condition *A*).

Given that a number of different data processing approaches can be employed, the literature has largely assumed that these differences do not affect the model parameter estimates. For example, both De Roia *et al*. (2012) and Gurd *et al*. (2009) examined the effect of a priming bout of heavy-intensity exercise on $\dot{V}O_{2p}$ kinetics during a subsequent bout of moderate-intensity exercise in older adults. Whereas De Roia *et al.* (2012) modelled 1-s interpolated and ensemble-averaged data (second-by-second), Gurd *et al.* (2009) modelled 1-s interpolated and ensemble-averaged data that were further averaged into 5-s time bins. In addition, both of these studies utilized different linear-interpolation

techniques. Using these two studies as an example, results from this study strongly indicate that the characterizations of phase II $\dot{V}O_{2p}$ responses from both of these studies are comparable and that the different processing techniques likely did not alter the underlying physiological response signal of their data.

Recently, Francescato *et al*. (2014) examined the effect of various data treatment methods on optimizing confidence intervals for $\dot{V}O_{2p}$ kinetic parameters using simulated data. Their analysis showed that depending on data processing treatment, the confidence intervals obtained from the mono-exponential may be narrower than the actual ones (as dictated by a defined SD for breath-by-breath noise); however the average parameter estimates were generally close to the theoretical values (used to simulate datasets). Whereas, Francescato *et al.* (2014) offered some theoretical insight into $\dot{V}O_{2p}$ data processing strategy, our study utilized actual $\dot{V}O_{2p}$ collected during repeated step-transitions within the moderate-intensity domain, not simulated responses, in groups of young and older adults. Also with the groups of subjects used in the present study, the breath-by-breath "noise" and $\Delta\dot{V}O_{2pSS}$ were highly variable between subjects (rather than "controlled" as occurs in simulated responses). Depending on individual subjects, breath-to-breath $\dot{V}O_{2p}$ fluctuations ranged from 85 $ml \cdot min^{-1}$ to 314 $ml \cdot min^{-1}$, moreover within a given subject (across four trials) the SD of the noise ranged from 10 $ml \cdot min^{-1}$ to 144 $ml \cdot min^{-1}$ (Table 2.3 and 2.4). These results demonstrate considerable between and with-in subject $\dot{V}O_{2p}$ noise variability which are difficult to replicate in simulated data. In combination with the results from Francescato *et al.* (2014), both studies demonstrate that the methods employed to increase the signal-to-noise ratio do not influence the dynamic characteristics of the $\dot{V}O_{2p}$ response.

The magnitude of the $\dot{V}O_{2p}$ signal-to-noise ratio is drastically affected by $\Delta\dot{V}O_{2pSS}$ in response to a step-transition such that smaller amplitudes will result in lower signal-to-noise ratios and greater CI_{95} for $\tau\dot{V}O_{2p}$. This issue is often observed in older individuals (or diseased populations) who have reduced $\dot{V}O_{2max}$ and thus a smaller spectrum of absolute intensity (work rates) by which exercise transitions can be performed within the moderate-intensity domain. For example, in the present study, the mean on-transient A_p was 800 ± 250 ml·min^{-1} (young) and 560 ± 200 ml·min^{-1} (older) and the mean $\dot{V}O_{2p}$ noise associated with the steady-state $\dot{V}O_{2p}$ at 90% $\hat{\theta}_L$ was 139 ml·min^{-1} (young) and 119 ml·min^{-1} (older). If the confidence interval for estimation of $\tau\dot{V}O_{2p}$ from a step-transition is proportional to the SD of inter-breath fluctuations (i.e. noise) divided by the change in $\dot{V}O_{2p}$ steady-state (A_p) (Lamarra *et al*. 1987), it is clear that for an equal number of repetitions CI_{95} will be much larger. In this study, older and young group differences were not apparent; however in Table 2.4 it should be noted that older subjects may present a challenge in model fitting as 2 of the 9 subjects had very high breath "noise" with lower $\dot{V}O_{2p}$ amplitude. Therefore the results of this study are applicable to future work with older adults (or in populations having respiratory, cardiovascular, or metabolic disease) whereby the data processing technique could be selected in order to minimize the number of repetitions and laboratory visits while maximizing the confidence in estimating the phase II $\dot{V}O_{2p}$ kinetics.

Similar to Lamarra *et al.* (1987), the inter-breath $\dot{V}O_{2p}$ fluctuations for a group of young subjects during steady-state cycling at baseline and moderate work rates were well approximated by a Gaussian probability-density function (Figure 2.4 and 2.6). In addition, this study was the first to show that the $\dot{V}O_{2p}$ noise statistics of older adults also were approximated by the standard normal distribution (Figure 2.5 and 2.6). Furthermore,

breath-to-breath fluctuations in $\dot{V}O_{2p}$ appeared to be independent of WR (120 ± 39 ml·min^{-1} and 119 ± 37 ml·min^{-1}, mean ± SD for 20 W and 90% $\hat{\theta}_L$ cycling, respectively) and also did not differ in the younger compared to the older group of subjects (0.32 versus 0.26 for CV, young versus older, respectively; Table 2.3 and 2.4). These results substantiate the notion that the statistics of "noise" are largely independent of WR, but also that the "noise" variance can drastically vary between subjects. However, there does not appear to be a difference in the "noise" characteristics of young and older groups (see mean and range CV for both groups; Tables 2.4 and 2.5) and therefore confidence in estimation of phase II $\dot{V}O_{2p}$ kinetics likely will vary considerably between individuals (regardless of age).

The applicability of these results may extend beyond $\dot{V}O_{2p}$ kinetics to characterizing the behaviour of other biological signals. Indeed similar kinetic analysis has been applied to on-transient behaviour of heart rate and near-infrared spectroscopy-associated parameters (Murias *et al*. 2011b; Spencer *et al*. 2013a) bulk leg blood flow (Chin *et al*. 2013; MacPhee *et al*. 2005), dynamics of microvascular and intracellular PO_2 (Behnke *et al*. 2001; Kindig *et al*. 2003) and vasoactive responses *in vitro* (Murias *et al*. 2013a; Murias *et al*. 2013b). Depending on the inherent noise associated with the measurement of any of these signals, issues with confidence intervals could be addressed *a priori* by selecting a data processing technique that optimizes the confidence in modeling a system's behaviour.

In conclusion, the results of the present study demonstrate that when modeling phase II $\dot{V}O_{2p}$ kinetics, data processing does not influence the parameter estimates describing the response but does increase the "confidence" (indicated by CI_{95}) in estimating $\tau\dot{V}O_{2p}$. The goodness of fit was highest and confidence in parameter estimation

of $\tau\dot{V}O_{2p}$ greatest (i.e., narrowest confidence interval) when the non-linear regression model was applied following linear-interpolation of individual trials and ensemble-averaging.

References

Babcock MA, Paterson DH, Cunningham DA & Dickinson JR (1994). Exercise on-transient gas exchange kinetics are slowed as a function of age. *Med Sci Sports Exerc.* **26**, 440-446.

Beaver WL, Lamarra N & Wasserman K (1981). Breath-by-breath measurement of true alveolar gas exchange. *J Appl Physiol* **51**, 1662-1675.

Beaver WL, Wasserman K & Whipp BJ (1986). A new method for detecting anaerobic threshold by gas exchange. *J Appl Physiol* **60**, 2020-2027.

Behnke BJ, Kindig CA, Musch TI, Koga S & Poole DC (2001). Dynamics of microvascular oxygen pressure across the rest-exercise transition in rat skeletal muscle. *Respir Physiol* **126**, 53-63.

Bell C, Paterson DH, Kowalchuk JM, Padilla J & Cunningham DA (2001). A comparison of modelling techniques used to characterise oxygen uptake kinetics during the on-transient of exercise. *Exp Physiol* **86**, 667-676.

Chin LM, Heigenhauser GJ, Paterson DH & Kowalchuk JM (2013). Effect of voluntary hyperventilation with supplemental CO_2 on pulmonary O_2 uptake and leg blood flow kinetics during moderate-intensity exercise. *Exp Physiol* **98**, 1668-1682.

De Roia G, Pogliaghi S, Adami A, Papadopoulou C & Capelli C (2012). Effects of priming exercise on the speed of adjustment of muscle oxidative metabolism at the onset of moderate-intensity step transitions in older adults. *Am J Physiol Regul Integr Comp Physiol* **302**, R1158-66.

Francescato MP, Cettolo V & Bellio R (2014). Confidence Intervals for the parameters estimated from simulated O_2 uptake kinetics: effects of different data treatments. *Exp Physiol* **99**, 187-195.

Grassi B, Poole DC, Richardson RS, Knight DR, Erickson BK & Wagner PD (1996). Muscle O_2 uptake kinetics in humans: implications for metabolic control. *J Appl Physiol* **80**, 988-998.

Gurd BJ, Peters SJ, Heigenhauser GJ, *et al.* (2009). Prior heavy exercise elevates pyruvate dehydrogenase activity and muscle oxygenation and speeds O_2 uptake kinetics during moderate exercise in older adults. *Am J Physiol Regul Integr Comp Physiol* **297**, R877-84.

Kindig CA, Kelley KM, Howlett RA, Stary CM & Hogan MC (2003). Assessment of O_2 uptake dynamics in isolated single skeletal myocytes. *J Appl Physiol* **94**, 353-357.

Krustrup P, Jones AM, Wilkerson DP, Calbet JA & Bangsbo J (2009). Muscular and pulmonary O_2 uptake kinetics during moderate- and high-intensity sub-maximal knee-extensor exercise in humans. *J Physiol* **587**, 1843-1856.

Lamarra N, Whipp BJ, Ward SA & Wasserman K (1987). Effect of interbreath fluctuations on characterizing exercise gas exchange kinetics. *J Appl Physiol* **62**, 2003-2012.

MacPhee SL, Shoemaker JK, Paterson DH & Kowalchuk JM (2005). Kinetics of O_2 uptake, leg blood flow, and muscle deoxygenation are slowed in the upper compared with lower region of the moderate-intensity exercise domain. *J Appl Physiol* **99**, 1822-1834.

Murias JM, Campos OA, Hall KE, McDonald MW, Melling CW & Noble EG (2013a). Vessel-specific rate of vasorelaxation is slower in diabetic rats. *Diab Vasc Dis Res* **10**, 179-186.

Murias JM, Dey A, Campos OA, *et al.* (2013b). High-intensity endurance training results in faster vessel-specific rate of vasorelaxation in type 1 diabetic rats. *PLoS One* **8**, e59678.

Murias JM, Kowalchuk JM & Paterson DH, (2011). Speeding of VO_2 kinetics in response to endurance-training in older and young women. *Eur J Appl Physiol* **111**, 235-243.

Murias JM, Kowalchuk JM & Paterson DH (2010). Speeding of VO_2 kinetics with endurance training in old and young men is associated with improved matching of local O_2 delivery to muscle O_2 utilization. *J Appl Physiol* **108**, 913-922.

Murias JM, Spencer MD, Kowalchuk JM & Paterson DH (2011). Influence of phase I duration on phase II VO_2 kinetics parameter estimates in older and young adults. *Am J Physiol Regul Integr Comp Physiol* **301**, R218-24.

Rossiter HB, Howe FA, Ward SA, Kowalchuk JM, Griffiths JR & Whipp BJ (2000). Intersample fluctuations in phosphocreatine concentration determined by 31P-magnetic resonance spectroscopy and parameter estimation of metabolic responses to exercise in humans. *J Physiol* **528 Pt 2**, 359-369.

Rossiter HB, Ward SA, Kowalchuk JM, Howe FA, Griffiths JR & Whipp BJ (2001). Effects of prior exercise on oxygen uptake and phosphocreatine kinetics during high-intensity knee-extension exercise in humans. *J Physiol* **537**, 291-303.

Spencer MD, Keir DA, Nederveen JP, Murias JM, Kowalchuk JM & Paterson DH (2013a). Prolonged moderate-intensity exercise oxygen uptake response following heavy-intensity priming exercise with short- and longer-term recovery. *Appl Physiol Nutr Metab* **38**, 566-573.

Spencer MD, Murias JM, Kowalchuk JM & Paterson DH (2013b). Effect of moderate-intensity work rate increment on phase II tauVO_2, functional gain and Delta[HHb]. *Eur J Appl Physiol* **113**, 545-557.

Whipp BJ, Ward SA, Lamarra N, Davis JA & Wasserman K (1982). Parameters of ventilatory and gas exchange dynamics during exercise. *J Appl Physiol Respir Environ Exerc Physiol* **52**, 1506-1513.

CHAPTER III: The influence of metabolic and circulatory heterogeneity on the expression of pulmonary $\dot{V}O_2$ kinetics in humans

Introduction

After a step-change in moderate-intensity exercise work rate (WR) (i.e., below the lactate threshold), pulmonary O_2 uptake ($\dot{V}O_{2p}$) increases in an exponential-like manner towards a new steady-state O_2 requirement following a brief cardiodynamic period (phase I). The exponential increase in $\dot{V}O_{2p}$ (phase II) is closely associated with the dynamic adjustment of skeletal muscle $\dot{V}O_2$ ($\dot{V}O_{2m}$) (Barstow *et al.* 1990; Grassi *et al.* 1996; Krustrup *et al.* 2009) and is characterized by both its rate (quantified by the time constant for $\dot{V}O_{2p}$ [$\tau\dot{V}O_{2p}$]) and amplitude (quantified by the functional $\dot{V}O_{2p}$ gain [G_P: $\Delta\dot{V}O_{2p}/\Delta WR$]) (Whipp *et al.* 1982).

During exercise initiated from a common, low, baseline WR, both phase II $\tau\dot{V}O_{2p}$ and G_P are invariant, and independent of the subsequent moderate-intensity WR performed (Özyener *et al.* 2001; Spencer *et al.* 2013). This kinetic behavior implies that phase II $\dot{V}O_{2p}$ kinetics are consequent to a first order rate reaction; specifically, linked, to mitochondrial ADP feedback (Rossiter, 2011; Wüst *et al.* 2011). However, when exercise is initiated from a raised baseline WR and metabolic rate, $\dot{V}O_{2p}$ kinetics are slowed: both $\tau\dot{V}O_{2p}$ and G_P are increased (Brittain *et al.* 2001; MacPhee *et al.* 2005; Spencer *et al.* 2011; Bowen *et al.* 2011; Williams *et al.* 2013; Keir *et al.* 2014). This behavior was suggested to be evidence that $\dot{V}O_{2p}$ kinetics do not conform to a first order rate reaction (Robergs, 2014). However, others interpreted this kinetic slowing to be reflective of the physiological properties of the activated musculature (Brittain *et al.* 2001), where individual fibers operate through a first-order ADP-feedback reaction, but where mitochondrial volume-density differs among the

activated muscle fibers (Rossiter, 2011). In other words, preferential activation of highly oxidative muscle fibers at low baseline WR will have inherently faster $\dot{V}O_{2p}$ kinetics than less-oxidative fibers activated at higher work rates; yet within each fiber $\dot{V}O_{2p}$ kinetics are first order (Brittain *et al.* 2001).

Recently, Keir *et al.* (2014) reported that moderate-intensity $\dot{V}O_{2p}$ kinetics were strongly related to baseline metabolic rate, but not to the baseline WR or the magnitude of the increase in WR during the exercise bout (ΔWR). This suggested that the intramuscular metabolic status (e.g. [ADP]/[ATP], and/or free energy of ATP), rather than kinetic characteristics of the recruited motor units, influence $\dot{V}O_{2p}$ kinetics; a conclusion supported by Bowen *et al.* (2011) using a model of incomplete muscle recovery, and by Wüst *et al.* (2014) with exercise transitions in electrically-stimulated dog hind limb muscle. However, DiMenna *et al.* (2010), using high-intensity exercise, found that baseline metabolic rate did not influence subsequent $\dot{V}O_{2p}$ kinetics, supporting the recruitment hypothesis.

To shed light on this controversy we aimed to determine the relationship between baseline metabolic rate and $\dot{V}O_{2p}$ kinetics during exercise initiated from several different rates of baseline metabolism, each using an identical work rate increment (ΔWR) within the moderate-intensity domain; previous investigations having used only two different baseline work rates. This would allow us to determine whether $\dot{V}O_{2p}$ kinetics are slowed in relation to baseline $\dot{V}O_{2p}$. Additionally, to account for potential confounding effects of regional O_2 delivery on muscle $\dot{V}O_{2p}$ (Hughson & Morrissey, 1982; MacPhee *et al.* 2005; Koga *et al.* 2007; Wüst *et al.* 2014), we simultaneously measured regional muscle deoxygenation (hemoglobin (Hb) + myoglobin (Mb); hereafter referred to as "[HHb]") by near-infrared spectroscopy, which reflects the relationship between microvascular O_2

delivery to O_2 utilization (Murias *et al.* 2014). In addition, it is well understood that $\dot{V}O_{2m}$ kinetics can be modulated by circulatory dynamics on transition to their pulmonary expression as phase II $\dot{V}O_{2p}$ (Hoffmann *et al.* 2013; Benson *et al.* 2013). To account for this we used a previously validated circulatory model (Benson *et al.* 2013) to determine whether a dissociation between $\dot{V}O_{2m}$ and phase II $\dot{V}O_{2p}$ kinetics – via circulatory dynamics – could explain a progressive slowing of $\dot{V}O_{2p}$ kinetics with progressively greater baseline work rate.

Thus, the purpose of this study was to determine in the same participants: 1) $\dot{V}O_{2p}$ and [HHb] kinetics over a range of moderate-intensity WR increments initiated from a constant baseline metabolic rate, i.e., the same baseline metabolism with variable ΔWR (constant baseline condition); 2) the relationship between baseline metabolic rate and $\dot{V}O_{2p}$ and [HHb] kinetics for a constant WR increment within the moderate-intensity domain, i.e., variable baseline metabolism with the same ΔWR (variable baseline condition); and 3) the extent to which circulatory dynamics may contribute to the slowed $\dot{V}O_{2p}$ kinetics from progressively increasing baseline metabolic rate. We hypothesized that, unlike in the constant baseline condition, in the variable baseline condition $\tau\dot{V}O_{2p}$ and G_P would increase linearly with baseline $\dot{V}O_{2p}$ independent of [HHb] dynamics, and that these differences could not be explained by circulatory modulation of muscle $\dot{V}O_2$ kinetics. Accepting this hypothesis would suggest an association between instantaneous muscle metabolism and $\tau\dot{V}O_{2p}$ and G_P in moderate intensity exercise, which is inconsistent with simple first order kinetic control theory.

Methods

Ethical approval. The study was conducted according to the Declaration of Helsinki and all procedures were approved by The University of Western Ontario Ethics Committee for Research on Human Subjects. All participants volunteered and gave informed written consent to participate in the study.

Participants. Fourteen healthy young adult men (mean ± SD values: age, 24 ± 3 yrs; body mass, 83 ± 5 kg; height, 180 ± 8 cm; $\dot{V}O_{2peak}$, 48.1 ± 5.9 $mL \cdot kg^{-1} \cdot min^{-1}$) volunteered for the study. All participants were non-smokers who were free of any known musculoskeletal, respiratory, cardiovascular, and metabolic conditions, and who were not taking any medications that might influence cardiorespiratory or metabolic responses to exercise. Participants were selected on the basis that their WR at the estimate lactate threshold ($\hat{\theta}_L$) was at least 130 W, allowing all step-transitions used in the protocol to begin within the moderate-intensity domain.

Ramp Incremental Exercise. Each participant reported to the laboratory to perform a symptom-limited ramp incremental (RI) exercise test (20 W baseline for 4 min followed by a 25 $W \cdot min^{-1}$ ramp) on a magnetically-braked cycle ergometer (model: Velotron, RacerMate Inc., Seattle, WA, USA) for determination of peak $\dot{V}O_{2p}$ ($\dot{V}O_{2peak}$) and peak WR (WR_{peak}). Participants were asked to maintain a cadence of ~60 rpm during the test. $\dot{V}O_{2peak}$ was defined as the greatest 20 s $\dot{V}O_{2p}$ computed from a rolling average and WR_{peak} was defined as the WR achieved at termination of the RI test. Additionally, the $\hat{\theta}_L$ was

determined by visual inspection using standard ventilatory and gas exchange indices as previously described (Beaver *et al.* 1986).

Constant Work Rate Exercise Protocols. Participants performed 3-5 repetitions of 40W step-increments (i.e., Δ40) from a baseline WR of 20, 40, 60, 80, 100, and 120 W (i.e., variable baseline condition). Step-transitions were 6 min of baseline WR followed by an instantaneous step-increase in WR to 40 W above the baseline for 6 min. With the exception of the step-transitions from 20 W and 40 W, all other transitions were preceded by 6 min of baseline cycling at 20 W, which provided an opportunity to examine step-transitions from a common 20 W baseline and different WR increments (i.e., Δ40, Δ60, Δ80, Δ100; constant baseline condition). Therefore, one-third of the exercise protocols were 12 min in duration (those initiated from 20 and 40 W) and the other two-thirds were 18 min. A maximum of two exercise protocols were completed per visit with a minimum of 20 min seated rest between exercise bouts. For each participant, the sequence of exercise protocols was randomized in a counterbalanced order and it was assumed that exercise duration did not affect physiological outcome measures.

Data Collection. During each trial participants wore a noseclip and breathed through a mouthpiece for breath-by-breath gas-exchange measurements. Inspired and expired volumes and flow rates were measured using a low dead space (90 mL) bidirectional turbine (Alpha Technologies, VMM 110) and pneumotach (Hans Rudolph, Model 4813) positioned in series from the mouthpiece (total apparatus dead space was 150 mL); respired air was continuously sampled at the mouth and analysed by mass spectrometry (Innovision,

AMIS 2000, Lindvedvej, Denmark) for fractional concentrations of O_2 and CO_2. The volume turbine was calibrated before each test using a syringe of known volume (3 L) over a range of flow rates and the pneumotach was adjusted for zero flow. Gas concentrations were calibrated with precision-analyzed gas mixtures. The time delay between an instantaneous, square-wave change in fractional gas concentration at the sampling inlet and its detection by the mass spectrometer was measured electronically by computer. Respiratory volumes, flow, and gas concentrations were recorded in real-time used to build a profile of each breath. Alveolar gas exchange was calculated on a breath-by-breath basis using the algorithms of Swanson (1980).

Local muscle deoxygenation ([HHb]) of the quadriceps *vastus lateralis* muscle was measured using a frequency domain multi-distance near-infrared spectroscopy (NIRS) system (Oxiplex TS, Model 92505, ISS, Champaign, USA) as described elsewhere (Spencer *et al.* 2012). Briefly, the system was comprised of a single channel consisting of eight laser diodes operating at two wavelengths (λ = 690 and 828 nm, four at each wavelength) that were pulsed in a rapid succession down a photomultiplier tube. A rigid plastic NIRS probe (connected to laser diodes and photomultiplier tube by optical fibers) consisted of two parallel rows of light emitter fibers and one detector fiber bundle; the source-detector separations for this probe were 2.0, 2.5, 3.0, and 3.5 cm for both wavelengths. The probe was placed on the belly of the muscle, at the distal end of the *vastus lateralis* muscle. NIRS measurements were collected continuously for the entire duration of each trial. The NIRS was calibrated at the beginning of each testing session following an instrument warm-up period of at least 20 min. Throughout each testing session, continuous measurements of the absolute scattering (μ_s) and absorption (μ_a) coefficients

for each wavelength were determined by measuring the intensity of modulated light entering and traversing the tissue (determined from the average component of the modulated light waves [DC], amplitude of the modulation [AC], and the phase shift [Φ] between those two signals) at the four source - detector distances (R). The coefficients of AC and Φ were plotted as a function of distance R at both wavelengths to determine μ_s and μ_a, which were used to resolve the absolute concentrations of HHb (in μM) using the Beer-Lambert equation. Data were stored online at an output frequency of 25 Hz, but were reduced to 1 s bins for all subsequent analyses.

Data Analysis. Breath-by-breath $\dot{V}O_{2p}$ data were edited on an individual basis by removing aberrant data that lay 3 SD from the local mean (Lamarra *et al.*, 1987). Within each participant, like-repetitions were linearly interpolated on a second-by-second basis, ensemble-averaged and time-aligned such that time "zero" represented the onset of the transition. The on-transient of each profile was modeled with the following mono-exponential function:

$$y(t) = y_{BSL} + A \cdot (1 - e^{-(t\text{-}TD)/\tau}) \qquad (3.1)$$

where, $y(t)$ is the value of the dependent variable at any time during the transition, y_{BSL} is the pre-transition baseline value (determined from the ~60 s before a transition), A is the steady-state increase in y above the baseline value, TD is the time delay, and τ is the time constant of the response (or the time for y to increase to 63% of the new steady-state after TD). The functional gain (G_P: $\Delta\dot{V}O_{2p}/\Delta WR$) of the response was determined by dividing A (in $mL \cdot min^{-1}$) by the change in WR (in W). Data were fit using the Levenberg-Marquardt algorithm to find the minimum sum of squared residuals between the mono-exponential

function and the experimental data (using Origin 8.5; OriginLab, Northampton, MA). The end of the fitting window was set to ~ 5 times the estimated time constant in order to restrict the modeling to data lying within the transient phase. For those individuals who transitioned into the heavy-intensity domain, the end of the phase II fitting window was determined by examining the change in τ, CI_{95}, χ^2, and plotted residuals in response to progressive increases in the end of the fitting window. The point immediately preceding a systematic increase in τ, CI_{95}, and χ^2 was considered as the end of phase II. The mean response time (MRT-$\dot{V}O_{2p}$) of $\dot{V}O_{2p}$ was characterized from a fit of the $\dot{V}O_{2p}$ response from t=0 to the end of the exercise

The TD for the [HHb] ([HHb]-TD) response was determined using second-by-second data and corresponded to the time, after the onset of exercise, at which the [HHb] signal increased above 1 SD of the pre-transition baseline value. Determination of the [HHb]-TD was made on each individual's ensemble-averaged response and the data were modeled using equation 1. Different fitting strategies ranging from 90-180 s into a transition resulted in minimal differences in estimates of τ[HHb]. The MRT for [HHb] (MRT-[HHb]) described the overall time for [HHb] to increase from the start of exercise to 63% of the "steady-state" value and was calculated as the sum of τ[HHb] and [HHb]-TD.

In silico simulations. The validated multi-compartmental model (MCM) of Benson *et al.* (2013) was used to investigate the dissociation between muscle and pulmonary $\dot{V}O_2$ kinetics. Briefly, mathematical expressions for O_2 delivery ($\dot{Q}$), muscle O_2 uptake, and a lumped compartment representing the rest of the body were joined in parallel by a single

arterial compartment and multiple compartments on the venous side (representing blood draining the muscle, the rest of the body, and a mixed compartment approximating the blood volume proximal to the common femoral veins). The fractions of total metabolic rate (from muscle: 0.57; from body 0.43), cardiac output ($\dot{Q}_{tot}$; to muscle: 0.57; to body 0.43) and venous blood volume associated with muscle (0.7 L), body (0.1 L), and mixed compartments (2.3 L) were fixed while the WR and kinetic variables for muscle and body $\dot{Q}$ ($\dot{Q}_m$ and $\dot{Q}_b$) and $\dot{V}O_2$ ($\dot{V}O_{2m}$ and $\dot{V}O_{2b}$) were manipulated experimentally to mimic the pre-transition conditions of the *in vivo* experiments and predict phase I and phase II $\dot{V}O_{2p}$ kinetics. The output of the model was instantaneous $\dot{V}O_{2p}(t)$:

$$\dot{V}O_{2p}(t) = \dot{Q}_{tot}(t) \cdot (C_aO_2 - C_{\bar{v}}O_2)(t) \quad (3.2)$$

where C_aO_2 is arterial content (fixed to 20 mL O_2 per 100 mL of blood), $C_{\bar{v}}O_2$ is mixed venous O_2 content, and $\dot{Q}_{tot}$ is cardiac output. During the simulated exercise step-transitions, $\dot{Q}_m$ and $\dot{V}O_{2m}$ increased exponentially according to equation 3.1 (with TD = 0), toward their WR-dependent steady-state values with a steady-state relationship of 6 $L \cdot min^{-1}$ per 1 $L \cdot min^{-1}$ of $\dot{V}O_2$. The intercept of the $\dot{Q}_{tot}$-to-$\dot{V}O_2$ relationship was set to 3.6 $L \cdot min^{-1}$ (Benson *et al.* 2013). Values of $\dot{V}O_2$ were dependent on WR inputs and functional gains (i.e., $\Delta\dot{V}O_2/\Delta W$) of 9.5, 11.0, and -1.5 $mL \cdot min^{-1} \cdot W^{-1}$ for $\dot{V}O_{2p}$, $\dot{V}O_{2m}$, and $\dot{V}O_{2b}$, respectively as previously described (Benson *et al.* 2013). Values for $\dot{Q}$ in the various compartments were based on the aforementioned $\dot{Q}$-to-$\dot{V}O_2$ relationship.

Essentially, the MCM links two theoretical compartments representing the "muscle" and "rest-of-body" via a single venous volume (V_v) to the pulmonary circulation. In this model, muscle and body venous effluents travel down a separate V_v before both are mixed in a flow-weighted manner on transit to the lung (see schematic Figure 3.1). The

input to the model is a WR profile (i.e., a step-change). The change in $\dot{V}O_{2m}$ is determined by the functional gain (9.5 $mL \cdot min^{-1} \cdot W^{-1}$) and the change in $\dot{Q}_m$ is then determined by the $\dot{Q}$-to-$\dot{V}O_2$ relationship (i.e., a linear relationship with a slope of 6.0 and a y-intercept of 3.6 $L \cdot min^{-1}$). The manner by which $\dot{V}O_{2m}$ and $\dot{Q}_{tot}$ get to their respective new steady-state values is determined by their kinetics, which are inputted as parameters to the model. In this way, the model can predict the $\dot{V}O_{2p}$ and be used to investigate how different circulatory conditions in specific conditions (i.e., increasing baseline WR or WR increment) may contribute to dissociations between $\dot{V}O_2$ kinetics between muscle and lung.

Exercise was simulated for moderate-intensity transitions by specifying a step-change in WR. Initially, the steady-state $\dot{V}O_{2p}$ baseline for 20 W was set to 0.75 $L \cdot min^{-1}$ and $\tau\dot{V}O_{2m}$ and $\tau\dot{Q}_m$ were modulated in order to generate a $\tau\dot{V}O_{2p}$ value that corresponded to the group mean $\tau\dot{V}O_{2p}$ from the 20 W to 60 W step. Thereafter, simulations were done for Δ40W step-changes from 40, 60, 80, 100, and 120 W and for Δ60W, Δ80W, and Δ100W step-changes from 20 W with fixed parameter inputs for $\tau\dot{V}O_{2m}$ and $\tau\dot{Q}_m$ in order to determine the degree by which circulatory dynamics modulate the dynamics of $\dot{V}O_{2p}$ at a constant $\tau\dot{V}O_{2m}$ and varying moderate-intensity baseline WR and WR increments. In addition, simulations were produced to examine the influence of slowing $\dot{Q}_m$ dynamics on the $\dot{V}O_{2p}$ profile; for each of the Δ40W step-changes, $\tau\dot{V}O_{2m}$ was fixed to each of 20, 30, and 40 s, and a series of simulations of $\dot{V}O_{2p}$ was produced where $\tau\dot{Q}_m$ was varied (MacPhee *et al.* 2005). In all experimental conditions, the phase II region of the $\dot{V}O_{2p}$ output from the simulations was fitted to equation 1, with the end of phase I being identified precisely from the profile of simulated $C_{\bar{v}}O_2$.

To investigate how the homogenized $\dot{V}O_{2p}$ response to a step-change in WR from 20 to 120 W may be influenced by multiple muscle compartments with heterogeneous metabolic and circulatory dynamics, the group mean dynamic responses of $\dot{V}O_{2p}$ and [HHb] from each of the equal WR increment steps (variable baseline condition) were used to infer the $\dot{V}O_{2m}$ and $\dot{Q}_m$ kinetics of six theoretical muscle compartments ($\tau\dot{V}O_{2m}$ = 15, 20, 25, 30, 35, 40 s and $\tau\dot{Q}_m$ = 20, 25, 30, 35, 40, 45 s for compartments 1 – 6, respectively) assuming that both $\tau\dot{V}O_{2m}$ and $\tau\dot{Q}_m$ linearly increase as a function of WR (see Figure 3.2 for multi-muscle compartment MCM). Assuming simultaneous activation and equal contributions of each of the six compartments, the homogenized $\dot{V}O_{2p}$ response to a step-change in WR from 20 to 120 W was simulated for each compartment and combined into a single homogenized response. The averaged $\dot{V}O_{2p}$ output was modeled as previously mentioned and kinetics were compared to the actual group mean $\dot{V}O_{2p}$ response to the step-change in WR from 20 to 120 W.

Statistical Analysis. Data are presented as means ± SD. A one-way analysis of variance (ANOVA) for repeated measures was used to compare kinetic parameters and variables between conditions. Where significant main effects were found, a Tukey's *post hoc* analysis was performed for multiple comparisons testing. All statistical analyses were performed using SigmaPlot Version 11.0, (Systat Software Inc., San Jose, CA). Statistical significance was accepted at an alpha level of 5%.

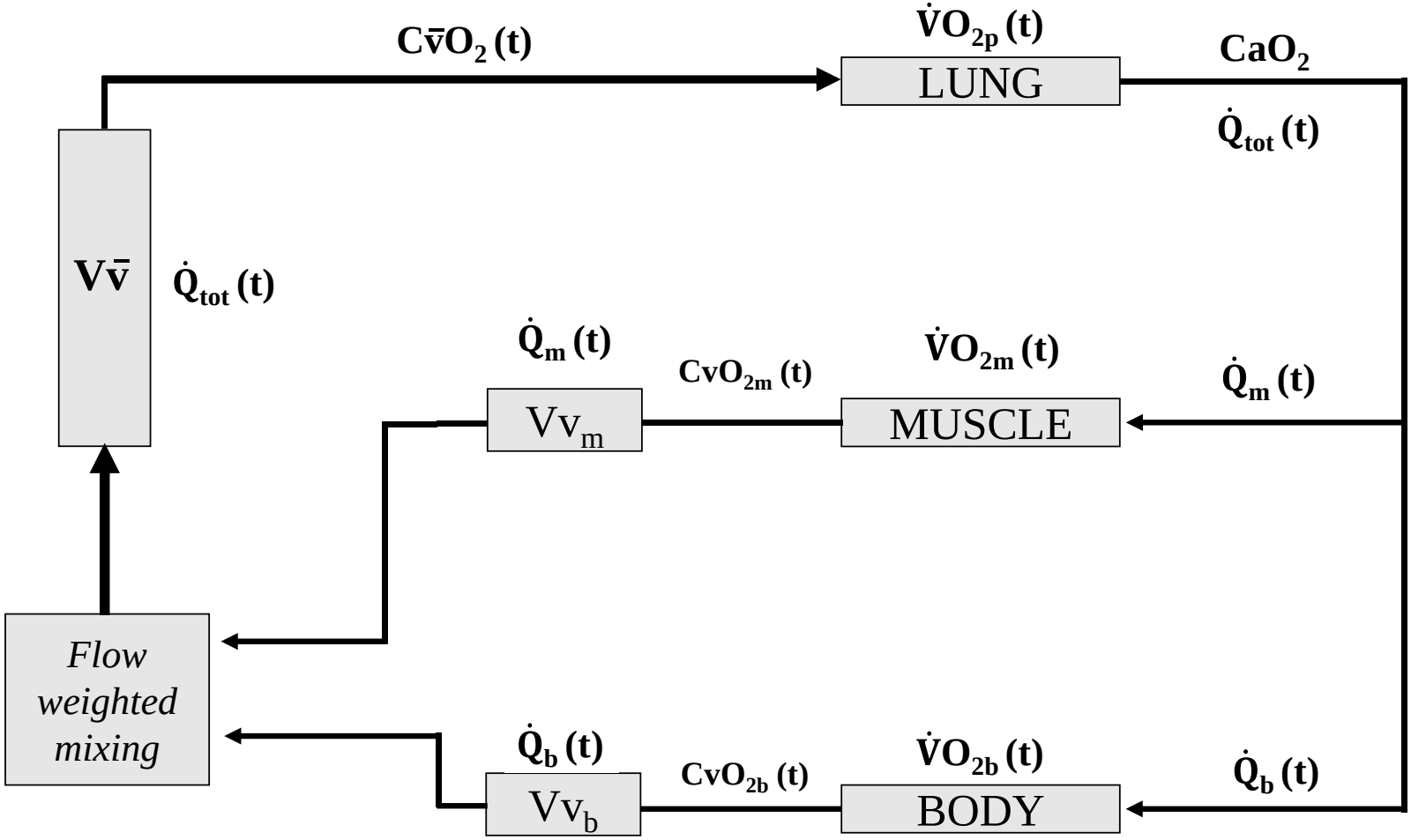

Figure 3.1. Schematic of the multi-compartment model (MCM; adapted from Benson *et al.* (2013)), where muscle and body venous effluents travel down separate venous volumes (V_V; i.e., V_{Vm} (muscle) and V_{Vb} (body) respectively) before flow-weighted mixing occurs. The MCM default parameters are provided in text. The output of the model is $\dot{V}O_{2p}$. See text also for abbreviations and model details.

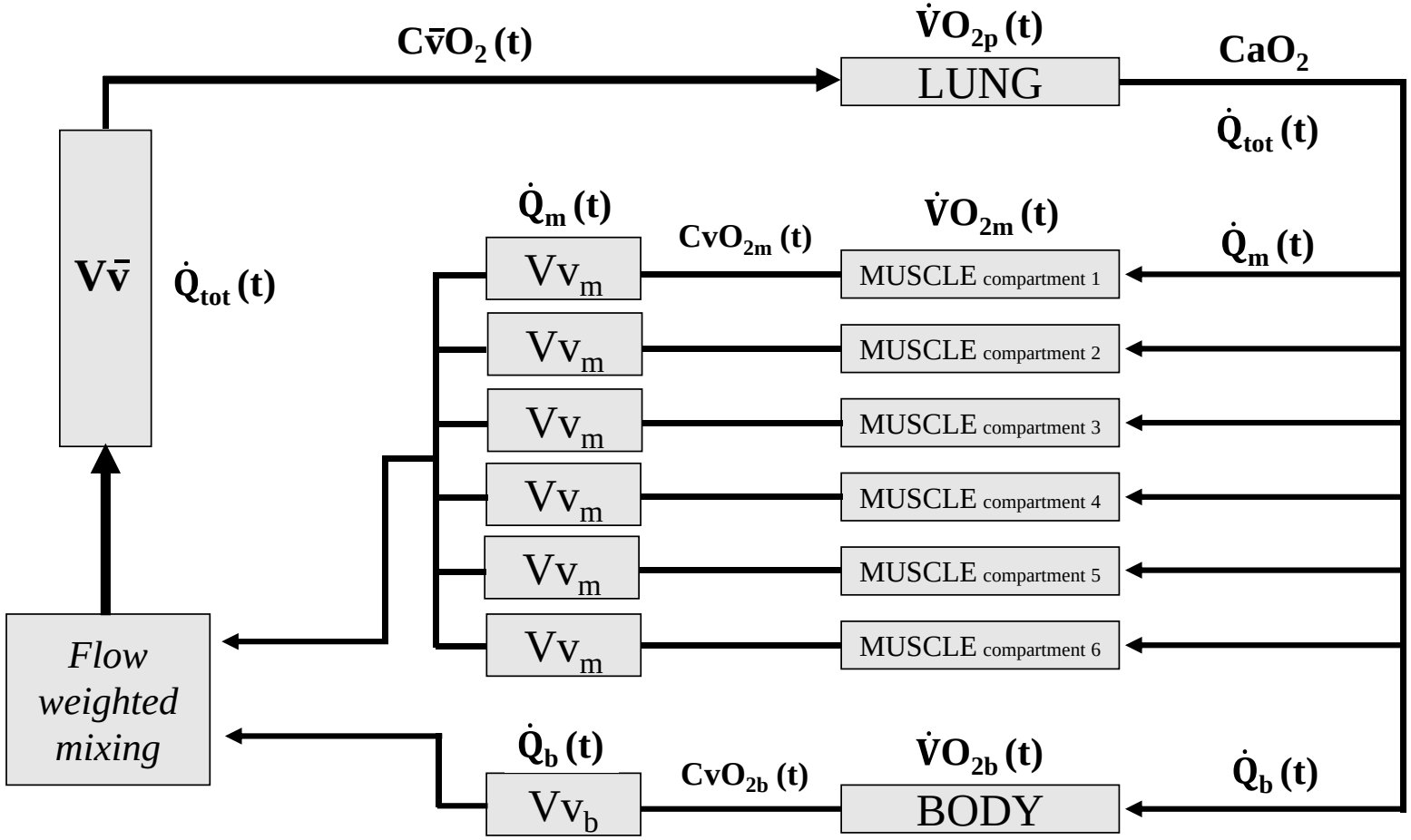

Figure 3.2. Schematic of the multi-compartment model (MCM; modified from Benson *et al.* (2013)), where muscle (comprised of six equal "compartments") and body venous effluents travel down separate venous volumes (V_V; i.e., V_{Vm} (muscle) and V_{Vb} (body) respectively) before flow-weighted mixing occurs. The MCM default parameters are provided in text. See text also for abbreviations and model details.

Results

The group mean $\hat{\theta}_L$ was 2.22 ± 0.32 L·min^{-1} (range: 1.85 – 3.00 L·min^{-1}), which corresponded to a mean WR of 161 ± 34 W (range: 130 – 240 W). Therefore, the WR associated with $\hat{\theta}_L$ for all participants was greater than the maximum baseline WR from which step-transitions were initiated in the experimental protocol (i.e., 120 W). The 40 W transitions from baselines of 20, 40, 60, 80, 100, and 120 W corresponded to 35 ± 6, 43 ± 7, 51 ± 8, 60 ± 9, 68 ± 10, 78 ± 12 % of $\dot{V}O_{2p}$ at $\hat{\theta}_L$, and the steady-state $\dot{V}O_{2p}$ achieved corresponded to 50 ± 8, 60 ± 9, 68 ± 10, 78 ± 11, 87 ± 12, 97 ± 14 % of $\hat{\theta}_L$. Based on the steady-state $\dot{V}O_{2p}$ achieved, four (of 14) participants transitioned into the heavy-intensity domain at 160 W and one at 140 W. However, removal of these data *post hoc* did not alter the overall study outcomes described below.

Table 3.1 shows the phase II $\dot{V}O_{2p}$ parameters for each of the variable baseline conditions. The ensemble-averaged group profiles of $\dot{V}O_{2p}$ for the variable baseline condition are displayed in Figure 3.3. In each panel, a mono-exponential fit derived from the group mean parameter estimates (from equation 3.1) is superimposed over the data. As designed, $\dot{V}O_{2pBSL}$ increased ($p<0.05$) progressively from the 20 W to 120 W baseline transitions (Table 3.1). Despite constant ΔWR, the parameter estimates for A, G_P and $\tau\dot{V}O_{2p}$ increased progressively with increasing baseline WR ($p<0.05$; see Table 3.1 and Figure 3.4 for pairwise differences).

The group mean parameter estimates from the phase II $\dot{V}O_{2p}$ fits for the constant baseline condition exercise transitions are displayed in Table 3.2. Figure 3.5 shows the mean $\dot{V}O_{2p}$ responses for Δ40, Δ60, Δ80, Δ100 W transitions from a 20 W baseline. As designed, $\dot{V}O_{2pBSL}$ did not change ($p>0.05$) amongst these step-transitions and A increased

($p<0.05$) with increasing WR increment. The G_P increased ($p<0.05$, main effect) during transitions to increasing moderate-intensity WRs, but there was no difference in $\tau\dot{V}O_{2p}$ among the different ΔWR conditions ($p>0.05$). The relationships between A, $\tau\dot{V}O_{2p}$ or G_P, and the WR increment are shown in Figure 3.6.

The kinetic parameters of [HHb] under the variable and constant baseline conditions are shown in Tables 3.3 and 3.4 and the group means responses are displayed in Figures 3.7 and 3.8. Similar to $\dot{V}O_{2p}$, τ[HHb] increased with increasing $\dot{V}O_{2pBSL}$ ($p<0.05$, main effect). Baseline [HHb] increased ($p<0.05$, main effect) and [HHb]-TD decreased ($p<0.05$, main effect) with increasing baseline WR (see Table 3.3 for multiple comparisons). The Δ[HHb] and MRT-[HHb] were not different ($p>0.05$) when the WR increment was constant (variable baseline condition; Table 3.3) but, as expected, Δ[HHb] increased ($p<0.05$) with increasing ΔWR (constant baseline condition; Table 3.4). There was no influence of WR increment ($p>0.05$) on $[HHb]_{BSL}$, [HHb]-TD, MRT-[HHb], or τ[HHb] in the constant baseline condition (Table 3.4).

The relationship between phase II $\dot{V}O_{2p}$ kinetics and [HHb] kinetics was examined by computing the difference in "time to reach steady-state" for both signals (i.e., ($4*\tau\dot{V}O_{2p}$) for $\dot{V}O_{2p}$ and ([HHb]-TD + $4*\tau$[HHb]) for [HHb], in s) (Figure 3.8). A "steady-state" for [HHb] was reached ~ 45 s earlier than for $\dot{V}O_{2p}$ for all Δ40W WR transitions (Figure 3.9A) and ~37 s earlier for WR transitions from a common 20 W baseline (Figure 3.9B); responses were similar between and within variable and constant baseline conditions ($p>0.05$, Figures 3.9A and 3.9B).

The *in silico* simulations using the *in vivo* estimated parameters for $\dot{V}O_{2p}$ kinetics are presented in Figure 3.10. First, the outcomes from simulations performed to determine

values of $\tau\dot{V}O_{2m}$ and $\tau\dot{Q}_m$ that would elicit a $\tau\dot{V}O_{2p}$ of 22 s for the Δ40W step-transition from 20 W were 26.1 s and 28.5 s for $\tau\dot{V}O_{2m}$ and $\tau\dot{Q}_m$, respectively. These values were then used to determine the extent to which $\tau\dot{V}O_{2p}$ would be modified by increasing WR increment (constant baseline condition; Figure 3.10A) and baseline WR (variable baseline condition; Figure 3.10B) assuming $\dot{V}O_{2m}$ and $\dot{Q}_m$ kinetics were unaltered. As shown in Figure 3.10A, the influence on increasing the WR increment in the constant baseline condition is that $\tau\dot{V}O_{2p}$ is reduced from 22.0 s (at Δ40W) to 20.3 s (at Δ100W). The opposite occurs in the variable baseline condition with common Δ40W WR increments, where $\tau\dot{V}O_{2p}$ increases from 22.0 s (at 20 W baseline) to 24.4 s (at 120 W baseline) (Figure 3.10B). In addition, we also tested the effect of allowing $\dot{Q}_m$ kinetics to become slower as baseline WR was increased ($\tau\dot{Q}_m$ was increased by 5 s per 20 W increase in baseline). Figure 3.9C shows that the difference between $\tau\dot{V}O_{2m}$ and $\tau\dot{V}O_{2p}$ tends to become smaller as the baseline WR is increased (variable baseline condition).

Figure 3.10 displays the results of the simulated six muscle compartment model to a step change from 20 to 120 W. Based on the dynamic responses of $\dot{V}O_{2p}$ and [HHb] from the group means of the equal WR increment steps, the $\dot{V}O_{2m}$ and $\dot{Q}_m$ kinetics for six theoretical muscle compartments were determined: $\tau\dot{V}O_{2m}$ = 15, 20, 25, 30, 35, 40 s and $\tau\dot{Q}_m$ = 20, 25, 30, 35, 40, 45 s (for compartments 1 – 6, respectively). The resultant $\tau\dot{V}O_{2p}$ of the averaged $\dot{V}O_{2p}$ output was 23.5 s, which was less than the mean $\tau\dot{V}O_{2m}$ of all compartments (27.5 s) and very similar to the measured $\dot{V}O_{2p}$ response of 21.8 s (Figure 3.11).

Table 3.1. Mean parameter estimates (± SD) for phase II $\dot{V}O_{2p}$ kinetics during 40 W exercise transitions from six different baseline work rates (variable baseline condition).

	Step-transition power output (W)					
n = 14	**20 → 60**	**40 → 80**	**60 → 100**	**80 → 120**	**100 → 140**	**120 → 160**
$\dot{V}O_{2pBSL}$ ($L \cdot min^{-1}$)*	0.75 ± 0.07	0.93 ± 0.06	1.10 ± 0.07	1.30 ± 0.06	1.48 ± 0.06	1.71 ± 0.08
A ($L \cdot min^{-1}$)	0.35 ± 0.02^{cdef}	0.37 ± 0.02^{def}	0.39 ± 0.02^{af}	0.40 ± 0.20^{ab}	0.41 ± 0.03^{ab}	0.42 ± 0.04^{abc}
$\dot{V}O_{2pSS}$ ($L \cdot min^{-1}$)*	1.10 ± 0.07	1.30 ± 0.06	1.49 ± 0.07	1.70 ± 0.07	1.90 ± 0.07	2.12 ± 0.08
TD (s)	12 ± 6	10 ± 4	7 ± 6	6 ± 6	6 ± 3	7 ± 3
$\tau\dot{V}O_{2p}$ (s)	22 ± 5^{cdef}	23 ± 5^{def}	28 ± 6^{af}	31 ± 7^{ab}	34 ± 6^{ab}	35 ± 9^{abc}
CI_{95} (s)	3 ± 1	3 ± 1	3 ± 1	4 ± 1	4 ± 1	4 ± 1
MRT-$\dot{V}O_{2p}$ (s)	34 ± 6^{ef}	32 ± 4^{ef}	36 ± 7^{f}	38 ± 6	41 ± 6^{ab}	45 ± 13^{abc}
O_{2Def} (mL)	193 ± 32^{def}	197 ± 26^{ef}	233 ± 43^{f}	251 ± 47^{af}	285 ± 51^{ab}	319 ± 115^{abcd}
G_P ($mL \cdot min^{-1} \cdot W^{-1}$)	8.7 ± 0.6^{cdef}	9.2 ± 0.5^{def}	9.7 ± 0.6^{af}	10.0 ± 0.6^{ab}	10.3 ± 0.8^{ab}	10.5 ± 0.9^{abc}

$^{a\text{-}f}$ indicate significant differences between conditions ($p<0.05$). "^{a}" indicates difference from "**20 → 60**", "^{b}" indicates difference from "**40 → 80**", and so forth. * indicates significant differences amongst all conditions ($p<0.05$).

Table 3.2. Mean parameter estimates (± SD) for phase II $\dot{V}O_{2p}$ kinetics during exercise transitions from 20W to four different work rates (constant baseline condition).

	Step-transition power output (W)			
n = 14	**20 → 60**	**20 → 80**	**20 → 100**	**20 → 120**
$\dot{V}O_{2pBSL}$ ($L \cdot min^{-1}$)	0.75 ± 0.07	0.75 ± 0.06	0.76 ± 0.06	0.76 ± 0.06
A ($L \cdot min^{-1}$)*	0.35 ± 0.02	0.54 ± 0.02	0.72 ± 0.04	0.93 ± 0.04
$\dot{V}O_{2pSS}$ ($L \cdot min^{-1}$)*	1.10 ± 0.07	1.30 ± 0.06	1.47 ± 0.05	1.68 ± 0.07
TD (s)	12 ± 6	11 ± 4	12 ± 3	11 ± 3
$\tau\dot{V}O_{2p}$ (s)	22 ± 5	20 ± 4	22 ± 6	22 ± 5
CI_{95} (s)	3 ± 1	2 ± 1	2 ± 1	1 ± 0
MRT-$\dot{V}O_{2p}$ (s)	34 ± 6	31 ± 3	33 ± 4	33 ± 5
O_{2Def} (mL)*	193 ± 32	276 ± 26	389 ± 47	501 ± 73
G_P ($mL \cdot min^{-1} \cdot W^{-1}$)	8.7 ± 0.6[bd]	9.0 ± 0.4[a]	8.9 ± 0.4	9.3 ± 0.4[a]

[a-d] indicate significant differences between conditions ($p<0.05$). "[a]" indicates difference from "**20 → 60**", "[b]" indicates difference from "**20 → 80**", and so forth. * indicates significant differences amongst all conditions ($p<0.05$).

Table 3.3. Mean parameter estimates and confidence interval of mono-exponential fit of [HHb] data for each 40W transition from progressively increasing baseline work rates (mean ± SD)

	Step-transition power output (W)					
	20 → 60	**40 → 80**	**60 → 100**	**80 → 120**	**100 → 140**	**120 → 160**
HHb_{bsl} (µM) *	19.2 ± 7.2 *	21.9 ± 8.1 *	22.3 ± 8.9 *	24.0 ± 9.5 *	24.5 ± 10.6 *	27.1 ± 11.5 *
ΔHHb_{amp} (µM)	3.4 ± 2.6	2.6 ± 1.4	2.6 ± 2.1	3.1 ± 2.8	2.7 ± 2.2	3.0 ± 2.5
[HHb]-TD (s)	16 ± 4[ef]	15 ± 3[e]	13 ± 4	11 ± 5	11 ± 4[a]	9 ± 5[ab]
τHHb (s)	9 ± 4[def]	11 ± 3	14 ± 7	17 ± 6[a]	18 ± 11[a]	18 ± 6[a]
MRT-HHb (s)	25 ± 6	26 ± 5	26 ± 6	28 ± 5	29 ± 9	28 ± 5
CI_{95} (s)	1 ± 1	2 ± 1	2 ± 1	2 ± 1	2 ± 1	2 ± 1

[a-f] indicate significant differences between conditions ($p<0.05$). "[a]" indicates difference from "**20 → 60**", "[b]" indicates difference from "**40 → 80**", and so forth. * indicates significant differences amongst all conditions ($p<0.05$).

Table 3.4. Mean parameter estimates and confidence interval of mono-exponential fit of [HHb] data for each ΔWR transition from a constant baseline of 20W (mean ± SD)

	Step-transition power output (W)			
	20 → 60	**20 → 80**	**20 → 100**	**20 → 120**
$[HHb]_{bsl}$ (μM)	19.2 ± 7.2	19.8 ± 7.1	19.2 ± 7.2	19.9 ± 7.6
$\Delta[HHb]_{amp}$ (μM)	3.4 ± 2.6 *	4.8 ± 3.3 *	6.3 ± 4.6 *	9.4 ± 2.8 *
[HHb]-TD (s)	16 ± 4	14 ± 3	13 ± 2	11 ± 3
τ[HHb] (s)	9 ± 4	10 ± 5	8 ± 3	8 ± 3
MRT-[HHb] (s)	25 ± 6	24 ± 7	20 ± 4	20 ± 4
CI_{95} (s)	1 ± 1	1 ± 1	1 ± 1	1 ± 0

[a-d] indicate significant differences between conditions ($p<0.05$). "[a]" indicates difference from "**20 → 60**", "[b]" indicates difference from "**20 → 80**", and so forth. * indicates significant differences amongst all conditions ($p<0.05$).

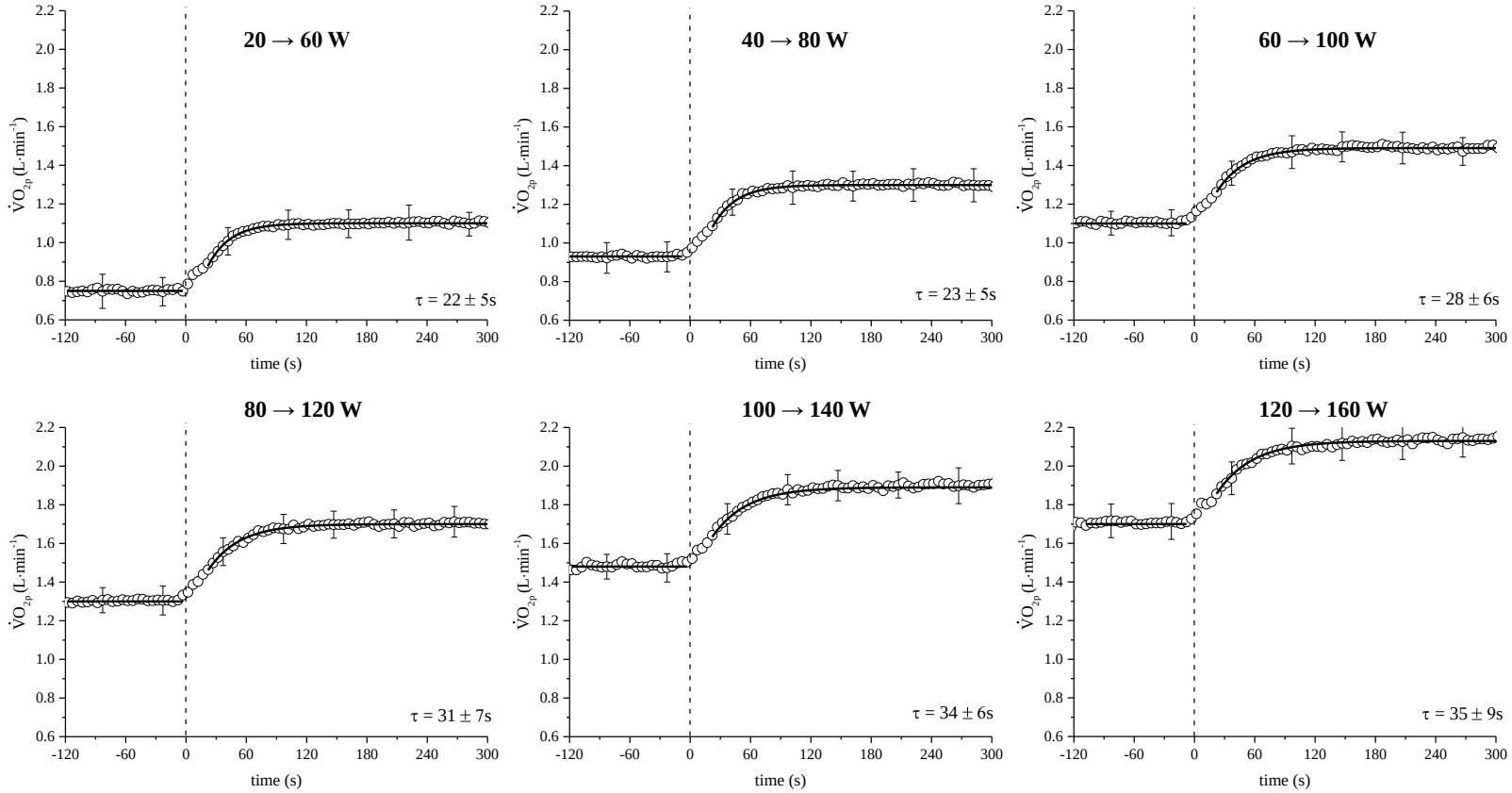

Figure 3.3. Ensemble-averaged group mean responses of $\dot{V}O_{2p}$ in the variable baseline condition: six 40 W transitions from different baseline work rates. Vertical dashed lines indicate the onset of the transition (time = 0 s). The group mean phase II kinetic responses for each condition are superimposed on the data (*dark lines*, fitted with a mono-exponential function using group mean parameter estimates). $\tau\dot{V}O_{2p}$ values (± SD) are inset under each transition and error bars at specific time points indicate SD.

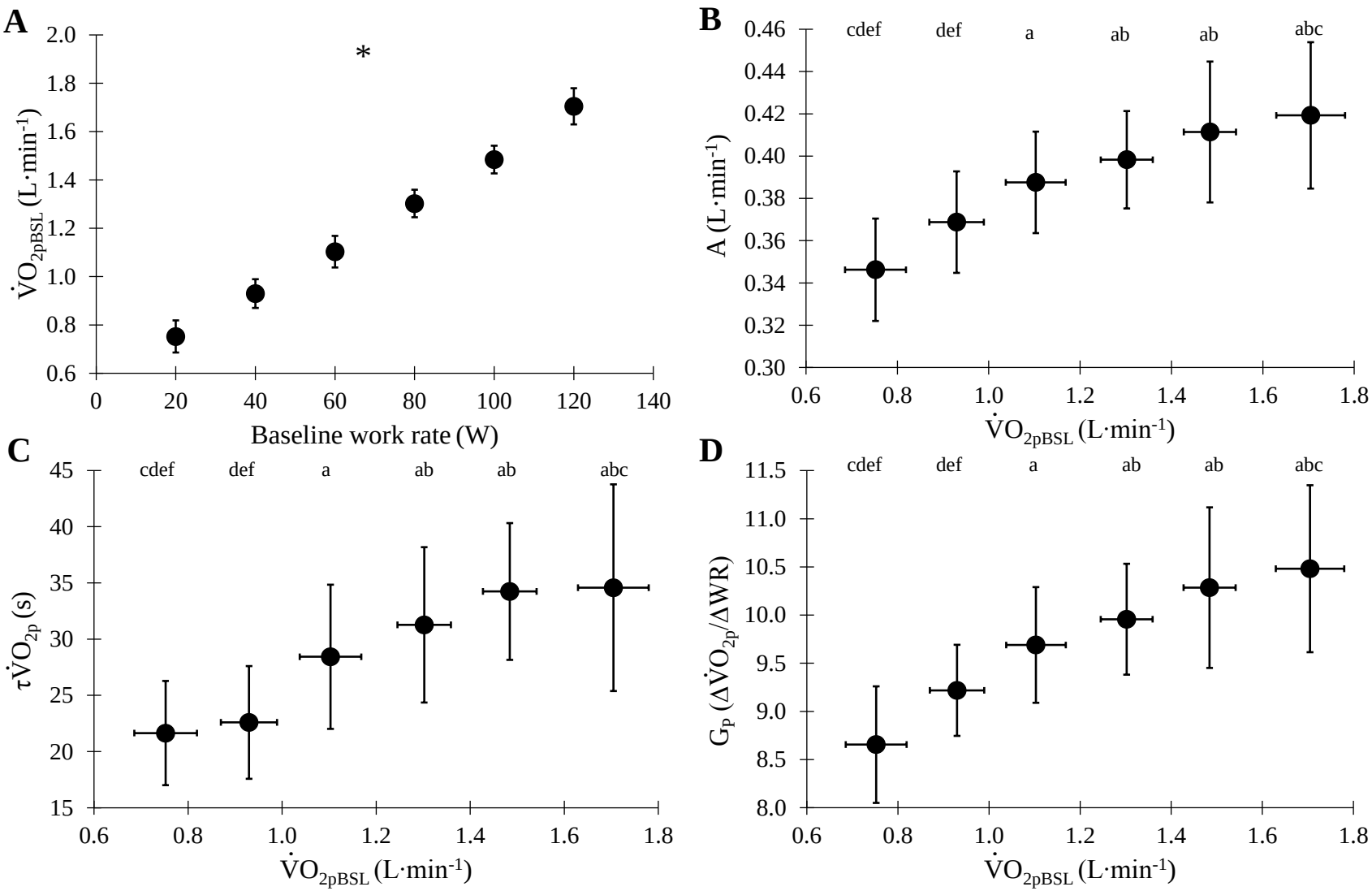
A
2.0
1.8
1.6
1.4
1.2
1.0
0.8
0.6
$\dot{V}O_{2pBSL}$ (L·min^{-1})
*
0
20
40
60
80
100
120
140
Baseline work rate (W)
B
0.46
0.44
0.42
0.40
0.38
0.36
0.34
0.32
0.30
A (L·min^{-1})
cdef
def
a
ab
ab
abc
0.6
0.8
1.0
1.2
1.4
1.6
1.8
$\dot{V}O_{2pBSL}$ (L·min^{-1})
C
45
40
35
30
25
20
15
$\tau\dot{V}O_{2p}$ (s)
cdef
def
a
ab
ab
abc
0.6
0.8
1.0
1.2
1.4
1.6
1.8
$\dot{V}O_{2pBSL}$ (L·min^{-1})
D
11.5
11.0
10.5
10.0
9.5
9.0
8.5
8.0
G_p ($\Delta\dot{V}O_{2p}/\Delta WR$)
cdef
def
a
ab
ab
abc
0.6
0.8
1.0
1.2
1.4
1.6
1.8
$\dot{V}O_{2pBSL}$ (L·min^{-1})

Figure 3.4. A) Baseline $\dot{V}O_{2p}$ ($\dot{V}O_{2pBSL}$) as a function of baseline WR. B) $\dot{V}O_{2p}$ amplitude (A) as function of $\dot{V}O_{2pBSL}$. C) $\dot{V}O_{2p}$ time constant ($\tau\dot{V}O_{2p}$) as function of $\dot{V}O_{2pBSL}$. D) Gain (G_P) as function of $\dot{V}O_{2pBSL}$. Symbols represent group mean ± SD. [a-f] indicate significant differences between conditions ($p<0.05$). "[a]" indicates difference from "**20 → 60**", "[b]" indicates difference from "**40 → 80**", and so forth. * indicates significant differences amongst all transitions ($p<0.05$).

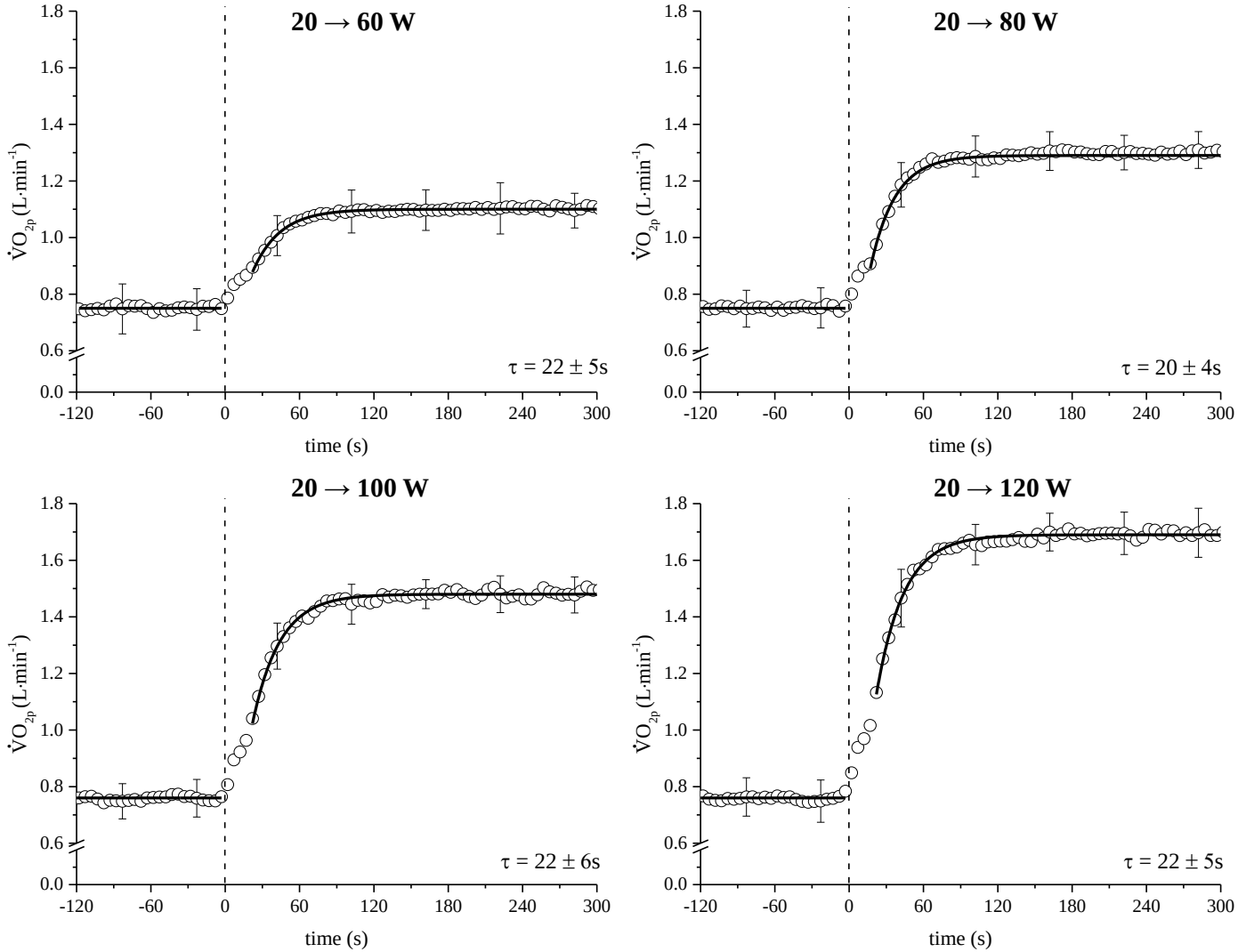
20 → 60 W
τ = 22 ± 5s
20 → 80 W
τ = 20 ± 4s
20 → 100 W
τ = 22 ± 6s
20 → 120 W
τ = 22 ± 5s
V̇O2p (L·min-1)
time (s)
1.8
1.6
1.4
1.2
1.0
0.8
0.6
0.0
-120
-60
0
60
120
180
240
300

Figure 3.5. Ensemble-averaged group mean responses of $\dot{V}O_{2p}$ in the constant baseline condition: four different increments in work rate (ΔWR) each from a 20 W baseline work rate. Vertical dashed lines indicate the onset of the transition (time = 0 s). The group mean phase II kinetic responses for each condition are superimposed over the data (*dark lines*, fitted with a mono-exponential function using group mean parameter estimates). $\tau\dot{V}O_{2p}$ values (± SD) are inset under each transition and error bars at specific time points indicate SD.

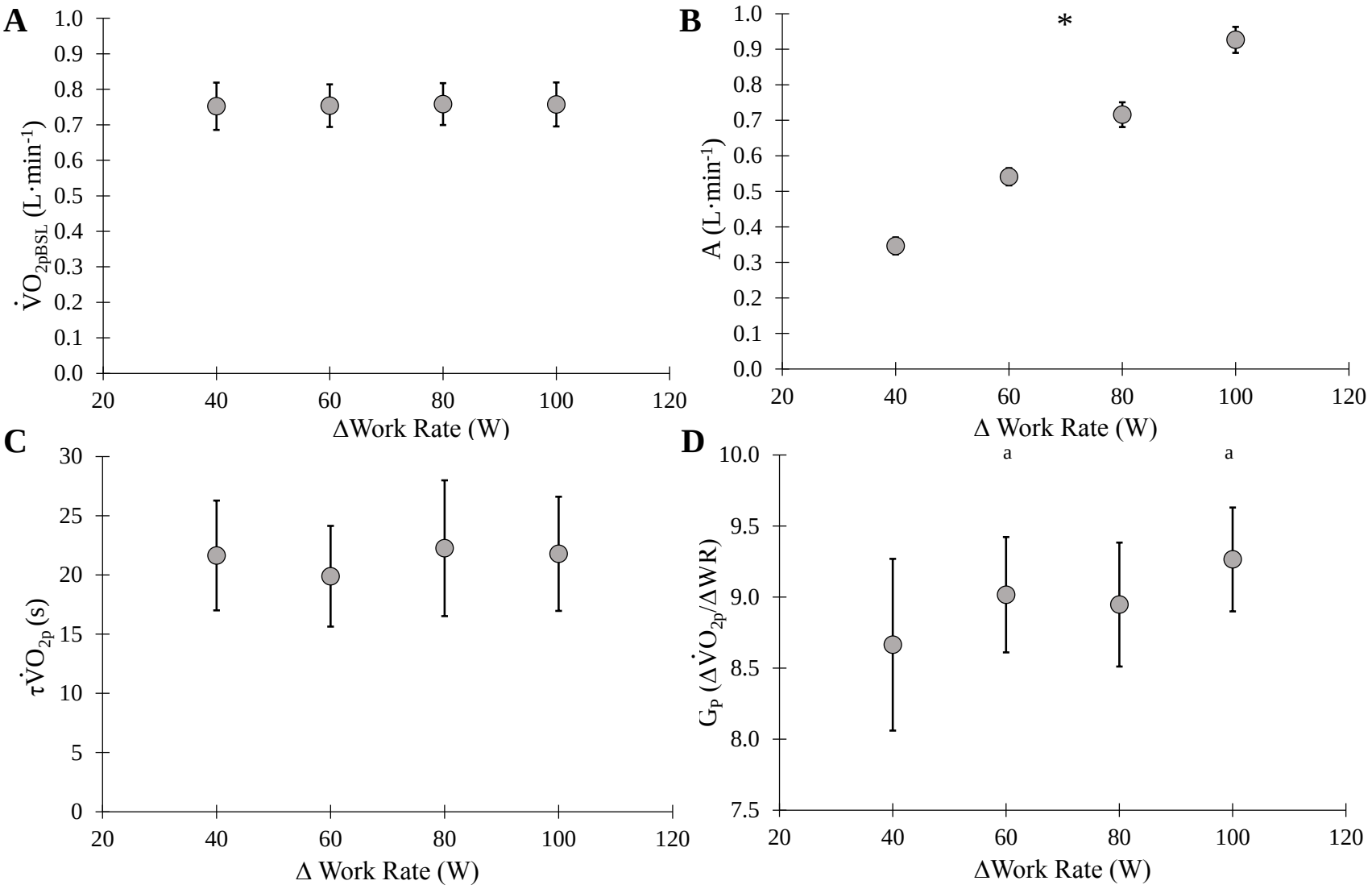
A
$\dot{V}O_{2pBSL}$ (L·min^{-1})
ΔWork Rate (W)
B
A (L·min^{-1})
*
Δ Work Rate (W)
C
$\tau\dot{V}O_{2p}$ (s)
Δ Work Rate (W)
D
G_p ($\Delta\dot{V}O_{2p}/\Delta WR$)
a
a
ΔWork Rate (W)

Figure 3.6. Comparison of A) baseline $\dot{V}O_{2p}$ ($\dot{V}O_{2pBSL}$); B) $\dot{V}O_{2p}$ amplitude (A); C) $\dot{V}O_{2p}$ time constant ($\tau\dot{V}O_{2p}$); and D) gain (G_P) as function of as a function of WR increment (ΔWR). Symbols represent group mean ± SD. [a-d] indicate significant differences between conditions ($p<0.05$). "[a]" indicates difference from "**20 → 60**", "[b]" indicates difference from "**20 → 80**", and so forth.* indicates significant differences amongst all transitions ($p<0.05$).

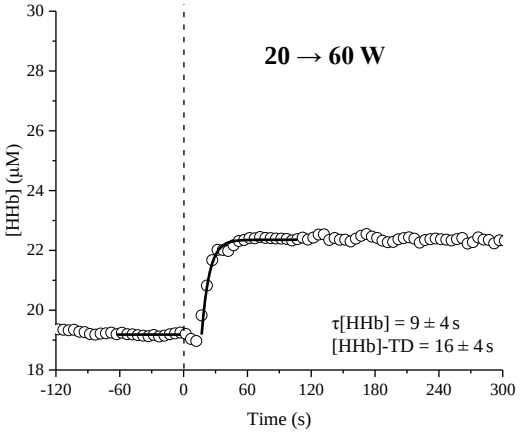
20 → 60 W
[HHb] (μM)
Time (s)
τ[HHb] = 9 ± 4 s
[HHb]-TD = 16 ± 4 s

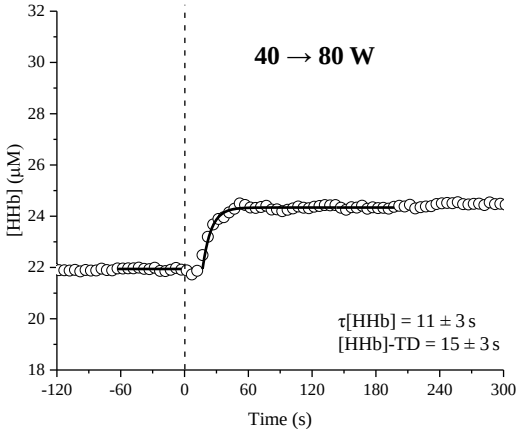
40 → 80 W
[HHb] (μM)
Time (s)
τ[HHb] = 11 ± 3 s
[HHb]-TD = 15 ± 3 s

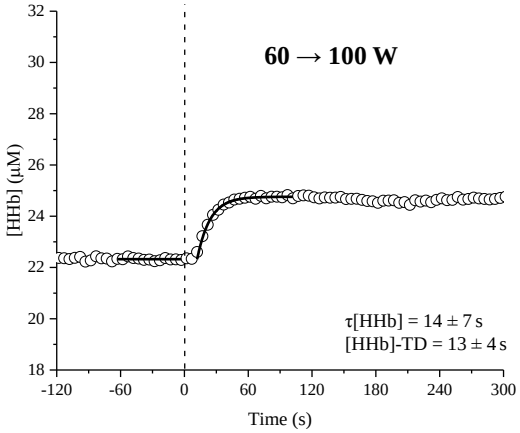
60 → 100 W
[HHb] (μM)
Time (s)
τ[HHb] = 14 ± 7 s
[HHb]-TD = 13 ± 4 s

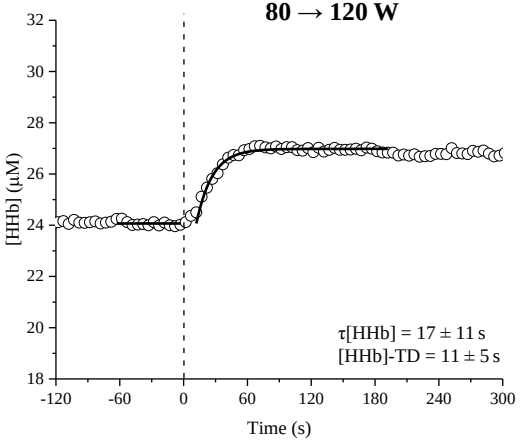
80 → 120 W
[HHb] (μM)
Time (s)
τ[HHb] = 17 ± 11 s
[HHb]-TD = 11 ± 5 s

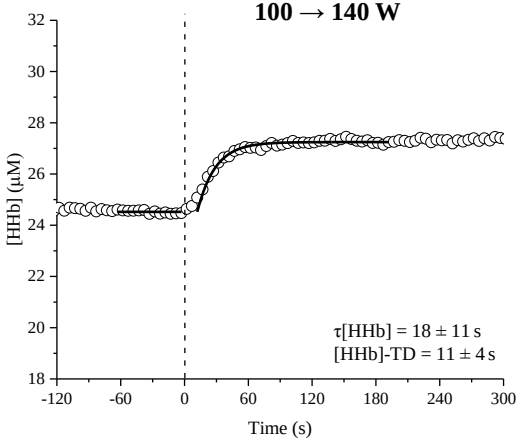
100 → 140 W
[HHb] (μM)
Time (s)
τ[HHb] = 18 ± 11 s
[HHb]-TD = 11 ± 4 s

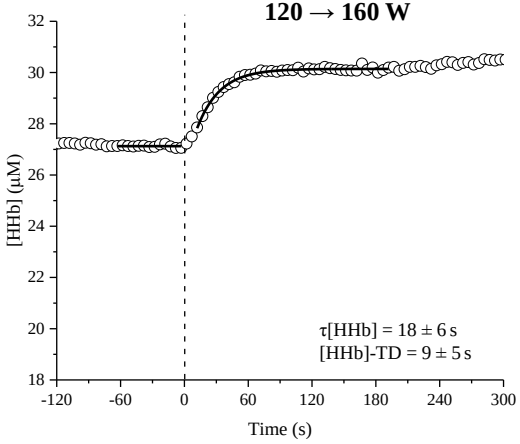
120 → 160 W
[HHb] (μM)
Time (s)
τ[HHb] = 18 ± 6 s
[HHb]-TD = 9 ± 5 s

Figure 3.7. Ensemble-averaged group mean responses of [HHb] in the variable baseline condition: six 40 W transitions from different baseline work rates. Vertical dashed lines indicate the onset of the transition (time = 0 s). The group mean phase II kinetic responses for each condition are superimposed on the data (*dark lines*, fitted with a mono-exponential function using group mean parameter estimates). τ[HHb] values (± SD) are inset under each transition and error bars at specific time points indicate SD. Error bars at specific time points are not displayed due to the large SD in [HHb] amongst subjects (see Table 3.3).

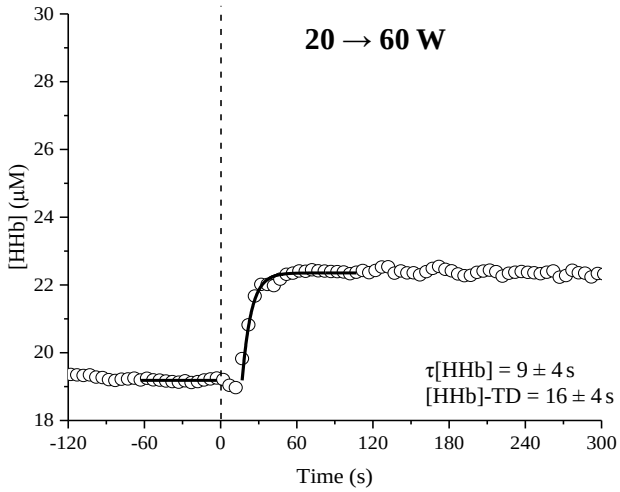
20 → 60 W
[HHb] (μM)
Time (s)
τ[HHb] = 9 ± 4 s
[HHb]-TD = 16 ± 4 s

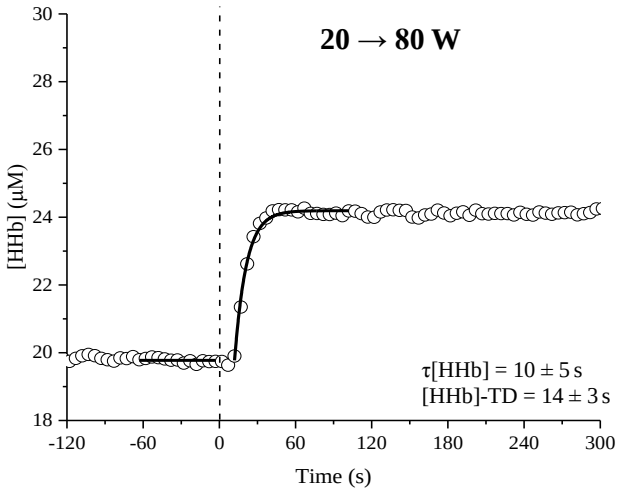
20 → 80 W
[HHb] (μM)
Time (s)
τ[HHb] = 10 ± 5 s
[HHb]-TD = 14 ± 3 s

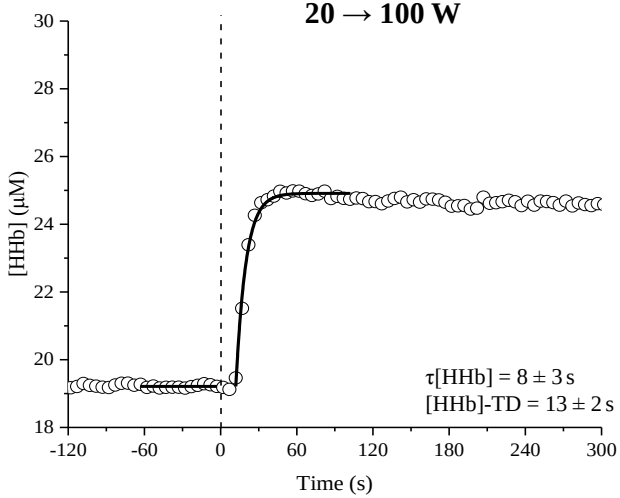
20 → 100 W
[HHb] (μM)
Time (s)
τ[HHb] = 8 ± 3 s
[HHb]-TD = 13 ± 2 s

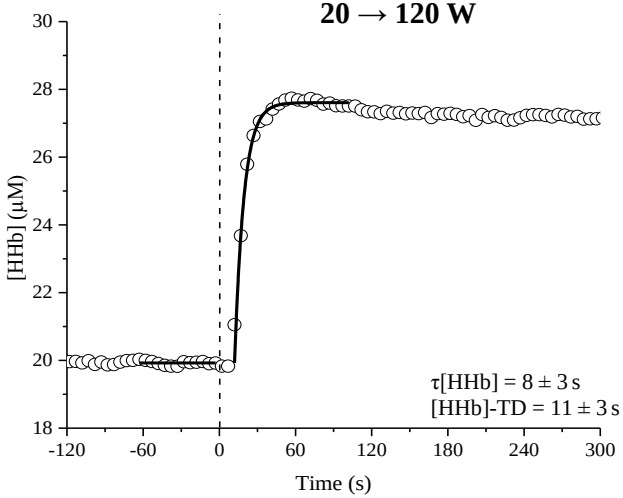
20 → 120 W
[HHb] (μM)
Time (s)
τ[HHb] = 8 ± 3 s
[HHb]-TD = 11 ± 3 s

Figure 3.8. Ensemble-averaged group mean responses of [HHb] in the constant baseline condition: four different increments in work rate (ΔWR) each from a 20 W baseline work rate. Vertical dashed lines indicate the onset of the transition (time = 0 s). The group mean phase II kinetic responses for each condition are superimposed over the data (*dark lines*, fitted with a mono-exponential function using group mean parameter estimates). τ[HHb] values (± SD) are inset under each transition. Error bars at specific time points are not displayed due to the large SD in [HHb] amongst subjects (see Table 3.4).

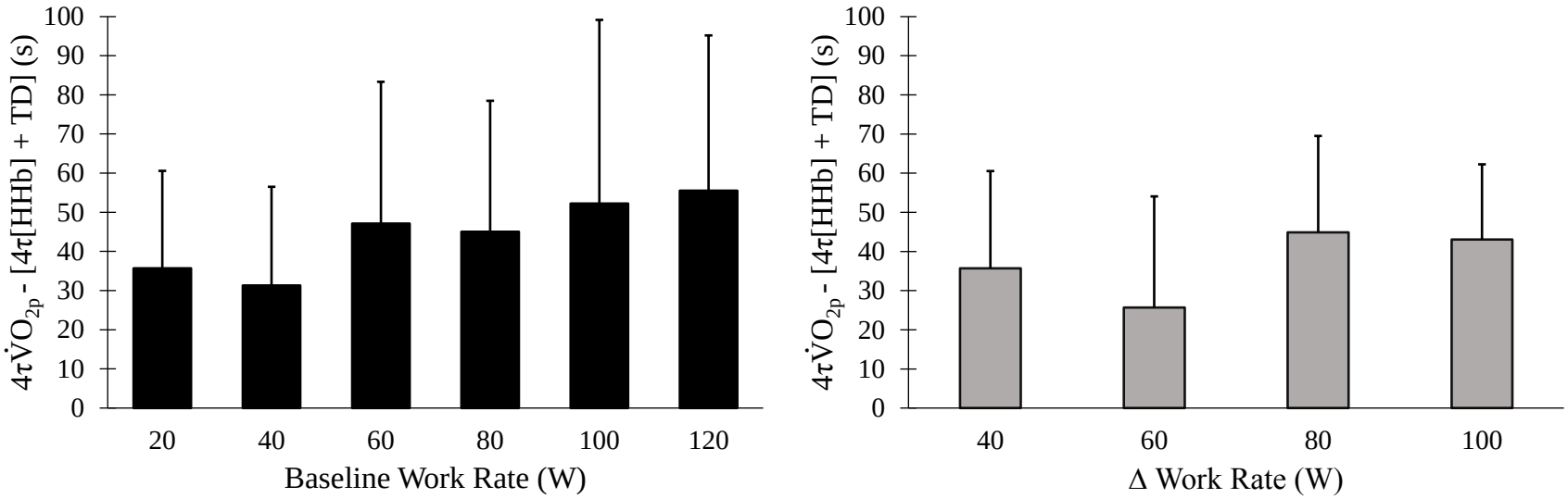

Figure 3.9. Comparison of the "time to reach steady-state" between $\dot{V}O_{2p}$ and NIRS-derived deoxygenated hemoglobin ([HHb]) signals following exercise onset. "Time to reach steady-state" was computed as the difference between the sum of 4 time constants for phase II $\dot{V}O_{2p}$ (4 x $\tau\dot{V}O_{2p}$) and 4 time constants plus the time delay for [HHb] ([HHb]-TD + (4 x τ[HHb])). Panel *A* shows group mean ± SD for the variable baseline condition; 40 W transitions from different baseline work rates (*black bars*). Panel *B* shows group mean ± SD for each the constant baseline condition; variable increments in work rate each from a 20 W baseline (*grey bar*). There were no differences amongst transitions ($p>0.05$).

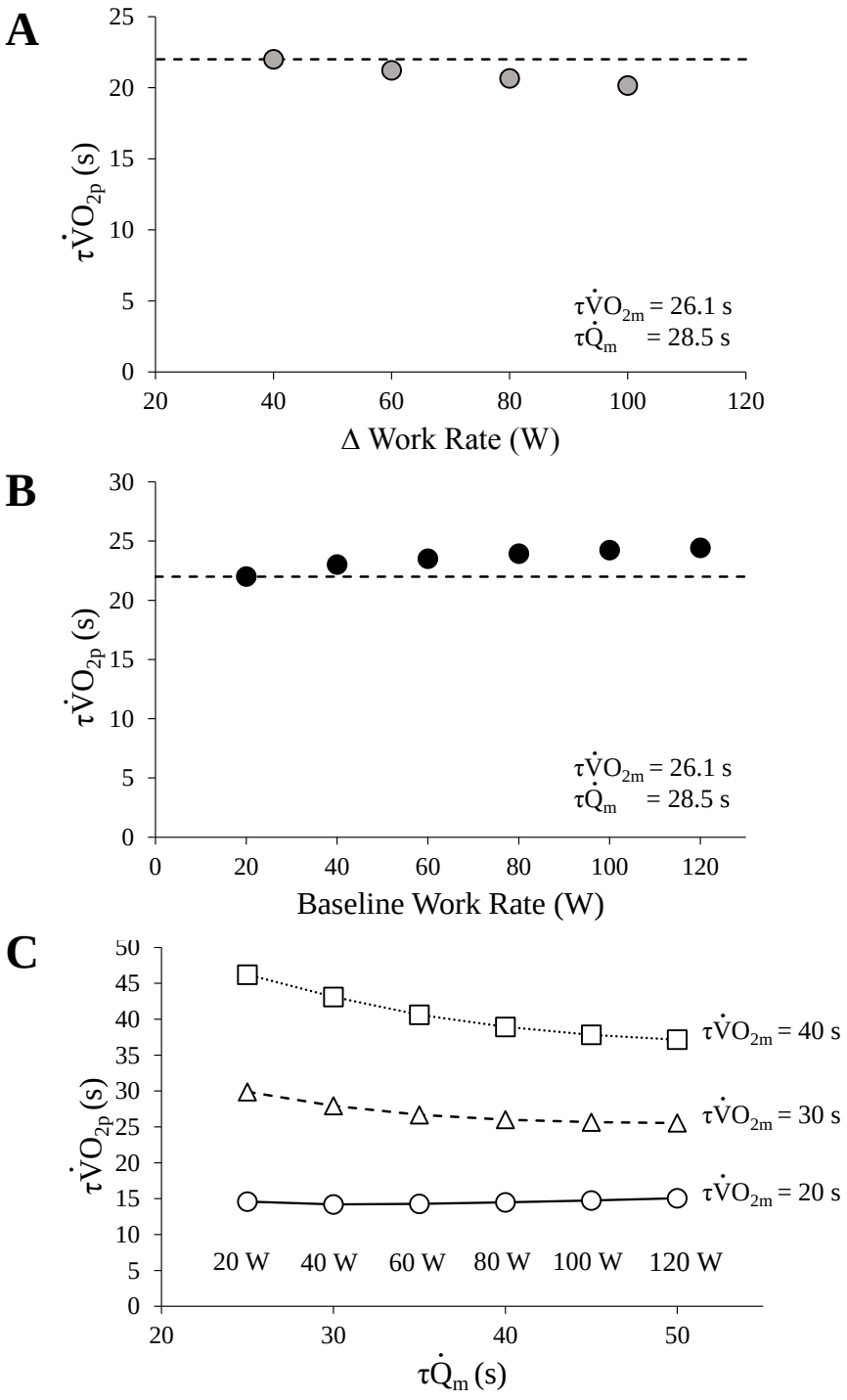
A
25
20
15
10
5
0
τV̇O2p (s)
τV̇O2m = 26.1 s
τQ̇m = 28.5 s
20
40
60
80
100
120
Δ Work Rate (W)
B
30
25
20
15
10
5
0
τV̇O2p (s)
τV̇O2m = 26.1 s
τQ̇m = 28.5 s
0
20
40
60
80
100
120
Baseline Work Rate (W)
C
50
45
40
35
30
25
20
15
10
5
0
τV̇O2p (s)
τV̇O2m = 40 s
τV̇O2m = 30 s
τV̇O2m = 20 s
20 W
40 W
60 W
80 W
100 W
120 W
20
30
40
50
τQ̇m (s)

Figure 3.10. The output of a dynamic computational simulation to illustrate the influence of circulatory dynamics on the phase II pulmonary $\dot{V}O_{2p}$ during exercise transitions in both the variable and constant baseline conditions. Modulation of $\tau\dot{V}O_{2p}$ at a fixed muscle $\tau\dot{V}O_2$ ($\tau\dot{V}O_{2m}$; 26.1 s) and muscle $\tau\dot{Q}$ ($\tau\dot{Q}_m$; 28.5 s) is examined for step-transitions from a 20 W baseline to increasing ΔWR increments (*panel A*) and for Δ40W step-transitions from increasing baseline WR (WR_{bsl}; *panel B*). *Panel C* displays the effect of circulatory dynamics on $\tau\dot{V}O_{2p}$ during simulated Δ40W exercise transitions from increasing baseline WRs at various $\tau\dot{V}O_{2m}$ (*circles*, 20 s; *triangles*, 30 s; *squares*, 40 s). The $\tau\dot{Q}_m$ values used in the simulations are based on data from MacPhee *et al.* (2005) who showed that $\dot{Q}_m$ dynamics slow with transitions from elevated metabolic rates. Note that as $\tau\dot{Q}_m$ increases with increasing baseline WR for each isopleth of $\tau\dot{V}O_{2m}$, $\tau\dot{V}O_{2p}$ becomes smaller (faster kinetics) which is opposite to the results from the *in vivo* data. See text for further explanation.

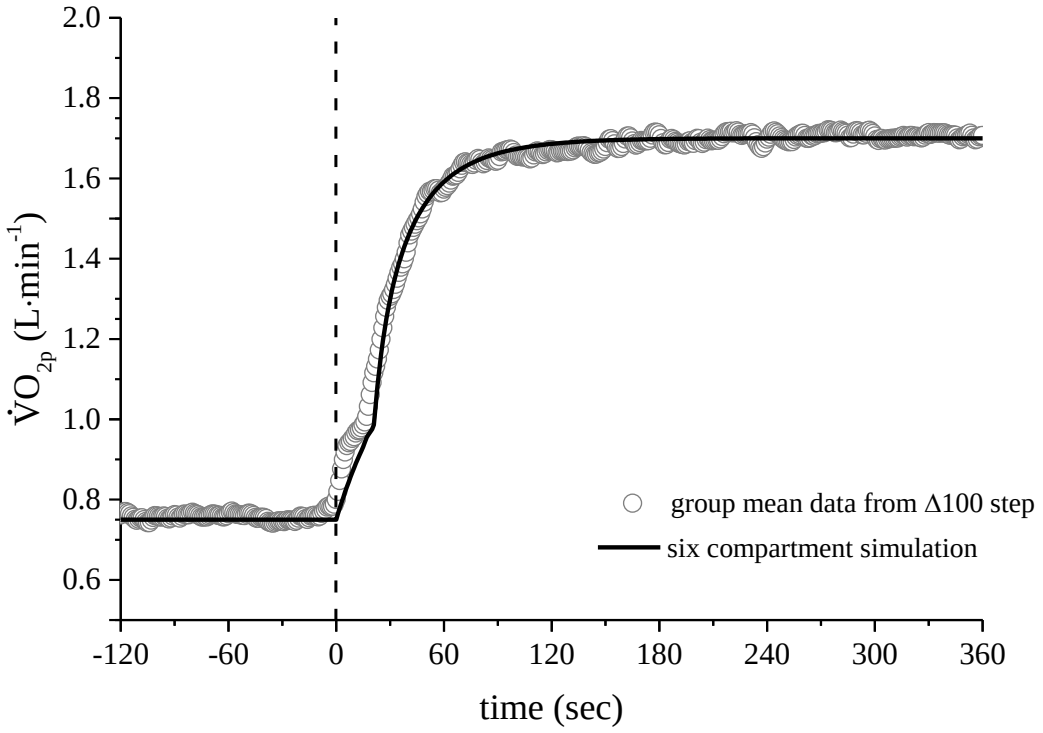

Figure 3.11. Ensemble-averaged group mean responses of $\dot{V}O_{2p}$ for the Δ100W step-transition from a 20 W baseline work rate. Vertical dashed lines indicate the onset of the transition (time = 0 s). A theoretical model containing six muscle compartments of equal size but varying $\dot{V}O_{2m}$ and $\dot{Q}_m$ kinetics ($\tau\dot{V}O_{2m}$ = 15, 20, 25, 30, 35, 40 s and $\tau\dot{Q}_m$ = 20, 25, 30, 35, 40, 45 s for compartments 1 – 6, respectively) was developed and computational simulations were used to investigate whether the conflation of $\dot{Q}_m$ dynamics amongst compartments may modulate the "summed" (or homogenized) $\dot{V}O_{2m}$ kinetics towards a faster $\tau\dot{V}O_{2p}$ response in a 100W step-change from 20 W. Assuming equal contributions from each compartment, the resultant $\dot{V}O_{2p}$ response (*black line*) is overlaid on the *in vivo* group mean response (*white circles*). The phase II $\tau\dot{V}O_{2p}$ from the six compartment model was 23.5 s, which is slightly faster than the mean $\tau\dot{V}O_{2m}$ of all compartments, 27.5 s and similar to the $\tau\dot{V}O_{2p}$ measured in the study participants (21.8 ± 4.8 s).

Discussion

The purpose of this study was to examine the relative stability of phase II $\dot{V}O_{2p}$ and [HHb] kinetics under a wide range of conditions with varying baseline work rate and work rate increment during moderate-intensity exercise. The main findings of the study were that: i) in the variable baseline condition, exercise transitions from a progressively greater baseline WR were associated with progressive increases in both $\tau\dot{V}O_{2p}$ and G_P – the relationships between baseline WR and $\tau\dot{V}O_{2p}$ or G_P were approximately linear; ii) in the constant baseline condition, but with progressively greater ΔWR increments, $\tau\dot{V}O_{2p}$ did not vary, but G_P increased, with increasing WR increment; iii) [HHb] kinetics were consistently faster than $\dot{V}O_{2p}$ kinetics by a magnitude that was essentially constant under all experimental conditions (i.e., a slowing of $\dot{V}O_{2p}$ kinetics was concomitant with a slowing of [HHb] kinetics) suggesting that both $\dot{V}O_{2m}$ and $\dot{Q}_m$ kinetics slowed in concert as baseline work rate increased; and iv) *in silico* simulations of the circulatory influences dissociating $\tau\dot{V}O_{2p}$ from $\tau\dot{V}O_{2m}$ showed that the slowed $\dot{V}O_{2p}$ kinetics observed in the variable baseline condition were unlikely to be consequent to altered circulatory dynamics. Thus, these data suggest that $\dot{V}O_{2p}$ kinetics may be dependent on the instantaneous metabolic rate from which they are initiated. However, the *in silico* simulations suggest that metabolic and circulatory dynamics can turn a heterogeneous (or summed) $\dot{V}O_{2m}$ response containing kinetically slow compartments into a uniformly fast $\dot{V}O_{2p}$ response. Therefore, we propose that intracellular O_2 utilization dynamics are first order and are intrinsically slower (in a progressive manner) in muscle fibres located at higher positions within the fibre recruitment hierarchy.

Mechanisms of $\dot{V}O_2$ kinetic control

Intriguingly, our finding that $\dot{V}O_{2p}$ kinetics were constant during different WR increments initiated from a common baseline (20 W) is consistent with the traditional suggestion that a first order rate reaction controls $\dot{V}O_{2p}$ kinetics (Whipp & Mahler, 1980; Barstow & Mole, 1991; Özyener *et al.* 2001; Scheuermann & Barstow, 2003; Spencer *et al.* 2013). However, the finding that $\dot{V}O_{2p}$ kinetics increased linearly with increasing baseline work rate is also consistent with the frequent and long-standing observation that moderate-intensity $\dot{V}O_{2p}$ kinetics are not first order (Hughson & Morrissey, 1982; Brittain *et al.* 2001; Robergs, 2014). Importantly, these findings were made within the same group of participants, ruling-out individual participant differences as an explanation for differences when comparing amongst published studies.

When two identical step-WR increments (between 20 W and 90% $\hat{\theta}_L$) bisecting the moderate-intensity domain are performed, the kinetics of $\dot{V}O_{2p}$ are consistently slower in the upper compared to the lower step-transition (Brittain *et al.* 2001; MacPhee *et al.* 2005; Bowen *et al.* 2011; Williams *et al.* 2013; Keir *et al.* 2014). By examining a range of pre-transition baseline work and metabolic rates spanning the entire moderate-intensity domain, the present study extends previous findings to show that both $\tau\dot{V}O_{2p}$ and G_P increase as a function of pre-transition baseline WR and metabolic rate in an approximately linear manner. This phenomenon has been previously explained by two hypotheses. The first is a fibre activation pattern favouring "kinetically-faster", more efficient fibres, to perform lower intensities and a progressive incorporation of "kinetically-slower" fibres to perform greater external WRs (Brittain *et al.* 2001). An alternative view proposes that $\dot{V}O_{2p}$ kinetics are influenced by the pre-transition metabolic rate such that greater reductions in intracellular energy state cause less free energy delivery from the mitochondria and

increase the demand for mitochondrial ATP production (Bowen *et al.* 2011; Wüst *et al.* 2014). It currently is not possible to know whether the muscle motor units recruited to transition to low work rates are the same or different from those recruited to transition to greater work rates. Thus, we cannot distinguish whether the present results are due to recruitment of motor units innervating muscle fibres with inherently different mitochondrial volume-density, or whether our findings were consequent to a progressive contribution of increasing metabolic rate within a uniform fibre population.

It has been suggested that the free energy associated with ATP hydrolysis (ΔG_{ATP}, i.e., ~58 $kJ \cdot mol^{-1}$) is greater than the activation energy required for acto-myosin crossbridge cycling (~ 40 $kJ \cdot mol^{-1}$ (Sheetz *et al.* 1984) but close to that for SERCA ATPase function (~ 52 $kJ \cdot mol^{-1}$) under normal physiological conditions (Grassi *et al.* 2015). Since the concentration of metabolites that affect ΔG_{ATP} (i.e., [ADP_{free}] and [Pi]) are elevated at greater baseline metabolic rates, less negative ΔG_{ATP} could prevent some acto-myosin crossbridge or SERCA ATPase regions from receiving sufficient energy to activate. The resultant effect would be a progressively larger and possibly less "square wave" change in ATP required for a given change in WR, thereby altering the exponential-nature of the response leading to an increase in both $\tau\dot{V}O_{2p}$ and G_P. However, this hypothesis is difficult to reconcile in moderate-intensity cycling exercise, where muscle fatigue appears to be absent (Cannon *et al.*, 2011). An alternative mechanism could be that $\dot{V}O_{2m}$ of individual fibers does operate through a unimolecular reaction of ADP-feedback to its mitochondrial network; when these same fibers are recruited at a greater level of metabolic activity, the intracellular [ADP_{free}] exceeds the K_m and thus the sensitivity of $\dot{V}O_{2m}$ to increases in [ADP_{free}] may decrease, manifesting as a slower rate of adjustment in $\dot{V}O_{2p}$ with a greater

baseline metabolic rate. Nevertheless, this also seems unlikely in moderate exercise where intramyocellular disturbance in [ADP_{free}] in the active fibres is likely small and thus an alternative explanation is required.

In silico simulations

Using *in silico* simulations based on a validated multi-compartmental model of circulatory dynamics (Figure 3.1), Benson *et al.* (2013) demonstrated that kinetic dissociations between phase II $\dot{V}O_{2p}$ and $\dot{V}O_{2m}$ can occur dependent on both the dynamics of muscle and whole body $\dot{Q}$ and flow-weighted mixing of muscle and whole body venous effluents. In the present study, this model was applied to assess whether altered circulatory dynamics with transitions from increasing baseline WRs might distort, by "slowing", the dynamic adjustment of the $\dot{V}O_{2p}$ profile despite $\dot{V}O_{2m}$ kinetics being "constant" when transitioning from progressively higher starting baseline metabolic rates. When assuming constant kinetics for $\dot{V}O_{2m}$ ($\tau\dot{V}O_{2m}$, 26.1 s) and $\dot{Q}_m$ (28.5 s) (see Methods), simulations showed that constant Δ40W step-transitions initiated from progressively higher baseline WRs (from 20 to 120W) were associated with a slight ~ 2 s increase in $\tau\dot{V}O_{2p}$ (22.0 to 24.2 s); however, this effect was not large enough to explain the observed $\tau\dot{V}O_{2p}$ which increased from 22 s to 35 s under the same conditions. This suggests that significant "distortion" of the $\dot{V}O_{2m}$ profile at the lung because of circulatory dynamics and mixing of muscle and other body venous compartments, while potentially contributory, likely were not responsible for the major progressive slowing of $\dot{V}O_{2p}$ kinetics observed in this study (Bowen *et al.* 2011).

That [HHb] kinetics were consistently faster than $\dot{V}O_{2p}$ kinetics suggests that, overall, during the on-transient phase, a greater rate of O_2 extraction was required relative

to the rate of muscle O_2 utilization. Since, the magnitude by which kinetics of both signals differed did not change as a function of baseline WR (Figure 3.9) suggests that the underlying microvascular blood flow ($\dot{Q}_m$) dynamics were slightly slower than $\dot{V}O_{2m}$ and that $\dot{Q}_m$ became progressively slower with transitions from greater baseline WRs. Given that MacPhee *et al.* (2005) also reported a twofold increase in the time constant for bulk leg blood flow when equal WR increment step-transitions were initiated from WRs midway between 20W and 90% $\hat{\theta}_L$ compared to a baseline of 20W, we examined the effect of progressively increasing $\tau\dot{Q}_m$ (by a factor of ~5 s per 20W increase in baseline; MacPhee *et al.* (2005)) on the modulation of $\tau\dot{V}O_{2p}$ for a range of $\tau\dot{V}O_{2m}$ (from 20 – 40 s; Figure 3.10C). For any given $\tau\dot{V}O_{2m}$, $\tau\dot{V}O_{2p}$ was reduced as baseline WR and $\tau\dot{Q}_m$ increased (a relationship opposite to that observed experimentally in the present study). This further supports the notion that the slowing of $\dot{V}O_{2p}$ kinetics coincident with higher baseline metabolic rates, seen in this and other studies, reflects an actual slowing of $\dot{V}O_{2m}$ kinetics, and is not a consequence of circulatory-induced "distortions" of an unchanging $\dot{V}O_{2m}$ profile.

Since It has been suggested that the dynamics of O_2 delivery are regionally heterogeneous within human quadriceps muscle (Koga *et al.* 2007), we further used this model to provide an additional explanation to reconcile why $\dot{V}O_{2p}$ kinetics were slowed (from ~ 22 s to ~ 35 s) in transitions initiated from progressively higher baseline WRs but are fast (~ 20 s) and unchanged with transitions initiated from a 20 W baseline but increasing ΔWR increment. In accordance with Koga *et al.* (2007), we proposed that "kinetically-faster" fibre pools (presumably those with a greater mitochondrial volume and better blood supply) dominate the collective, or homogenized, $\dot{V}O_{2p}$ response by exerting

a greater influence on C_vO_2 of the blood draining the muscle during the early portion of the transition. To explore this suggestion we used a model broadly based on the six muscle "compartments" derived from the responses to the six Δ40W steps that were examined in this study. We assumed that each compartment was of equal size but varied in $\dot{V}O_{2m}$ and $\dot{Q}_m$ kinetics. We examined the average $\dot{V}O_{2p}$ response to a step-change in WR from 20 to 120 W derived from the simultaneous activation of these compartments (see Figure 3.2 and Methods). $\dot{V}O_{2m}$ and $\dot{Q}_m$ kinetics for each compartment were determined *ad-hoc* and were selected to reflect the kinetics (as inferred from $\dot{V}O_{2p}$ and [HHb]) from the group means of the equal WR increment steps ($\tau\dot{V}O_{2m}$ = 15, 20, 25, 30, 35, 40 s and $\tau\dot{Q}_m$ = 20, 25, 30, 35, 40, 45 s for compartments 1 – 6, respectively). The resultant $\tau\dot{V}O_{2p}$ was 23.5 s which was less than the mean $\tau\dot{V}O_{2m}$ of all compartments (27.5 s) and very similar to the measured $\dot{V}O_{2p}$ response of 22 s (Figure 3.11). This suggests that the conflation of $\dot{Q}_m$ dynamics amongst compartments may modulate the "summated" $\dot{V}O_{2m}$ kinetics towards a faster $\tau\dot{V}O_{2p}$ via disproportionate and time-dependent contributions (of those compartments) to the dynamics of C_vO_2 of blood draining the muscle. Therefore, it is possible that the $\tau\dot{V}O_{2p}$ from the larger step-changes (i.e., greater WR increments) may have been influenced by the blood flow and metabolic heterogeneity and differences in circulatory and metabolic dynamics existing within the pool of muscle fibres recruited to support the change in WR. Although $\dot{Q}_m$ dynamics were not directly measured, microvascular O_2 pressure ($P_{mv}O_2$) has been shown to drop at a faster rate and to a greater extent at the onset of contraction in rat muscle comprised predominately of fast- compared to slow-muscle fibres (Behnke *et al.* 2003; McDonough *et al.* 2005). Therefore, it is conceivable that human skeletal muscle

may also express diversity in $\dot{Q}_m$ dynamics such that muscle fibres with slow $\dot{V}O_{2m}$ kinetics may also have slower blood flow dynamics.

Reconciling models of $\dot{V}O_{2p}$ kinetic control

Thus, while distinguishing among the various hypotheses for $\dot{V}O_{2p}$ kinetic control will require complex and detailed descriptions of $\dot{V}O_{2m}$ and intramyocellular signalling dynamics under a range of conditions (such as those used in this study), our combined *in vivo* and *in silico* data propose a unifying hypothesis. That $\dot{V}O_{2p}$ kinetics were invariant in the moderate domain with constant baseline WR is consistent with first order control. While the progressive increase in $\tau\dot{V}O_{2p}$ with increasing baseline work rates appears to subvert the requirements of a first order system, we propose that these findings can be reconciled by the understanding of the heterogeneity in both dynamics of muscle motor unit recruitment (of fibres with different a volume of mitochondrial network) and of blood flow (where the microvascular blood flow dynamics may vary to a similar magnitude to $\dot{V}O_{2p}$ kinetics). Thus, the transit and mixing of blood draining kinetically variable motor units are later combined to form a $\dot{V}O_{2p}$ kinetic response that is dominated by the influence of the motor units where both $\dot{V}O_{2m}$ and $\dot{Q}_m$ kinetics are fast. These features can explain both the main findings of $\dot{V}O_{2p}$ kinetic behaviour in this study and remain consistent with the assumptions of apparent first order control.

Conclusion

The main finding of the present study was that $\dot{V}O_{2p}$ kinetics are not altered when step-changes are initiated from a 20 W baseline WR, but get progressively slower with increasing baseline work rate. The observed slowing of $\dot{V}O_{2p}$ kinetics with increasing baseline intensity could not be attributed to limitations in O_2 delivery (since the magnitude

of the difference between kinetic adjustments of [HHb] and $\dot{V}O_{2p}$ was unchanged regardless of baseline WR or ΔWR increment). However, a model combining heterogeneous metabolism and blood flow kinetics was able to reconcile these apparently conflicting findings. Collectively, these data suggest that within the moderate-intensity domain phase II $\dot{V}O_{2p}$ kinetics are influenced by pre-transition WR, becoming slower as baseline WR increases, and are strongly influenced by heterogeneity in the dynamic metabolic and circulatory properties of the active muscles. Taken together, these data suggest that the work rate-dependent non-linear $\dot{V}O_{2p}$ responses may be attributable to "heterogeneity" within the range of muscle fibres recruited to address the exercise challenge. Importantly, each of these muscle fibres may independently behave as a linear, first order system.

References

Barstow TJ, Lamarra N & Whipp BJ (1990). Modulation of muscle and pulmonary O_2 uptakes by circulatory dynamics during exercise. *J Appl Physiol* **68,** 979–989.

Barstow TJ & Mole PA (1991). Linear and nonlinear characteristics of oxygen uptake kinetics during heavy exercise. *J Appl Physiol* **71,** 2099–2106.

Beaver WL, Wasserman K & Whipp BJ (1986). A new method for detecting anaerobic threshold by gas exchange. *J Appl Physiol* **60,** 2020–2027.

Behnke BJ, McDonough P, Padilla DJ, Musch TI & Poole DC (2003). Oxygen exchange profile in rat muscles of contrasting fibre types. *J Physiol* **549,** 597–605.

Benson AP, Grassi B & Rossiter HB (2013). A validated model of oxygen uptake and circulatory dynamic interactions at exercise onset in humans. *J Appl Physiol* **115,** 743–755.

Bowen TS, Murgatroyd SR, Cannon DT, Cuff TJ, Lainey AF, Marjerrison AD, Spencer MD, Benson AP, Paterson DH, Kowalchuk JM & Rossiter HB (2011). A raised metabolic rate slows pulmonary O_2 uptake kinetics on transition to moderate-intensity exercise in humans independently of work rate. *Exp Physiol* **96,** 1049–1061.

Brittain CJ, Rossiter HB, Kowalchuk JM & Whipp BJ (2001). Effect of prior metabolic rate on the kinetics of oxygen uptake during moderate-intensity exercise. *Eur J Appl Physiol* **86,** 125–134.

Cannon DT, White AC, Andriano MF, Kolkhorst FW & Rossiter HB (2011). Skeletal muscle fatigue precedes the slow component of oxygen uptake kinetics during exercise in humans. *J Physiol* **589,** 727–739.

DiMenna FJ, Bailey SJ, Vanhatalo A, Chidnok W & Jones AM (2010). Elevated baseline VO_2 per se does not slow O_2 uptake kinetics during work-to-work exercise transitions. *J Appl Physiol* **109,** 1148–1154.

Grassi B, Poole DC, Richardson RS, Knight DR, Erickson BK & Wagner PD (1996). Muscle O_2 uptake kinetics in humans: implications for metabolic control. *J Appl Physiol* **80,** 988–998.

Grassi B, Rossiter HB & Zoladz JA (2015). Skeletal muscle fatigue and decreased efficiency: two sides of the same coin? *Exerc Sport Sci Rev* **43,** 75–83.

Hoffmann U, Drescher U, Benson AP, Rossiter HB & Essfeld D (2013). Skeletal muscle VO_2 kinetics from cardio-pulmonary measurements: assessing distortions through O_2 transport by means of stochastic work-rate signals and circulatory modelling. *Eur J Appl Physiol* **113,** 1745–1754.

Hughson RL & Morrissey M (1982). Delayed kinetics of respiratory gas exchange in the transition from prior exercise. *J Appl Physiol* **52,** 921–929.

Keir DA, Nederveen JP, Paterson DH & Kowalchuk JM (2014). Pulmonary O_2 uptake kinetics during moderate-intensity exercise transitions initiated from low versus elevated metabolic rates: insights from manipulations in cadence. *Eur J Appl Physiol* **114,** 2655–2665.

Koga S, Poole DC, Ferreira LF, Whipp BJ, Kondo N, Saitoh T, Ohmae E & Barstow TJ (2007). Spatial heterogeneity of quadriceps muscle deoxygenation kinetics during cycle exercise. *J Appl Physiol (Bethesda, Md 1985)* **103,** 2049–2056.

Krustrup P, Jones AM, Wilkerson DP, Calbet JAL & Bangsbo J (2009). Muscular and pulmonary O_2 uptake kinetics during moderate- and high-intensity sub-maximal knee-extensor exercise in humans. *J Physiol* **587,** 1843–1856.

Lamarra N, Whipp BJ, Ward SA & Wasserman K (1987). Effect of interbreath fluctuations on characterizing exercise gas exchange kinetics. *J Appl Physiol* **62,** 2003–2012.

MacPhee SL, Shoemaker JK, Paterson DH & Kowalchuk JM (2005). Kinetics of O_2 uptake, leg blood flow, and muscle deoxygenation are slowed in the upper compared with lower region of the moderate-intensity exercise domain. *J Appl Physiol* **99,** 1822–1834.

McDonough P, Behnke BJ, Padilla DJ, Musch TI & Poole DC (2005). Control of microvascular oxygen pressures in rat muscles comprised of different fibre types. *J Physiol* **563,** 903–913.

Murias JM, Spencer MD & Paterson DH (2014). The critical role of O_2 provision in the dynamic adjustment of oxidative phosphorylation. *Exerc Sport Sci Rev* **42,** 4–11.

Özyener F, Rossiter HB, Ward SA & Whipp BJ (2001). Influence of exercise intensity on the on- and off-transient kinetics of pulmonary oxygen uptake in humans. *J Physiol* **533,** 891–902.

Robergs RA (2014). A critical review of the history of low- to moderate-intensity steady-state VO_2 kinetics. *Sport Med* **44,** 641–653.

Rossiter HB (2011). Exercise: Kinetic Considerations for Gas Exchange. *Compr Physiol* **1,** 203–244.

Scheuermann BW & Barstow TJ (2003). O_2 uptake kinetics during exercise at peak O_2 uptake. *J Appl Physiol* **95,** 2014–2022.

Sheetz MP, Chasan R & Spudich J a. (1984). ATP-dependent movement of myosin in vitro: Characterization of a quantitative assay. *J Cell Biol* **99,** 1867–1871.

Spencer MD, Murias JM, Kowalchuk JM & Paterson DH (2011). Pulmonary O_2 uptake and muscle deoxygenation kinetics are slowed in the upper compared with lower region of the moderate-intensity exercise domain in older men. *Eur J Appl Physiol* **111,** 2139–2148.

Spencer MD, Murias JM, Kowalchuk JM & Paterson DH (2013). Effect of moderate-intensity work rate increment on phase II tauVO_2, functional gain and Delta[HHb]. *Eur J Appl Physiol* **113,** 545–557.

Spencer MD, Murias JM & Paterson DH (2012). Characterizing the profile of muscle deoxygenation during ramp incremental exercise in young men. *Eur J Appl Physiol* **112,** 3349–3360.

Swanson GD (1980). Breath-to-breath considerations for gas exchange kinetics. In *Exercise Bioenergetics and Gas Exchange*, ed. Cerretelli P & Whipp BJ, pp. 211–222. Elsevier, Amsterdam.

Whipp BJ & Mahler M (1980). Dynamics of pulmonary gas exchange during exercise. In *Pulmonary Gas Exchange, Vol II, Organism and Environment*, ed. West JB, pp. 33–96. Academic Press, New York.

Whipp BJ, Ward SA, Lamarra N, Davis JA & Wasserman K (1982). Parameters of ventilatory and gas exchange dynamics during exercise. *J Appl Physiol* **52,** 1506–1513.

Williams AM, Paterson DH & Kowalchuk JM (2013). High-intensity interval training speeds the adjustment of pulmonary O_2 uptake, but not muscle deoxygenation, during moderate-intensity exercise transitions initiated from low and elevated baseline metabolic rates. *J Appl Physiol* **114,** 1550–1562.

Wüst RC, McDonald JR, Sun Y, Ferguson BS, Rogatzki MJ, Spires J, Kowalchuk JM, Gladden LB & Rossiter HB (2014). Slowed muscle oxygen uptake kinetics with raised metabolism are not dependent on blood flow or recruitment dynamics. *J Physiol* **592,** 1857–1871.

Wüst RCI, Grassi B, Hogan MC, Howlett R a, Gladden LB & Rossiter HB (2011). Kinetic control of oxygen consumption during contractions in self-perfused skeletal muscle. *J Physiol* **589,** 3995–4009.

CHAPTER IV: Influence of muscle metabolic heterogeneity in determining the $\dot{V}O_{2p}$ response to ramp-incremental exercise

Introduction

The pulmonary O_2 uptake ($\dot{V}O_{2p}$) response to ramp-incremental exercise increases linearly with work rate (WR), following an early exponential phase (Davis *et al.* 1982; Meyer *et al.* 1998; Boone & Bourgois, 2012). The dynamics of this $\dot{V}O_{2p}$ response have been well described by a mono-exponential function with a single time constant (τ) and gain (G: $\Delta\dot{V}O_{2p}/\Delta WR$) (Whipp *et al.* 1981; Hughson & Inman, 1986; Swanson & Hughson, 1988), which is consistent with the action of a first-order control system. This means that, for a given change in WR (input), the $\dot{V}O_{2p}$ response (output) for any individual should be predictable based on invariant values of τ and G, regardless of the forcing function used to initiate the change in $\dot{V}O_{2p}$ (e.g., step-increments vs ramp-increments) (Rossiter, 2011).

Accordingly, in response to a step-change in WR, the profile of $\dot{V}O_{2p}$ projects, exponentially, towards a new steady-state (termed the 'fundamental', or phase II component of the response), following a brief cardiodynamic period (phase I) reflective of an increase in pulmonary blood flow (Whipp *et al.* 1982). Both the 'fundamental' phase II and the overall profile (including phase I) of the $\dot{V}O_{2p}$ response, may be described by a mono-exponential transfer function which dictates that for a given change in WR the instantaneous rate of change of $\dot{V}O_{2p}$ (dy/dt) at any time, t, is directly proportional to the difference between the actual $\dot{V}O_{2p}$ and the projected steady-state $\dot{V}O_{2p}$ (Whipp *et al.* 1981). Typically, this proportionality is described by the phase II time constant for $\dot{V}O_{2p}$ ($\tau\dot{V}O_{2p}$) or the mean response time (MRT; describing the overall response).

A tenet of a system under dynamically linear control is that it must conform to the law of superposition (Fujihara *et al.* 1973). For $\dot{V}O_{2p}$, this principle dictates that the time constant and gain for a given input (i.e., ΔWR) are independent of both the starting point (e.g., baseline WR) and the amplitude of the change in WR. However, $\dot{V}O_{2p}$ kinetic responses to step-exercise have consistently demonstrated non-linear characteristics (for review see (DiMenna & Jones, 2009)) particularly when measured at supra-lactate threshold (LT) work rates (Whipp & Mahler, 1980; Whipp *et al.* 2002) or when $\dot{V}O_{2p}$ changes are initiated from elevated baseline work rates (Brittain *et al.* 2001; MacPhee *et al.* 2005; Wilkerson & Jones, 2007; DiMenna *et al.* 2010; Bowen *et al.* 2011; Williams *et al.* 2013; Keir *et al.* 2014). The kinetic behaviour of sub- vs supra-LT exercise has been explained on the basis of the kinetic and metabolic properties of muscle fibre pools located at lower and higher positions within the recruitment hierarchy (Brittain *et al.* 2001; Wilkerson & Jones, 2006), and on the influence of fatigue on muscle metabolism and motor unit recruitment (Cannon *et al.* 2011; Grassi *et al.* 2015). Therefore, given that incremental exercise typically spans a range of power outputs for which non-linear $\dot{V}O_{2p}$ responses have been demonstrated, it is surprising that the $\dot{V}O_{2p}$ response is well described by a mono-exponential model with a single time constant and gain (Whipp *et al.* 1981; Hughson & Inman, 1986; Swanson & Hughson, 1988). This implies that the dynamic responses of the underlying muscle fibre populations that vary with WR throughout a ramp protocol are metabolically and kinetically homogenous.

In attempt to reconcile this dichotomy it was suggested that the incremental $\dot{V}O_{2p}$ response may reflect the interaction of time constant and gain increasing progressively as a function of WR (Whipp *et al.* 2002; Rossiter, 2011): this would seemingly yield a "linear"

$\dot{V}O_{2p}$ profile, but obscure the underlying heterogeneous kinetic properties of the muscle fibres that contribute to the overall response. To explore this possibility we examined $\dot{V}O_{2p}$ kinetic responses to step-incremental exercise to establish a relationship between baseline WR and $\dot{V}O_{2p}$ kinetics, and used these parameters to determine whether the incremental $\dot{V}O_{2p}$ response would be best explained by constant or variable time constant and gain values in the same participants. Finally, computational simulations were used to evaluate the implications of the outcome. It was hypothesized that a function based on a variable relationship between $\tau\dot{V}O_{2p}$ and WR, and G and WR established from step-incremental exercise, would better characterise the $\dot{V}O_{2p}$ response to incremental exercise than one based on a constant $\tau\dot{V}O_{2p}$ and G.

Methods

Participants. Nine healthy young adult men (mean ± SD values: age, 25 ± 4 yrs; body mass, 84 ± 12 kg; height, 182 ± 7 cm; $\dot{V}O_{2max}$, 51.0 ± 5.8 $mL \cdot kg^{-1} \cdot min^{-1}$) volunteered and gave written informed consent to participate in the study. All procedures were approved by The University of Western Ontario Ethics Committee for Research on Human Subjects. All volunteers were non-smokers who were free of any known musculoskeletal, respiratory, cardiovascular, and metabolic conditions, and were not taking any medications that might influence cardiorespiratory or metabolic responses to exercise. Participants were included on the basis that their peak WR achieved during ramp-incremental exercise (WR_{peak}) was at least 350 W. This was to ensure that enrolled participants would be able to meet the requirements of the experimental protocol.

Experimental Protocol. Each participant reported to the laboratory to perform: i) three repetitions of a symptom-limited ramp-incremental (RI) exercise test (50 W baseline for 4 min followed by a 30 $W \cdot min^{-1}$ ramp); and ii) at least 3 repetitions of two different step-incremental (SI) exercise protocols (Protocol A and Protocol B; Figure 1). Both SI protocols consisted of four step-transitions of 60 W increments starting from a 6 min baseline of either 20 W cycling (Protocol A) or 50 W cycling (Protocol B). The first two step-changes in WR in each protocol lasted 6 min and the subsequent two step-changes were 8 min in duration; for a total duration of 34 min (Figure 1). All exercise protocols were performed in a randomized order on an electromagnetically-braked cycle ergometer (model: Velotron, RacerMate Inc., Seattle, WA, USA). Participants were allowed to select a preferred cadence during the first testing session. Thereafter, each participant was asked to maintain their self-selected cadence for all exercise protocols.

Data Collection. During each trial participants wore a noseclip and breathed through a mouthpiece for breath-by-breath gas-exchange measurements. Inspired and expired volumes and flow rates were measured using a low dead space (90 mL) bidirectional turbine (Alpha Technologies, VMM 110) and pneumotach (Hans Rudolph, Model 4813) positioned in series from the mouthpiece (total apparatus dead space was 150 mL); respired air was continuously sampled at the mouth and analysed by mass spectrometry (Innovision, AMIS 2000, Lindvedvej, Denmark) for fractional concentrations of O_2 and CO_2. The volume turbine was calibrated before each test using a syringe of known volume (3 L) over a range of flow rates and the pneumotach was adjusted for zero flow. Gas concentrations were calibrated with precision-analyzed gas mixtures. The time delay between an

instantaneous square-wave change in fractional gas concentration at the sampling inlet and its detection by the mass spectrometer was measured electronically by computer. Respiratory volumes, flow, and gas concentrations were recorded in real-time at a sampling frequency of 100 Hz and transferred to a computer, which aligned gas concentrations with volume signals as measured by the turbine. Flow from the pneumotach was used to resolve inspiratory-expiratory phase transitions and the turbine was used for volume measurement. The computer executed a peak-detection program to determine end-tidal PO_2, end-tidal PCO_2 and inspired and expired volumes and durations to build a profile of each breath. Breath-by-breath alveolar gas exchange was calculated using the algorithms of Swanson (Swanson, 1980).

During one of the repeats of protocol A and protocol B, blood lactate concentration ($[La^-]$; mM) was measured in arterialized-capillary blood samples (~5 µL) taken from the heated earlobe using a Lactate Scout (Sports Resource Group, Hawthorne, NY). Samples were obtained at the fourth minute of each constant-load WR (Figure 4.1) and analyzed immediately

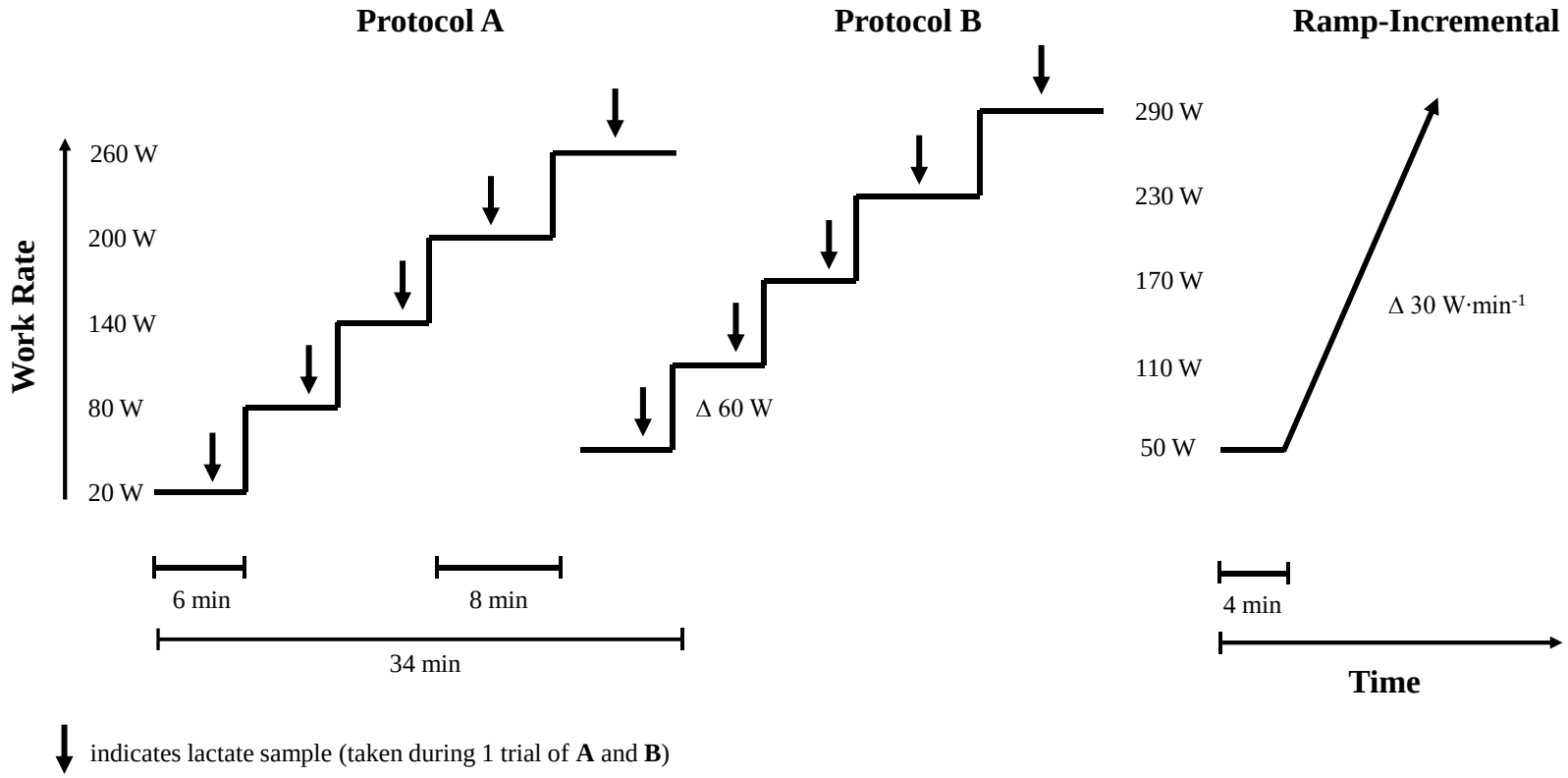

Figure 4.1. Schematic of experimental protocols and procedures. *1. Left,* step-incremental protocol "A" beginning from a baseline intensity of 20 W with step-increments of 60 W every 6 min for the first two steps and 8 min for the last two steps. *2. Middle,* step-incremental protocol "B" beginning from a baseline intensity of 50 W with step-increments of 60 W every 6 min for the first two steps and 8 min for the last two steps. *3. Right,* Ramp-incremental protocol beginning from a baseline WR of 50 W and increasing by 30 W per min. Downward arrows in Protocols A and B denote blood lactate sample.

Data Analysis. Breath-by-breath $\dot{V}O_{2p}$ data were edited on an individual basis by removing aberrant data that lay 3 SD from the local mean (Lamarra *et al.* 1987). After editing, like-repetitions were linearly interpolated on a second-by-second basis, ensemble-averaged and time-aligned such that time "zero" represented the onset of the SI or RI protocol.

Ramp-Incremental: The $\dot{V}O_{2p}$ data from the ramp-incremental protocol were fitted with a mono-exponential function (Whipp *et al.*, 1981), using non-linear least squares regression (Origin 2015; OriginLab, Northampton, MA):

$$\dot{V}O_{2p}(t) = \dot{V}O_{2pBSL} + \Delta\dot{V}O_{2pSS} \cdot (t - \tau' [1 - e^{-t/\tau'}]) \quad (4.1)$$

where, $\dot{V}O_{2p}(t)$ is the value of $\dot{V}O_{2p}$ at any time during the ramp, $\dot{V}O_{2pBSL}$ is the pre-ramp baseline value, $\Delta\dot{V}O_{2pSS}$ is the increment above $\dot{V}O_{2pBSL}$ required for the WR at time *t*, and τ' is the effective time constant of the response (note that τ' includes phase I data). The fitting window was constrained from the onset of the ramp ($t = 0$) to the end of the RI. Note that the gain of the response is measured with respect to time ($\Delta\dot{V}O_{2pSS}$; $mL \cdot min^{-1} \cdot s^{-1}$), but was simply converted (WR is linear with time during RI) to be expressed with respect to WR ($G_{ramp} = \Delta\dot{V}O_{2pSS}/\Delta WR$ in $mL \cdot min^{-1} \cdot W^{-1}$).

$\dot{V}O_{2peak}$ was defined as the greatest $\dot{V}O_{2p}$ computed from a 20 s rolling average, and WR_{peak} was defined as the WR achieved at termination of the RI test. $\dot{V}O_{2max}$ was confirmed in the RI test repeats. Additionally, the lactate threshold (LT) and the respiratory compensation point (RCP) were determined by visual inspection using standard ventilatory

and gas exchange indices as previously described (Whipp *et al.* 1986). LT was corroborated by examining the [La^-] dynamics obtained during the SI protocols.

Step-Incremental. The on-transient of each step-change in WR during SI protocols was fitted with a mono-exponential function:

$$\dot{V}O_{2p}(t) = \dot{V}O_{2pBSL} + \Delta\dot{V}O_{2pSS} \cdot (1 - e^{-(t\text{-}TD)/\tau}) \qquad (4.2)$$

where, $\dot{V}O_{2p}(t)$ is the value of $\dot{V}O_{2p}$ at any time during the transition, $\dot{V}O_{2pBSL}$ is the pre-transition baseline value, $\Delta\dot{V}O_{2pSS}$ is the steady-state increase in $\dot{V}O_{2p}$ above the baseline value, τ is the time constant of the response, and TD is the time delay. The end of the phase II fitting window was set to ~ 5 times the estimated time constant in order to restrict the modeling to data lying within the transient phase. For those individuals who transitioned into the heavy-intensity domain, the end of the phase II fitting window was determined by examining the change in τ, CI_{95}, χ^2, and plotted residuals in response to progressive increases in the end of the fitting window. The point immediately preceding a systematic increase in τ, CI_{95}, and χ^2 was considered as the end of phase II. The phase II gain (G_P; $mL \cdot min^{-1} \cdot W^{-1}$) was determined by dividing $\Delta\dot{V}O_{2pSS}$ by the ΔWR. The mean response time (MRT) of $\dot{V}O_{2p}$ was characterized from a fit of the $\dot{V}O_{2p}$ response from t=0 to the end of the exercise stage. The total gain of each step-increment (G_{tot}) was determined by dividing the overall $\Delta\dot{V}O_{2pSS}$ from the MRT fit by ΔWR.

Modeling the ramp response with variable time constant and gain. Since phase II responses likely best represent the metabolic properties among muscle fibre pools recruited, we

expected that predictions based on phase II fits from SI exercise would best represent the $\dot{V}O_{2p}$ response to RI exercise. However, since pulmonary blood flow dynamics change throughout RI exercise, we also included predictions based on the MRT, which includes the SI phase I kinetics. For this reason, two predictive models (phase II and MRT; see below) were generated.

The group mean kinetic parameters from the SI protocols were plotted as a function of WR and the relationship was fit with a first- and second-order polynomial, and linear piecewise model. The Akaike's information criterion (AIC) was used to determine the best fit model. The best fit models for rate ($\tau\dot{V}O_{2p}$ and MRT) and gain (G_P and G_{tot}) were the second-order polynomial and first-order polynomial (i.e., linear), respectively (lower AIC score). These models were used to determine the relationships between kinetic parameter values and WR as follows:

$$\tau\dot{V}O_{2p}(WR) = (A * WR^2) + (B * WR) + C \quad (4.3)$$

$$G_P(WR) = (m * WR) + b \quad (4.4)$$

$$MRT(WR) = (A * WR^2) + (B * WR) + C \quad (4.5)$$

$$G_{tot}(WR) = (m * WR) + b \quad (4.6)$$

where A, B, and C are the parameters of the second-order polynomial function and m and b are the slope and intercept parameters of the linear function. Three participants were unable to complete the last step in SI Protocol B (from 230 W to 290 W), and therefore the kinetic data associated with that transition were excluded from the individual's model fit.

To predict the $\dot{V}O_{2p}$ response to RI exercise from the kinetic data collected in the SI protocols, i.e., where time constant and gain were variable, the τ and $\Delta\dot{V}O_{2pSS}$ parameters in equation 1 were replaced with equations 4.3 and 4.4 (with the gain term converted from W to time in seconds; i.e., 30 $W \cdot min^{-1}$ = 0.5 $W \cdot s^{-1}$ and therefore, 10 $mL \cdot min^{-1} \cdot W^{-1}$ = 5 $mL \cdot min^{-1} \cdot s^{-1}$). A similar substitution was made for MRT and G_{tot}, where equations 4.5 and 4.6 replaced τ and $\Delta\dot{V}O_{2pSS}$ parameters in equation 1. Thus, three prediction models for RI were obtained:

Model 1: Constant time constant and $\dot{V}O_{2p}$ gain (equation 4.1).

Model 2: Variable time constant and $\dot{V}O_{2p}$ gain using kinetic parameters isolated to phase II (equation 4.1, with substitution equations 4.3 and 4.4).

Model 3: Variable time constant and gain using the overall mean response kinetic parameters (equation 4.1, with substitution equations 4.5 and 4.6).

The resulting predicted $\dot{V}O_{2p}$ responses were superimposed over the measured $\dot{V}O_{2p}$ RI response for each individual. Since phase II kinetics do not account for limb-to-lung transit delays, modeled fits derived from phase II data (Model 2) were right-shifted by ~ 15 s to align the measured $\dot{V}O_{2p}$ RI response with predicted $\dot{V}O_{2p}$ responses.

Goodness of fit analyses. The sum of squared residuals were calculated for the three prediction models. Since Models 2 and 3 were derived from the time constant vs WR and gain vs WR relationships from step changes up to 230 W, and the values for the time constant and gain parameters were then extrapolated to fit RI responses at end exercise

(group mean WR_{peak} = 393 ± 25 W), the goodness of fit was examined at two levels of data inclusion. The two data inclusion windows began at RI onset and proceeded to: 1) the ramp-time corresponding to 230W (i.e., 360 s); and 2) end exercise. This allowed for comparisons to be made amongst models at each fitting window level.

In silico simulations of ramp-incremental transitions. Using the group mean relationships from equations 4.5 and 4.6, the $\dot{V}O_{2p}$ response to RI exercise of 15 $W \cdot min^{-1}$, 30 $W \cdot min^{-1}$, and 50 $W \cdot min^{-1}$ was predicted and compared. The group mean parameters for equation 4.5 and 4.6 were substituted for the τ and $\Delta\dot{V}O_{2pSS}$ parameters in equation 4.1 with the adjustments made to the gain to correct for the differences in the WR vs time relation for different simulated ramp rates (e.g., for a G of 10 $mL \cdot min^{-1} \cdot W^{-1}$; 15 $W \cdot min^{-1}$ = 2.5 $mL \cdot min^{-1} \cdot s^{-1}$; 30 $W \cdot min^{-1}$ = 5 $mL \cdot min^{-1} \cdot s^{-1}$, 50 $W \cdot min^{-1}$ = 8.3 $mL \cdot min^{-1} \cdot s^{-1}$).

In silico simulations of step-transitions. The validated multi-compartmental model (MCM) of Benson *et al.* (2013) was used to investigate the association between muscle and pulmonary $\dot{V}O_2$ responses to SI protocols. Briefly, mathematical expressions for O_2 delivery ($\dot{Q}$), muscle O_2 uptake, and a lumped compartment representing the rest of the body were joined in parallel by a single arterial compartment and multiple compartments on the venous side (representing blood draining the muscle, the rest of the body, and a mixed compartment approximating the blood volume proximal to the common femoral veins). The fractions of total metabolic rate (from muscle: 0.57; from body 0.43), cardiac output ($\dot{Q}_{tot}$; to muscle: 0.57; to body 0.43) and blood volume associated with muscle (0.7 L), body (0.1 L), and mixed compartments (2.3 L) were fixed while the WR and kinetic

variables for muscle and body $\dot{Q}$ ($\dot{Q}_m$ and $\dot{Q}_b$) and $\dot{V}O_2$ ($\dot{V}O_{2m}$ and $\dot{V}O_{2b}$) were manipulated experimentally to mimic the pre-transition conditions of the *in vivo* experiments and predict phase I and phase II $\dot{V}O_{2p}$ kinetics. The output of the model was instantaneous $\dot{V}O_{2p}(t)$:

$$\dot{V}O_{2p}(t) = \dot{Q}_t(t) \cdot (C_aO_2 - C_{\bar{v}}O_2)(t) \qquad (4.7)$$

where C_aO_2 is arterial O_2 content (fixed to 20 mL O_2 per 100 mL of blood), $C_{\bar{v}}O_2$ is mixed venous O_2 content, and $\dot{Q}_t$ is cardiac output. During the simulated exercise step-transitions, $\dot{Q}_m$ and $\dot{V}O_{2m}$ increased exponentially according to equation 2 (with TD = 0), toward their WR-dependent steady-state values with a steady-state relationship of 6 $L \cdot min^{-1}$ per 1 $L \cdot min^{-1}$ of $\dot{V}O_2$. The intercept of the $\dot{Q}$-to-$\dot{V}O_2$ relationship was set to 3.6 $L \cdot min^{-1}$ (Benson *et al.* 2013). Values of $\dot{V}O_2$ were dependent on WR inputs and functional gains (i.e., $\Delta\dot{V}O_2/\Delta W$). Values for $\dot{Q}$ in the various compartments were based on the $\dot{Q}$-to-$\dot{V}O_2$ relationship.

Simulations were undertaken to investigate how the homogenized $\dot{V}O_{2p}$ response to various single step-changes in WR from 20 W may be influenced by multiple muscle compartments that express heterogeneous metabolic properties (described by the $\tau\dot{V}O_{2p}$ and G_P vs WR relationships) and circulatory dynamics. Simulated step-changes from 20 W to 80 W, 160 W, 240 W, and 300 W were considered. A muscle compartments were created based on 5 W intervals beginning from 20 W and the number of muscle compartments recruited for a given step-change was determined by the ΔWR. Therefore, for a single step-change from 20 to 300 W, 57 muscle compartments were assumed to be simultaneously activated, whereas only 13, 29, and 45 muscle compartments were assumed activated for single step-changes from 20 to 80 W, 160 W and 240 W, respectively (assuming that the lower-order, more efficient muscle units are activated at the lower transitions with higher-order, less efficient muscle units being activated with greater step-changes in WR). The

$\tau\dot{V}O_{2m}$ and gain of a given compartment was determined by resolving the equation 4.3 and 4.4 using the compartment's corresponding WR (i.e., compartment #1 = 20 W, #2 = 25 W, #10 = 65….#57 = 300 W). $\tau\dot{Q}_m$ in each compartment was determined by assuming a ratio of $\tau\dot{V}O_{2m}$-to-$\tau\dot{Q}_m$ of 1.09 (Benson *et al.* 2013). The simulated $\dot{V}O_{2p}$ output was modeled using equation 4.2 with fitting window constrained from phase I to 180 s and from phase I to end exercise. Kinetics of the $\dot{V}O_{2p}$ simulation responses were compared amongst WR increments.

Statistical Analysis. Data are presented as mean ± SD. A two-way (model x fitting window) analysis of variance (ANOVA) with repeated measures was used to compare the sum of squared residuals of each model at various levels of data inclusion (fitting windows). Polynomial regression was used to characterize the effect of baseline WR on the kinetic parameters in the SI protocols. A one-way repeated measures ANOVA was also used to compare kinetic parameters and variables amongst the steps from SI. Where significant main effects were found, a Student Newman-Keul's *post hoc* analysis was performed for multiple comparisons testing. All statistical analyses were performed using SigmaPlot Version 11.0, (Systat Software Inc., San Jose, USA). Statistical significance was accepted at an alpha level less than 0.05.

Results

The $\dot{V}O_{2p}$ corresponding to the estimated LT averaged 2.18 ± 0.21 $L \cdot min^{-1}$ (range: 1.90 – 2.40 $L \cdot min^{-1}$), which corresponded to a mean WR of 162 ± 16 W (range: 135 – 180 W). This was corroborated in all participants by capillary blood lactate concentration

(Table 4.1). Table 4.1 shows the $\dot{V}O_{2p}$ kinetic parameters for the SI protocols. The $\dot{V}O_{2p}$ profile of a representative participant with phase II model fits and residuals for Protocols A and B are displayed in Figure 4.2. G_P and G_{tot} increased linearly with the baseline WR in SI ($p<0.05$), and $\tau\dot{V}O_{2p}$ and MRT increased in a curvilinear manner with baseline WR ($p<0.05$) (Figure 4.3). In all participants, the best fit models for rate ($\tau\dot{V}O_{2p}$ and MRT) and gain (G_P and G_{tot}) as a function of WR were a second-order polynomial and first-order polynomial, respectively (lowest AIC score). The group mean parameter estimates for the linear and curvilinear fits to the gain and time constant terms, respectively are presented in Figure 4.3.

Figure 4.4 displays the RI $\dot{V}O_{2p}$ response of three different representative participants with each model fit superimposed. For each participant, the $\dot{V}O_{2p}$ response to RI exercise was well described by a mono-exponential function (Model 1). The group mean τ' and G_{ramp} of the response (using equation 4.1) were 47 ± 19 s and 9.7 ± 0.63 $mL \cdot min^{-1} \cdot W^{-1}$, respectively. There was a model x window interaction ($p<0.05$) when the full RI $\dot{V}O_{2p}$ response was considered (i.e., fit from exercise onset to end exercise). The sum of squared error tended to be lower ($p<0.05$) in Model 1 (3.36 ± 0.84) compared to the Models 2 and 3 (12.51 ± 7.61 and 11.44 ± 9.22, respectively). However, there was no difference in the sum of squared residual error amongst model fits when the fit window included only data from exercise onset to 360 s (i.e., corresponding to WRs studied in the SI protocols). For this constrained fit window the sum of squared residuals were 0.92 ± 0.44, 1.32 ± 0.47, and 1.58 ± 0.61 for Models 1, 2, and 3, respectively ($p>0.05$).

The *in silico* simulations for RI exercise of varying ramp rates using the *in vivo* estimated parameters for $\dot{V}O_{2p}$ kinetics are presented in Figure 4.5. The group mean $\tau\dot{V}O_{2p}$

and G_P vs WR relationships depicted in Figure 4.3C and 4.3D were used to simulate the $\dot{V}O_{2p}$ response to RI exercise assuming three different ramp rates. $\dot{V}O_{2max}$ (using the group mean $\dot{V}O_{2max}$ of 4.23 $L \cdot min^{-1}$) was achieved at 315 W, 390 W, and 490 W for the 15 $W \cdot min^{-1}$, 30 $W \cdot min^{-1}$, and 50 $W \cdot min^{-1}$ ramps respectively (Figure 4.5A and 4.5B show $\dot{V}O_{2p}$ responses for each ramp rate plotted in relation to time and WR respectively). In contrast to the simulations of the 30 $W \cdot min^{-1}$ RI (where $\dot{V}O_{2p}$ responses were approximately linear), the $\dot{V}O_{2p}$ response profile was curvilinear upwards in the slow ramp (15 $W \cdot min^{-1}$) and curvilinear downwards in the fast ramp (50 $W \cdot min^{-1}$).

The *in silico* simulations for step-changes in WR from 20 W to 80 W, 160 W, 240 W, and 300 W are presented in Figure 4.6. Based on the group mean dynamic relationship of phase II $\tau\dot{V}O_{2p}$ and G_P vs WR, 57 theoretical muscle compartments were determined ($\tau\dot{V}O_{2m}$ and gain of each compartment was assigned in 5 W increments between 20 W and 300W based on the equations derived in Figure 4.3). The $\dot{V}O_{2p}$ output for each step-transition demonstrated that circulatory dynamics did not alter the $\dot{V}O_{2p}$ kinetics as phase II $\tau\dot{V}O_{2p}$ was 25 s, 33 s, 52 s, and 72 s for the Δ60 W, Δ140 W, Δ220 W, and Δ280 W steps, respectively; which was not appreciably different from the mean $\tau\dot{V}O_{2m}$ amongst muscle compartments included in each simulated step (mean $\tau\dot{V}O_{2m}$ of "recruited" compartments = 25 s, 36 s, 55 s, and 74 s). When only the first three minutes of the simulated $\dot{V}O_{2p}$ response were fit with a mono-exponential function, $\tau\dot{V}O_{2p}$ was greatly reduced in the two largest steps compared to the $\tau\dot{V}O_{2p}$ obtained from fitting the entire response ($\tau\dot{V}O_{2p}$ = 42 vs 52 s and 51 s vs 72 s for Δ220 W and Δ280 W, respectively). The end-exercise or "steady-state" $\dot{V}O_{2p}$ was well predicted from the group mean $\dot{V}O_{2p}$ response to RI exercise (these data were left-shifted by τ' to account for the early exponential phase and align $\dot{V}O_{2p}$

with WR) for the lowest intensity (20 to 80 W), however the simulated end-exercise or "steady-state" $\dot{V}O_{2p}$ was greater than predicted for the higher intensity steps with the magnitude of the difference increasing with increasing exercise intensity.

Table 4.1. Mean parameter estimates (± SD) for $\dot{V}O_{2p}$ kinetics during 60 W exercise transitions from eight different baseline work rates (Protocols A and B).

	Step-transition power output (W)							
n = 9	**20 → 80**	**50 → 110**	**80 → 140**	**110 → 170**	**140 → 200**	**170 → 230**	**200 → 260**	**230 → 290**
$\dot{V}O_{2pBSL}$ ($L \cdot min^{-1}$) *	0.86 ± 0.07	1.13 ± 0.07	1.38 ± 0.05	1.70 ± 0.06	1.98 ± 0.06	2.36 ± 0.07	2.67 ± 0.09	3.10 ± 0.14
A_P ($L \cdot min^{-1}$)	0.52 ± 0.04	0.56 ± 0.03	0.59 ± 0.02	0.63 ± 0.02^{abcfgh}	0.64 ± 0.03^{abcfgh}	0.67 ± 0.05	0.72 ± 0.12	0.72 ± 0.12
$\tau\dot{V}O_{2p}$ (s)	21 ± 5†	24 ± 5†	34 ± 12†	38 ± 6†	50 ± 13 †	66 ± 12†	84 ± 18^{a-f}	98 ± 20^{a-f}
G_P ($mL \cdot min^{-1} \cdot W^{-1}$)	8.7 ± 0.6†	9.3 ± 0.4†	9.8 ± 0.4†	10.4 ± 0.3^{abcfgh}	10.6 ± 0.5^{abcfgh}	11.1 ± 0.8†	11.8 ± 1.2†	12.0 ± 1.9†
$\dot{V}O_{2pEND}$ ($L \cdot min^{-1}$) *	1.39 ± 0.05	1.71 ± 0.06	1.99 ± 0.06	2.36 ± 0.07	2.67 ± 0.09	3.11 ± 0.14	3.52 ± 0.19	3.93 ± 0.30
MRT (s) *	30 ± 5	36 ± 7	46 ± 14	51 ± 6	71 ± 24	101 ± 26	135 ± 39	132 ± 40
G_{tot} ($mL \cdot min^{-1} \cdot W^{-1}$)	8.8 ± 0.6†	9.5 ± 0.4†	10.0 ± 0.4†	10.9 ± 0.3†	11.5 ± 0.7†	12.5 ± 1.2†	14.2 ± 2.0^{a-f}	13.7 ± 3.3^{a-f}
$Lactate_{BSL}$ (mM)	1.4 ± 0.1	1.5 ± 0.2	1.4 ± 0.2	1.6 ± 0.3	1.9 ± 0.5^{abcd}	2.5 ± 0.5^{abcde}	3.4 ± 0.8†	4.7 ± 1.1†

$^{a-h}$ indicate significant differences between conditions ($p<0.05$). "^{a}" indicates difference from "**20 → 80**", "^{b}" indicates difference from "**50 → 110**", and so forth. * indicates significant differences amongst all conditions ($p<0.05$). † indicates difference from all other conditions.

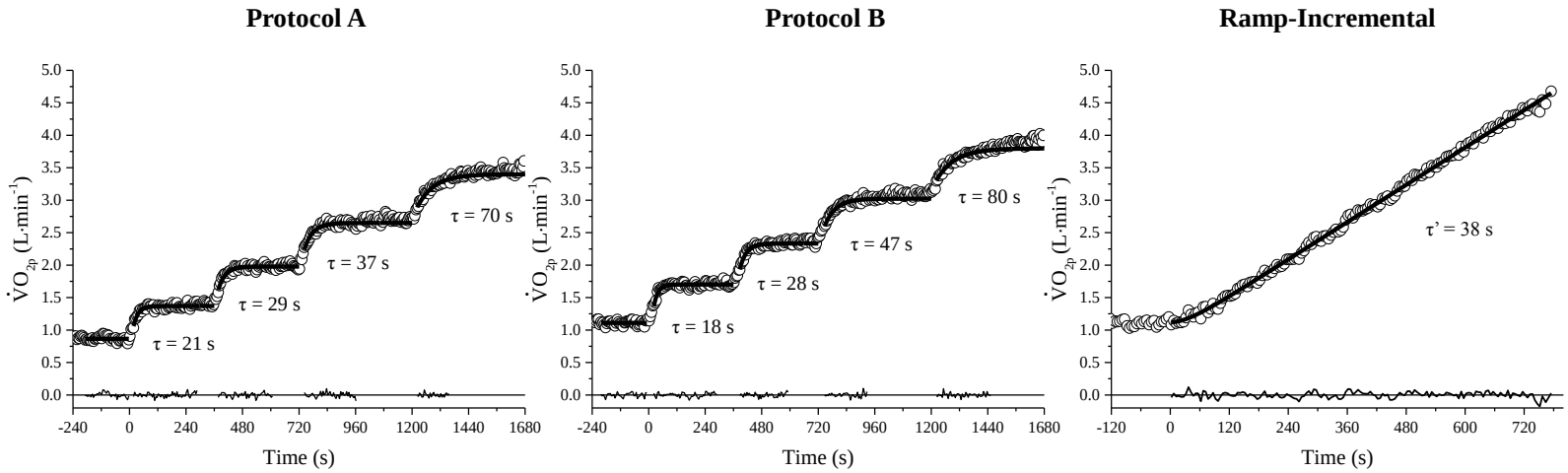

Figure 4.2. The $\dot{V}O_{2p}$ response profile of a representative participant from each exercise protocol (Protocol A, *left*; Protocol B, *centre*; and Ramp-incremental, *right*). Phase II kinetic responses for step-transitions from Protocols A and B and the mono-exponential fit to ramp-incremental exercise are superimposed over the data (*black lines*, fitted with a mono-exponential function). $\tau\dot{V}O_{2p}$ values (Protocols A and B) and the ramp mean response time (τ') value are inset under each transition. Residuals of each fit are shown about y = 0 (*grey line*).

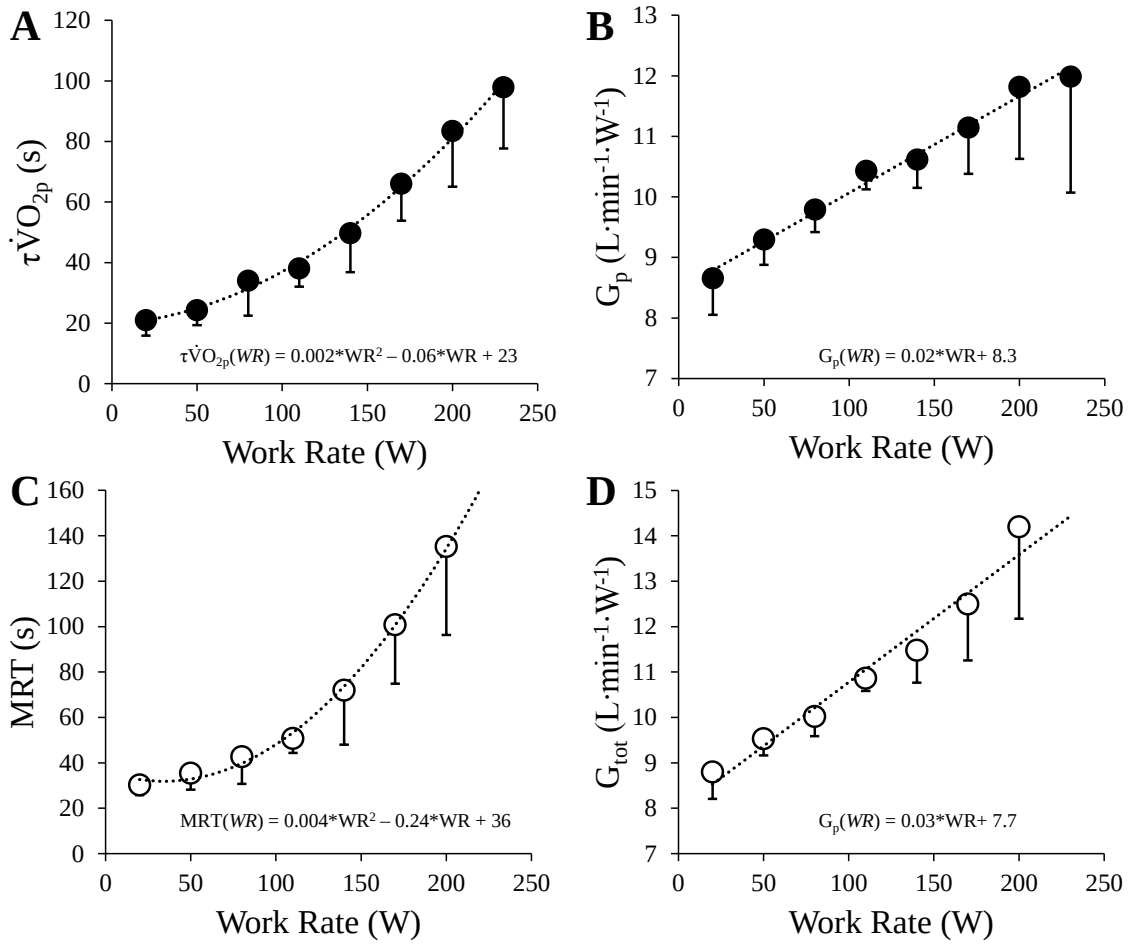

Figure 4.3. A) Phase II $\dot{V}O_{2p}$ time constant ($\tau\dot{V}O_{2p}$) as function of baseline work rate. B) Phase II functional gain (G_P) as function of baseline work rate. C) Mean response time (MRT) as function of baseline work rate. D) Total gain (G_{tot}) as function of baseline work rate. Symbols represent group mean ± SD. Three of the nine participants were unable to complete the full step-transition from a baseline of 230 W and most reached $\dot{V}O_{2max}$ during the 290 W intensity, thus the data point corresponding to this step-transition was excluded from the analysis for the model based on the overall step-change response (Model 3). The best fit models describing each parameter as a function of work rate are superimposed over each panel with equations displayed using group mean parameter estimates. Note that the $\tau\dot{V}O_{2p}$ and MRT vs work rate (WR) relationships are described by a second-order polynomial and the G_P and G_{tot} vs WR relationships are described by a first-order polynomial.

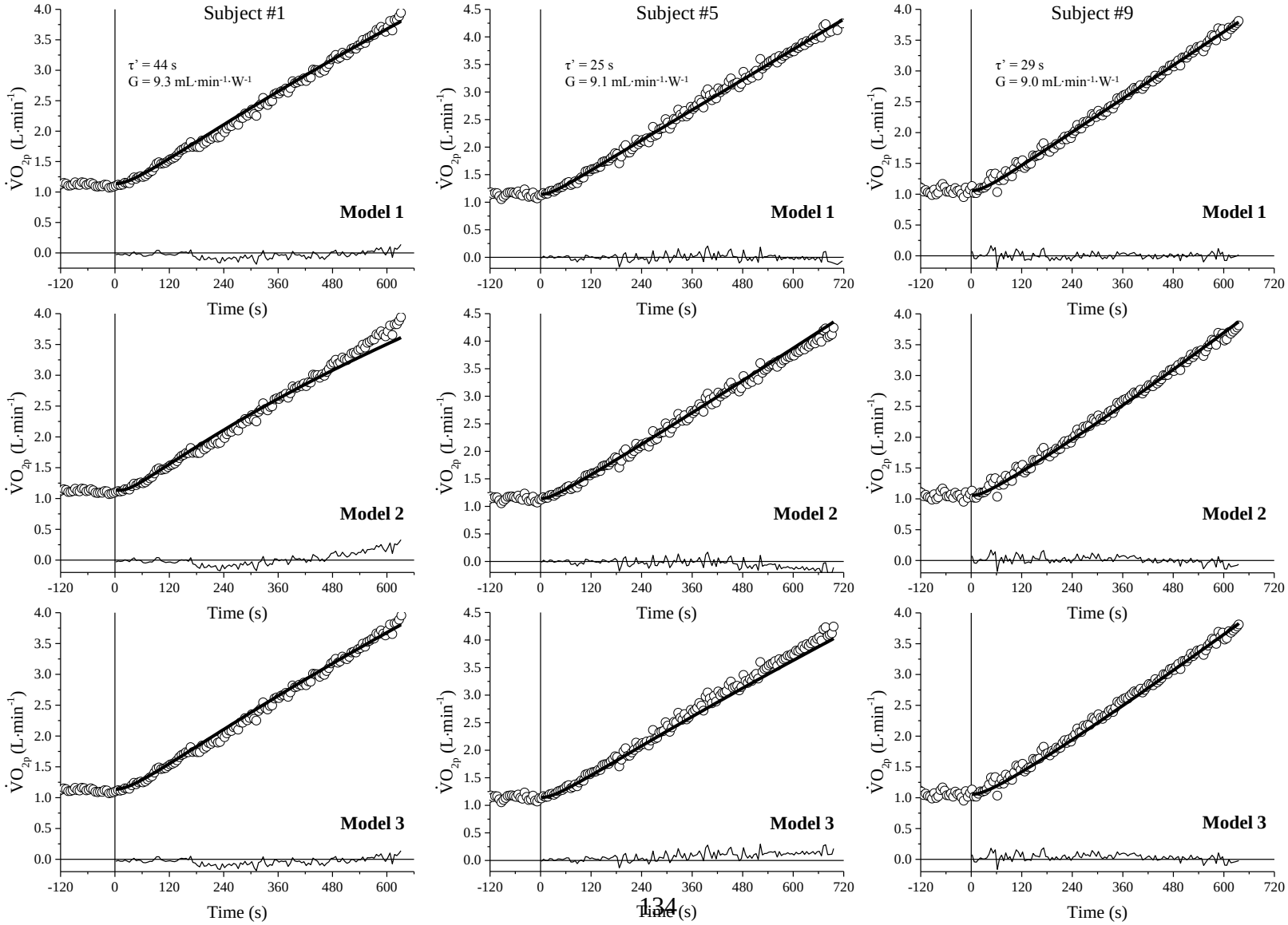
Subject #1
τ' = 44 s
G = 9.3 mL·min-1·W-1
Subject #5
τ' = 25 s
G = 9.1 mL·min-1·W-1
Subject #9
τ' = 29 s
G = 9.0 mL·min-1·W-1
Model 1
Model 2
Model 3
V̇O2p (L·min-1)
Time (s)

Figure 4.4. Comparison of model fits to ramp-incremental (RI) exercise for three representative individuals. *Top row*, Mono-exponential (Model 1) fits are superimposed over the data (*black lines*). The mean response time (τ') and gain (G) parameter values derived from the model are inset, and model residuals displayed about $y = 0$. *Middle row*, Model 2 simulation (based on the phase II variable time constant and gain) is superimposed over the $\dot{V}O_{2p}$ vs time response to RI exercise for the same three representative individuals as the top row. The phase II time constant and gain parameters at any time (t) were resolved based on polynomial regressions of each individual and substituted into equation 1 to derive Model 2 (see text for details). The predicted $\dot{V}O_{2p}$ RI response was left-shifted by ~15 s (to account for the limb-to-lung transit time); fit residuals are displayed about $y = 0$. *Bottom row*, Model 3 simulation (based on the overall time constant and gain) is superimposed over the $\dot{V}O_{2p}$ vs time response to RI. The mean response time (MRT) and total gain (G_{tot}) parameters at any time (t) were resolved based on polynomial regressions of each individual and substituted into equation 1 to derive Model 3; fit residuals are displayed about $y = 0$. The vertical line in each panel indicates the onset of RI exercise.

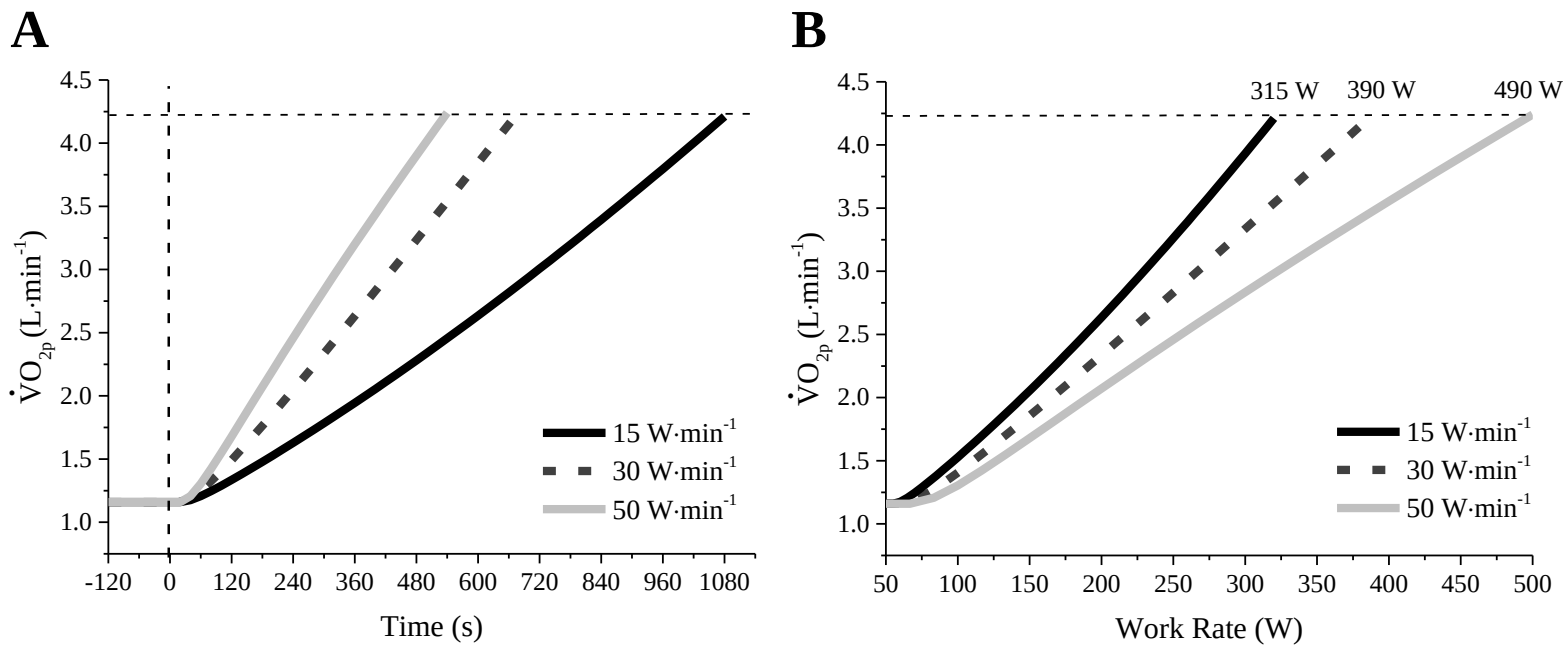

Figure 4.5. The phase II time constant ($\tau\dot{V}O_{2p}$) and gain (G_P) vs baseline WR relationships were used to simulate the $\dot{V}O_{2p}$ response to ramp-incremental exercise of varying slopes (30 W·min^{-1}, *dashed line*; 15 W·min^{-1}, *grey line*; and 50 W·min^{-1}, *black line*). The simulated $\dot{V}O_{2p}$ response predictions are presented as a function of time (panel A) and work rate (panel B). Note the deviation of the conventional "linear" $\dot{V}O_{2p}$ response (i.e., from RI exercise = 30 W·min^{-1}) in the slow (15 W·min^{-1}) and fast (50 W·min^{-1}) ramp protocols. In particular, the slow ramp protocol allows sufficient time for the kinetically slower and less oxidatively efficient muscle fiber populations associated with higher work rates to be expressed in the $\dot{V}O_{2p}$ response (see text for details).

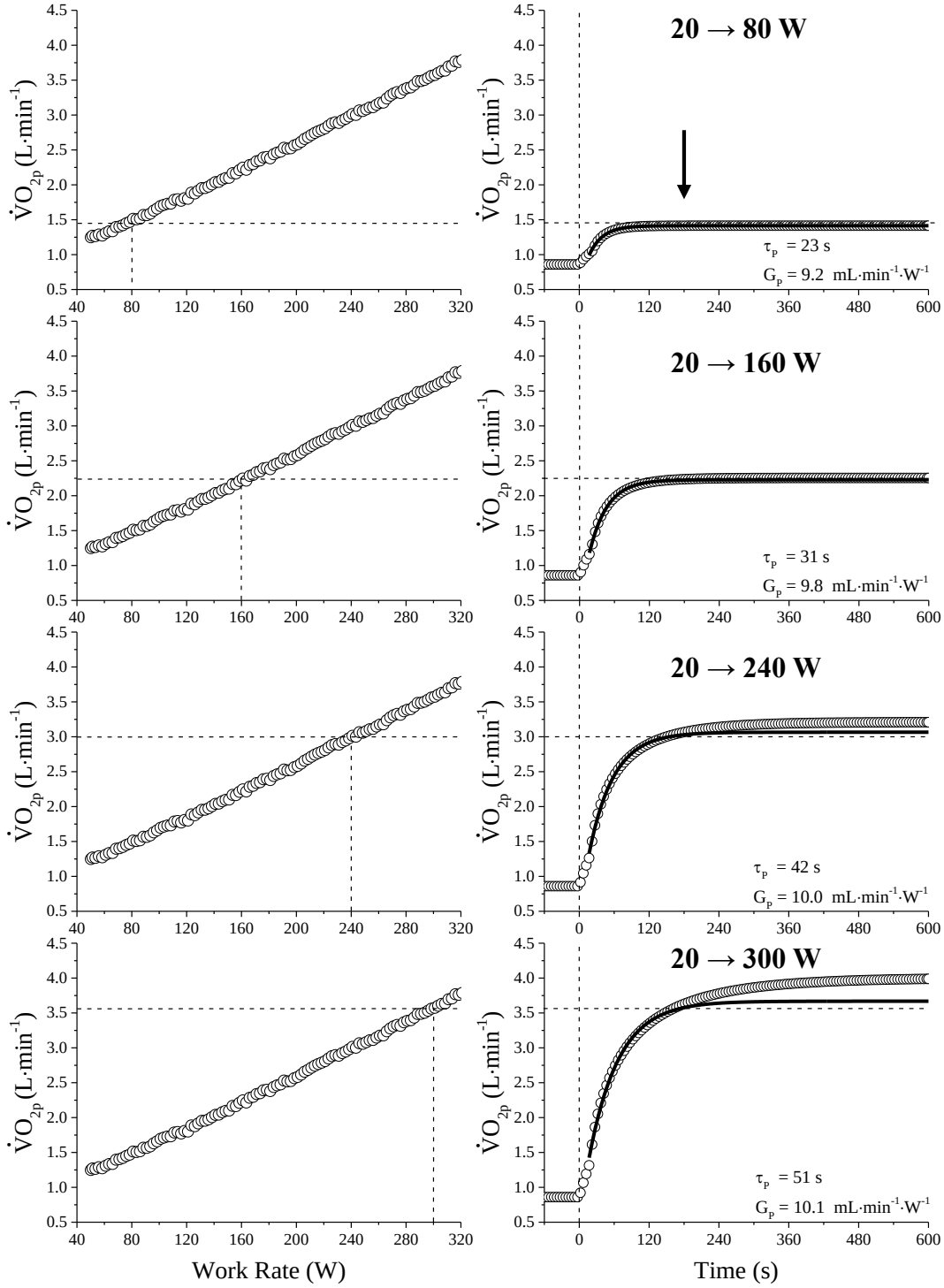
20 → 80 W
τp = 23 s
Gp = 9.2 mL·min-1·W-1
20 → 160 W
τp = 31 s
Gp = 9.8 mL·min-1·W-1
20 → 240 W
τp = 42 s
Gp = 10.0 mL·min-1·W-1
20 → 300 W
τp = 51 s
Gp = 10.1 mL·min-1·W-1
V̇O2p (L·min-1)
Work Rate (W)
Time (s)

Figure 4.6. Simulated $\dot{V}O_{2p}$ outputs for step-changes from 20 W to 80 W, 160 W, 240 W, and 300 W using a multi-compartment muscle model with variable inter-compartmental $\tau\dot{V}O_{2m}$ and gain based on the group mean $\tau\dot{V}O_{2p}$ and G_P vs WR relationships are portrayed (right panels). The left panels display the group mean $\dot{V}O_{2p}$ response to RI exercise plotted as a function of WR. These data were left-shifted by the group average ramp mean response time (τ') to account for the kinetic component of the ramp and to align WR with the local metabolic responses. *Dashed horizontal lines* indicate the predicted steady-state $\dot{V}O_{2p}$ expected based on the linear $\dot{V}O_{2p}$ vs WR relationship from RI exercise. Note that for higher intensities of exercise, the $\dot{V}O_{2p}$ output response projects above that predicted from the $\dot{V}O_{2p}$ vs WR relationship corresponding to the ramp. Mono-exponential model fits are superimposed over the $\dot{V}O_{2p}$ profile for each step-change in WR. The *dashed vertical line* indicates the onset of exercise at time "zero" and the downward arrow indicates the end of the fitting window (i.e., 180 seconds). This fitting window (end of phase I to 180 s) was used to model each of the step-changes; $\tau\dot{V}O_{2p}$ and G_P for each fit are inset within each panel.

Discussion

There is an apparent dichotomy for the control of $\dot{V}O_{2p}$ dynamics during exercise in that $\dot{V}O_{2p}$ kinetics vary with work rate in response to step-changes, but do not in ramp exercise. The purpose of this study was to examine $\dot{V}O_{2p}$ kinetic responses to SI and RI exercise, in the same participants, to determine whether work rate-dependent kinetics from SI exercise can result in an apparently linear $\dot{V}O_{2p}$ RI response. This was accomplished by establishing a relationship between $\dot{V}O_{2p}$ time constant and $\dot{V}O_{2p}$ gain vs WR (using $\dot{V}O_{2p}$ kinetic analyses during SI exercise) and comparing the measured $\dot{V}O_{2p}$ responses to ramp exercise to models consisting of constant (linear) or variable (non-linear) time constant and gain parameters. Although the $\dot{V}O_{2p}$ response to RI exercise appeared linear, and was well described by a mono-exponential function, we demonstrate that these dynamics were as well characterized when the $\dot{V}O_{2p}$ time constant and gain parameters were allowed to covary to a magnitude based on measurements in the same participants; both progressively increasing as a function of WR.

Interactions between $\dot{V}O_{2p}$ time constant and gain parameters during ramp-incremental exercise. In accordance with previous work using RI exercise of ~20-30 $W^{-1}{\cdot}min^{-1}$, the $\dot{V}O_{2p}$ response increased in a linear manner, after an initial lag phase, and well described by a mono-exponential function with τ' and G_{ramp} parameters. The values we found were similar to those reported in healthy populations (τ' ~ 45 s and G_{ramp} ~ 10 $mL{\cdot}min^{-1}{\cdot}W^{-1}$) (Whipp *et al.* 1981; Hughson & Inman, 1986; Swanson & Hughson, 1988). This finding supports the long standing notion that $\dot{V}O_{2p}$ kinetics are controlled by a dynamically linear, first-order process (Whipp *et al.* 1981; Rossiter, 2011). The principle of superposition mandates that were $\dot{V}O_{2p}$ control to be dynamically linear, the $\dot{V}O_{2p}$ responses to step-

increments should be characterized by τ and G values equal to that of ramp exercise (Barstow & Mole, 1991). In contrast, coherence between kinetic responses to RI and SI exercise was not observed. Rather, $\dot{V}O_{2p}$ kinetic analyses of SI exercise demonstrated that both phase II $\tau\dot{V}O_{2p}$ and MRT increase curvilinearly and G_P and G_{tot} increase linearly as a function of baseline WR (Figure 4.3). Therefore, while the $\dot{V}O_{2p}$ response dynamics to RI exercise appeared to be consistent with a system controlled by linear, first order process, the $\dot{V}O_{2p}$ kinetics from SI exercise were inconsistent with this assertion.

Differentiating amongst models

Based on the $\dot{V}O_{2p}$ kinetic relationships from SI exercise, we examined whether the linear $\dot{V}O_{2p}$ response to RI exercise could also be well described by an exponential function consisting of variable time constant and gain parameters (Models 2 and 3). To accomplish this, $\dot{V}O_{2p}$ ramp responses were predicted by substituting the time constant and gain parameter functions established from SI exercise into the exponential equation (equation 1) to obtain a $\dot{V}O_{2p}$ vs time relationship. Predicted $\dot{V}O_{2p}$ responses were then overlaid on the measured $\dot{V}O_{2p}$ vs time relationship (Models 2 and 3; Figure 4.4) and the sum of squared residuals were calculated to assess the goodness of fit of each model. Since Models 2 and 3 were derived from step-changes up to 230 W, and it was necessary to extrapolate these models to fit the entire ramp response (group mean WR_{peak}, 393 ± 25 W). We found that the mono-exponential fitted model (Model 1) had a lower sum of squared residuals (compared to Models 2 and 3) only when the entire $\dot{V}O_{2p}$ ramp response was considered. This was not surprising given that modeling of the full response for Models 2 and 3 included predicted $\dot{V}O_{2p}$ data based on extrapolated time constant and gain parameters. Nevertheless, these data demonstrate that the conflation between these variable time

constant and gain parameters estimates (through their relationship with WR) can produce a $\dot{V}O_{2p}$ ramp response that is approximately linear and closely resembles the kinetics *in vivo*.

Interestingly, Model 2 (derived from phase II kinetics) was not different from Model 3 (derived from the overall mean response). The early exponential phase of the $\dot{V}O_{2p}$ ramp response is described by τ' (or the MRT). Importantly, this parameter incorporates both a τ (reflective of the response dynamics of the system) and a time delay resulting from the time interval for local metabolic responses to reach the lungs. Thus, it is not possible to discriminate a single time delay in the $\dot{V}O_{2p}$ ramp response, because the limb-to-lung transit time varies throughout the ramp. For this reason, it was necessary to right-shift the predicted $\dot{V}O_{2p}$ response based on phase II $\dot{V}O_{2p}$ kinetics (Model 2) by ~ 15 s to account for the limb-lung transit delay. Given that both the phase II $\tau\dot{V}O_{2p}$ and G_P values (measured from SI exercise) were consistently lower than the MRT and G_{tot} values (as a function of WR), and that the variance in both time constants and gains were similarly well described by a second-order and first-order polynomial, respectively, the $\dot{V}O_{2p}$ response to RI predicted by each model fitted the measured response equally well.

That the $\dot{V}O_{2p}$ RI response was well-fitted by a mono-exponential function (Model 1) in addition to the variable fits (Models 2 and 3) makes it difficult to discriminate amongst models. The variable models (particularly Model 2) were constructed based on parameter values thought to represent the individual metabolic properties of the active muscle fibre pools, and therefore they may more closely reflect the underlying muscle-physiological properties that combine to determine the $\dot{V}O_{2p}$ RI response. It may also be considered whether the high goodness-of-fit of Model 1 could withstand further experimental scrutiny.

For example, in slowly incrementing ramp protocols, the $\dot{V}O_{2p}$ response is commonly observed to curve upwards sometime after the LT i.e., increase in excess of the expected linear response (Scheuermann & Kowalchuk, 1998; Zoladz & Korzeniewski, 2001). As a consequence, individuals have been reported to reach $\dot{V}O_{2max}$ and exercise intolerance at lower WRs in low slope protocols compared to the maximal WR that would be expected based on the linear, sub-LT $\dot{V}O_{2p}$ vs WR relationship, or from the maximal WR during faster incrementing ramp protocols (Davis *et al.*, 1982; Hansen *et al.*, 1988; Takaishi *et al.*, 1992; Boone & Bourgois, 2012). This phenomenon has been attributed to the low slope of the WR vs time relationship which affords sufficient time for the $\dot{V}O_{2p}$ "slow component" to be expressed (Zoladz & Korzeniewski, 2001).

Although we did not measure the $\dot{V}O_{2p}$ response to varying ramp slopes, the group mean time constant and gain vs WR relationships (Model 3) enabled us to simulate the $\dot{V}O_{2p}$ response to a slow (15 $W \cdot min^{-1}$), medium (30 $W \cdot min^{-1}$) and fast (50 $W \cdot min^{-1}$) incrementing ramp protocol. The output of those simulations (Figure 4.5) indicated that the $\dot{V}O_{2p}$ vs WR and $\dot{V}O_{2p}$ vs time relationships would be approximately linear for the 30 $W \cdot min^{-1}$ ramp protocol and would achieve $\dot{V}O_{2max}$ at 390 W, which was almost identical to our measured WR_{peak} of 393 ± 25 W. They also showed that the $\dot{V}O_{2p}$ response would be curvilinear upward for a slow ramp protocol achieving $\dot{V}O_{2max}$ at 315 W (an outcome identical to those reported comparing slow vs faster ramp protocols (Hansen *et al.* 1988; Takaishi *et al.* 1992; Scheuermann & Kowalchuk, 1998). Our simulations were also consistent with the finding of a steeper $\dot{V}O_{2p}$ vs WR slope for fast ramp protocols (50 $W \cdot min^{-1}$) (Takaishi *et al.* 1992; Scheuermann & Kowalchuk, 1998). Given that a mono-exponential model, by definition, would be unable to predict a $\dot{V}O_{2p}$ response to slow ramp

exercise that is curvilinear upward and that our variable model predicted a response similar to those previously reported, these analyses indicate that the mono-exponential model might fail to characterize the ramp response (where the variable model would) under a different set of ramp conditions. However, this remains to be tested. Interestingly, these analyses suggest that the curvilinear increase in $\dot{V}O_{2p}$ that appears during slow RI protocols may not necessarily reflect an "excess" $\dot{V}O_{2p}$, *per se*, i.e., reflecting a drop in mechanical efficiency, rather, it may reflect a progressive recruitment of higher-order, muscle fibres that are kinetically slower and require a greater O_2 cost of force production.

In silico analyses: considerations for step exercise

Phase II $\dot{V}O_{2p}$ kinetics have been reported to be invariant with WR increment (Barstow & Mole 1991; Özyener *et al.* 2001; Scheuermann & Barstow 2003; Spencer *et al.* 2013). However, Keir *et al.* (Chapter III) recently suggested that the invariant, fast, $\dot{V}O_{2p}$ kinetic responses may occur due to the transit and mixing of venous blood draining kinetically variable populations of muscle fibres that are later summed to form an on-transient $\dot{V}O_{2p}$ kinetic response that is dominated by the "kinetically fast" muscle fibre pools (at least within the moderate-intensity domain). The present study attempted to extend these findings beyond the confines of the moderate-intensity domain by investigating whether heterogeneity in both dynamics of muscle fibre recruitment (of fibres with a different volume of mitochondrial network) and of blood flow (where the red blood cell transit times vary to a similar magnitude to $\dot{V}O_{2p}$ kinetics) could also influence the later portion of the exercise on-transient (i.e., phase III) such that the "kinetically" slow muscle fibre populations (e.g., higher-order, type II fibres pools) are predominately expressed later in the response resulting in a $\dot{V}O_{2p}$ profile that takes longer to attain a

steady-state and that projects above the $\dot{V}O_{2p}$ that would be expected based on the $\dot{V}O_{2p}$ vs WR relationship from RI exercise (especially for those WRs above LT).

That the early portion (phase II) on transition to supra-LT exercise has been reported to be well described by a mono-exponential with similar or slightly slower kinetics to those within the moderate intensity domain (Paterson & Whipp 1991; Koga *et al.* 2001; Özyener *et al.* 2001; Jones *et al.* 2002; Pringle *et al.* 2003) provides the greatest evidence supporting an "extra" component of the $\dot{V}O_{2p}$ response that is of delayed onset (usually ~120 s). This finding challenges the assumption that $\dot{V}O_{2p}$ adapts to changes in metabolism with linear, first-order kinetics. Using *in silico* simulations based on a validated multi-compartmental model of circulatory dynamics (Benson *et al.* 2013) we were able to examine a theoretical multi-muscle compartment model to step-changes in WR from a baseline of 20 W to 80 W, 160 W, 240 W, and 300 W. Assuming that all muscle compartments were under first-order control and that activation of each compartment occurred simultaneously at exercise onset, the $\dot{V}O_{2p}$ output was modeled with a mono-exponential function with a fitting window including data from the end of phase I to: 1) the end of the transition and 2) to 3 min (roughly corresponding to typically reported phase III TD; see Figure 4.6). While $\tau\dot{V}O_{2p}$ was reduced only slightly from the mean $\tau\dot{V}O_{2m}$ amongst compartments for the low WR increment steps ($\tau\dot{V}O_{2p}$ Δ60 W = 25 s vs 23 s and $\tau\dot{V}O_{2p}$ Δ140 W = 36 vs 31 s, for full vs 3 min fits, respectively), a disparity became increasingly apparent for the larger WR increment steps ($\tau\dot{V}O_{2p}$ Δ220 W = 55 s vs 42 s and $\tau\dot{V}O_{2p}$ Δ280 W = 74 vs 51 s, for full vs. 3 min fits, respectively) indicating that fitting strategy can greatly affect $\dot{V}O_{2p}$ kinetic parameter estimates particularly at high exercise intensities.

Our *in silico* analyses suggest that the appearance of this "excess" $\dot{V}O_{2p}$ may, in part, be resultant of "kinetically slow" muscle fibre pools being expressed later at the pulmonary level. We hypothesized that the overall $\dot{V}O_{2p}$ response to a step-change in WR could be a distortion of the $\dot{V}O_{2m}$ signal where the early portion (i.e., the on-transient or phase II) appears relatively fast (dominated by the faster, lower-order fibre pools) and after some time has passed (phase III) the $\dot{V}O_{2p}$ signal is dominated by the slower, higher-order fibre pools manifesting as a slow developing or "excess" component of $\dot{V}O_{2p}$. Contrary to our hypothesis, we did not observe a definitive "breakpoint" in the homogenized $\dot{V}O_{2p}$ response indicative of a phase III time delay or the onset of a slow component. Heterogeneity did appear to be reflected in the pulmonary response, with slower compartments manifesting later in the transient, however their influence was smooth and gradual, likely due to the gradual changes in $\tau\dot{V}O_{2m}$ and $\tau\dot{Q}_m$ and relatively low venous volumes amongst compartments. Nevertheless, these data provide an alternative perspective as to why it takes longer for $\dot{V}O_{2p}$ to attain "steady-state" with step-transitions to higher intensities of constant-load exercise and also why the total $\dot{V}O_{2p}$ gain increases in an intensity-dependent manner, beyond what would be expected based on the linear $\dot{V}O_{2p}$ vs WR relationship obtained from conventional RI exercise.

In silico analyses: assumptions

It is acknowledged that the simulated responses presented in this paper were constructed based on a number of assumptions regarding human skeletal muscle. The major assumptions of our multi-compartment model were that human muscle consists of a range, or continuum, of muscle fibre pools that are: 1) under first-order control; 2) that have both progressively slower $\dot{V}O_{2m}$ and $\dot{Q}_m$ kinetics and that are progressively less efficient in their

use of O_2 for metabolism; 3) that are recruited in a progressive manner related to WR such that the most oxidative and kinetically efficient (presumably those with the highest mitochondrial volume and capillary density) are activated at very low intensities and the least oxidative (most glycolytic) and most kinetically inefficient fibres pools are reserved for higher intensities of muscular work; and 4) that are instantaneously and concurrently activated at exercise onset to address a given change in WR. However, all of these assumptions may, in part, be supported by the literature. For example, there is evidence to suggest that the on-transient response of single skeletal muscle fibres is well characterized by a first-order response (Kindig *et al.* 2003; Wüst *et al.* 2013). Additionally, it is well established that human skeletal muscle consists of populations of muscle fibres that are metabolically and spatially heterogeneous (Kalliokoski *et al.* 2000; Richardson *et al.* 2001) and regionally non-uniform in their capillary density (Porter *et al.* 2002; Groen *et al.* 2014) with slow oxidative fibres likely being perfused to a greater extent compared to fast glycolytic fibres (Laughlin *et al.* 1996). Thus, it may be expected that blood flow to and from these heterogeneous populations is unequally distributed both at rest and during exercise (Piiper, 2000; Behnke *et al.* 2003; McDonough *et al.* 2005) and that kinetics of blood flow are slower in higher- compared to lower-order muscle fibres (McDonough *et al.* 2005). Finally, using electromyography, it has been reported that muscle activation increases almost instantaneously at exercise onset and remains stable as long as WR remains constant (Scheuermann *et al.* 2001) supporting the notion that muscle fibres of varying order are concurrently recruited at exercise onset.

Conclusions

In accordance with the suggestion of Whipp *et al.* (2002), this study demonstrates that a continually varying time constant and gain throughout RI exercise can obscure the non-linear characteristics of $\dot{V}O_{2p}$ and yield a profile that appears to behave like a dynamically linear system. The implication of a "linear" RI $\dot{V}O_{2p}$ response that is well-described by variable time constant and gain parameters is that the muscle fibres that contribute to the response are kinetically heterogeneous. Based on this interpretation, our *in vivo* data suggest that in human skeletal muscle, there exists a continuum of $\dot{V}O_2$ kinetics within muscle fibre pools that are recruited in a hierarchical fashion. These pools respond to changes in metabolic demand with first-order $\dot{V}O_2$ kinetics that are progressively slower and progressively less efficient in their use of O_2 to synthesize energy as work rate increases. Furthermore, our *in silico* analyses indicated that this "muscle metabolic heterogeneity" can explain the curvilinear profile of $\dot{V}O_{2p}$ that is observed during slow ramp protocols, and the increase in total $\dot{V}O_{2p}$ gain during constant-load exercise at intensities above the lactate threshold.

References

Barstow TJ & Mole PA (1991). Linear and nonlinear characteristics of oxygen uptake kinetics during heavy exercise. *J Appl Physiol (1985)* **71**, 2099-2106.

Behnke BJ, McDonough P, Padilla DJ, Musch TI & Poole DC (2003). Oxygen exchange profile in rat muscles of contrasting fibre types. *J Physiol* **549**, 597-605.

Benson AP, Grassi B & Rossiter HB (2013). A validated model of oxygen uptake and circulatory dynamic interactions at exercise onset in humans. *J Appl Physiol (1985)* **115**, 743-755.

Boone J & Bourgois J (2012). The oxygen uptake response to incremental ramp exercise: methodogical and physiological issues. *Sports Med* **42**, 511-526.

Bowen TS, Murgatroyd SR, Cannon DT, et al. (2011). A raised metabolic rate slows pulmonary O_2 uptake kinetics on transition to moderate-intensity exercise in humans independently of work rate. *Exp Physiol* **96**, 1049-1061.

Brittain CJ, Rossiter HB, Kowalchuk JM & Whipp BJ, (2001). Effect of prior metabolic rate on the kinetics of oxygen uptake during moderate-intensity exercise. *Eur J Appl Physiol* **86**, 125-134.

Cannon DT, White AC, Andriano MF, Kolkhorst FW & Rossiter HB (2011). Skeletal muscle fatigue precedes the slow component of oxygen uptake kinetics during exercise in humans. *J Physiol* **589,** 727–739.

Davis JA, Whipp BJ, Lamarra N, Huntsman DJ, Frank MH & Wasserman K, (1982). Effect of ramp slope on determination of aerobic parameters from the ramp exercise test. *Med Sci Sports Exerc* **14**, 339-343.

DiMenna F & Jones AM, (2009). "Linear" versus "nonlinear" VO2 responses to exercise: reshaping traditional beliefs **7**, 67-84.

DiMenna FJ, Bailey SJ, Vanhatalo A, Chidnok W & Jones AM (2010). Elevated baseline VO_2 per se does not slow O_2 uptake kinetics during work-to-work exercise transitions. *J Appl Physiol (1985)* **109**, 1148-1154.

Fujihara Y, Hildebrandt JR & Hildebrandt J (1973). Cardiorespiratory transients in exercising man. I. Tests of superposition. *J Appl Physiol* 35, 58-67.

Grassi B, Rossiter HB & Zoladz JA (2015). Skeletal muscle fatigue and decreased efficiency: two sides of the same coin? *Exerc Sport Sci Rev* **43,** 75–83.

Groen BB, Hamer HM, Snijders T, et al. (2014). Skeletal muscle capillary density and microvascular function are compromised with aging and type 2 diabetes. *J Appl Physiol (1985)* **116**, 998-1005.

Hansen JE, Casaburi R, Cooper DM & Wasserman K (1988). Oxygen uptake as related to work rate increment during cycle ergometer exercise. *Eur J Appl Physiol Occup Physiol* **57**, 140-145.

Hughson RL & Inman MD (1986). Oxygen uptake kinetics from ramp work tests: variability of single test values. *J Appl Physiol (1985)* **61**, 373-376.

Jones AM, Carter H, Pringle JS & Campbell IT (2002). Effect of creatine supplementation on oxygen uptake kinetics during submaximal cycle exercise. *J Appl Physiol (1985)* **92**, 2571-2577.

Kalliokoski KK, Kemppainen J, Larmola K, et al. (2000). Muscle blood flow and flow heterogeneity during exercise studied with positron emission tomography in humans. *Eur J Appl Physiol* **83**, 395-401.

Keir DA, Nederveen JP, Paterson DH & Kowalchuk JM (2014). Pulmonary O_2 uptake kinetics during moderate-intensity exercise transitions initiated from low versus elevated metabolic rates: insights from manipulations in cadence. *Eur J Appl Physiol* **114**, 2655-2665.

Kindig CA, Kelley KM, Howlett RA, Stary CM & Hogan MC (2003). Assessment of O_2 uptake dynamics in isolated single skeletal myocytes. *J Appl Physiol* **94**, 353-357.

Koga S, Barstow TJ, Shiojiri T, et al. (2001). Effect of muscle mass on VO_2 kinetics at the onset of work. *J Appl Physiol (1985)* **90**, 461-468.

Lamarra N, Whipp BJ, Ward SA & Wasserman K (1987). Effect of interbreath fluctuations on characterizing exercise gas exchange kinetics. *J Appl Physiol* **62**, 2003-2012.

Laughlin MH, Korthuis RJ, Dunker DJ & Bache RJ (1996). Control of blood flow to cardiac and skeletal muscle during exercise. In Handbook of Physiology, Section 12, Exercise: Integration and Regulation of Multiple Systems. ed. Rowell LB & Shepherd JT, pp. 705-769. American Physiological Society, Bethesda, MD.

MacPhee SL, Shoemaker JK, Paterson DH & Kowalchuk JM (2005). Kinetics of O_2 uptake, leg blood flow, and muscle deoxygenation are slowed in the upper compared with lower region of the moderate-intensity exercise domain. *J Appl Physiol* **99**, 1822-1834.

McDonough P, Behnke BJ, Padilla DJ, Musch TI & Poole DC (2005). Control of microvascular oxygen pressures in rat muscles comprised of different fibre types. *J Physiol* **563**, 903-913.

Meyer K, Schwaibold M, Hajric R, et al., (1998). Delayed VO_2 kinetics during ramp exercise: a criterion for cardiopulmonary exercise capacity in chronic heart failure. *Med Sci Sports Exerc* **30**, 643-648.

Özyener F, Rossiter HB, Ward SA & Whipp BJ (2001). Influence of exercise intensity on the on- and off-transient kinetics of pulmonary oxygen uptake in humans. *J Physiol* **533**, 891-902.

Paterson DH & Whipp BJ (1991). Asymmetries of oxygen uptake transients at the on- and offset of heavy exercise in humans. *J Physiol* **443**, 575-586.

Piiper J (2000). Perfusion, diffusion and their heterogeneities limiting blood-tissue O_2 transfer in muscle. *Acta Physiol Scand* **168**, 603-607.

Porter MM, Stuart S, Boij M & Lexell J (2002). Capillary supply of the tibialis anterior muscle in young, healthy, and moderately active men and women. *J Appl Physiol* **92**, 1451-1457.

Pringle JS, Doust JH, Carter H, et al. (2003). Oxygen uptake kinetics during moderate, heavy and severe intensity "submaximal" exercise in humans: the influence of muscle fibre type and capillarisation. *Eur J Appl Physiol* **89**, 289-300.

Richardson RS, Haseler LJ, Nygren AT, Bluml S & Frank LR (2001). Local perfusion and metabolic demand during exercise: a noninvasive MRI method of assessment. *J Appl Physiol* **91**, 1845-1853.

Rossiter HB (2011). Exercise: Kinetic Considerations for Gas Exchange. *Comp Physiol* **1**, 203-244.

Scheuermann BW & Barstow TJ (2003). O_2 uptake kinetics during exercise at peak O_2 uptake. *J Appl Physiol* **95**, 2014-2022.

Scheuermann BW, Hoelting BD, Noble ML & Barstow TJ (2001). The slow component of O_2 uptake is not accompanied by changes in muscle EMG during repeated bouts of heavy exercise in humans. *J Physiol* **531**, 245-256.

Scheuermann BW & Kowalchuk JM (1998). Attenuated respiratory compensation during rapidly incremented ramp exercise. *Respir Physiol* **114**, 227-238.

Spencer MD, Murias JM, Kowalchuk JM & Paterson DH (2013). Effect of moderate-intensity work rate increment on phase II tauVO_2, functional gain and Delta[HHb]. *Eur J Appl Physiol* **113**, 545-557.

Swanson GD (1980). Breath-to-breath considerations for gas exchange kinetics. In Exercise Bioenergetics and Gas Exchange, ed. Cerretelli P & Whipp BJ, pp. 211-222. Elsevier, Amsterdam.

Swanson GD & Hughson RL (1988). On the modeling and interpretation of oxygen uptake kinetics from ramp work rate tests. *J Appl Physiol* **65**, 2453-2458.

Takaishi T, Ono T & Yasuda Y (1992). Relationship between muscle fatigue and oxygen uptake during cycle ergometer exercise with different ramp slope increments. *Eur J Appl Physiol Occup Physiol* **65**, 335-339.

Whipp BJ, Davis JA, Torres F & Wasserman K (1981). A test to determine parameters of aerobic function during exercise. *J Appl Physiol Respir Environ Exerc Physiol* **50**, 217-221.

Whipp BJ, Rossiter HB & Ward SA (2002). Exertional oxygen uptake kinetics: a stamen of stamina? *Biochem Soc Trans* **30**, 237-247.

Whipp BJ, Ward SA, Lamarra N, Davis JA & Wasserman K (1982). Parameters of ventilatory and gas exchange dynamics during exercise. *J Appl Physiol Respir Environ Exerc Physiol* **52**, 1506-1513.

Whipp BJ, Ward SA & Wasserman K (1986). Respiratory markers of the anaerobic threshold. *Adv Cardiol* **35**, 47-64.

Wilkerson DP & Jones AM (2007). Effects of baseline metabolic rate on pulmonary O_2 uptake on-kinetics during heavy-intensity exercise in humans. *Respir Physiol Neurobiol* **156**, 203-211.

Wilkerson DP & Jones AM (2006). Influence of initial metabolic rate on pulmonary O_2 uptake on-kinetics during severe intensity exercise. *Respir Physiol Neurobiol* **152**, 204-219.

Williams AM, Paterson DH & Kowalchuk JM (2013). High-intensity interval training speeds the adjustment of pulmonary O_2 uptake, but not muscle deoxygenation, during moderate-intensity exercise transitions initiated from low and elevated baseline metabolic rates. *J Appl Physiol* **114**, 1550-1562.

Wüst RC, van der Laarse WJ & Rossiter HB (2013). On-off asymmetries in oxygen consumption kinetics of single Xenopus laevis skeletal muscle fibres suggest higher-order control. *J Physiol* **591**, 731-744.

Zoladz JA & Korzeniewski B (2001). Physiological background of the change point in VO_2 and the slow component of oxygen uptake kinetics. *J Physiol Pharmacol* **52**, 167-184.

CHAPTER V: General Discussion and Conclusions

A linear, first-order system is one whose output variable values change proportionally with input variable values based on a single critical rate modulator. For example, it has been suggested that muscle O_2 utilization ($\dot{V}O_2$) increases in proportion to metabolic demand as controlled by the creatine kinase reaction (Meyer, 1988). Dynamic linearity implies that the time course of the system output is proportional to the system input, a consequence of which is that in response to a step-change in input, the output variable will respond with exponential dynamics whose kinetics will not change regardless of the initial input or the magnitude of the step-change in input (law of superposition). Though the pulmonary $\dot{V}O_2$ uptake ($\dot{V}O_{2p}$) response has been shown to be linearly related to WR (in some instances) and has been well described by a mono-exponential response, its kinetics have consistently displayed non-linear response dynamics. This thesis examined the non-linearity of $\dot{V}O_{2p}$ to provide perspective on what this behavior conveys in terms of the control of muscle O_2 utilization

Summary of Studies

The studies comprising this thesis relied heavily on non-invasive estimations of muscle $\dot{V}O_2$ derived from breath-by-breath measurements of pulmonary $\dot{V}O_2$ uptake ($\dot{V}O_{2p}$). For decades, this technique has been used to examine the mechanisms that control and limit the dynamics of $\dot{V}O_{2m}$ on transition to exercise in humans. A major challenge associated with the use of breath-by-breath $\dot{V}O_{2p}$ data resides in the variability of the measurement and thus it is common practice to perform multiple step-transitions which are subsequently processed to yield an ensemble-averaged profile with an improved signal-to-noise ratio. To combine multiple repetitions various data processing techniques may be

used. However it was unclear whether using different data processing strategies impacted model parameter estimation.

In Chapter II, the aim was to determine whether techniques used as common practice for processing breath-by-breath $\dot{V}O_{2p}$ data from repeated step-transitions in WR influence the model parameter estimations and confidence of describing the phase II $\dot{V}O_{2p}$ response. Using measured breath-by-breath $\dot{V}O_{2p}$ data our analyses showed that: 1) phase II $\dot{V}O_{2p}$ kinetic parameter estimates were not different when modeling $\dot{V}O_{2p}$ data using like-trials that were combined without processing of any kind, after interpolation, and/or after bin-averaging; 2) the "noise" statistics for $\dot{V}O_{2p}$ were highly variable both between subjects and within subject trial-repeats; 3) the amplitude of breath-by-breath $\dot{V}O_{2p}$ "noise" is not different between low- or moderate- exercise intensities, or between young and older individuals; and 4) the statistics of breath-by-breath $\dot{V}O_{2p}$ "noise" conformed to a predictable Gaussian distribution independent of age group or steady-state exercise intensity. Though data processing technique did not affect model parameter estimation, it did impact the 95% confidence intervals of best fit model parameters. Collectively, these analyses indicated that in practice, higher 'confidence' in modeling of phase II $\dot{V}O_{2p}$ could best be obtained by: collecting quality data and carefully fitting the phase II $\dot{V}O_{2p}$ response with attention paid to the parameters and statistical outcomes (CI_{95}, chi-square), and the goodness-of-fit of the model as determined by visual inspection of the model residuals, especially within the non-steady-state region of interest – it was by this mantra that data were collected and analyzed in the subsequent studies of this thesis.

The main focus of this thesis was to re-examine some of the experimental evidence refuting the assumption that $\dot{V}O_{2p}$ is controlled by a dynamically linear process that is close

to first-order (Chapters III and IV). Specifically, we focused on the slowed on-transient dynamics of $\dot{V}O_{2p}$ when initiated from elevated baseline intensities. Using $\dot{V}O_{2p}$ kinetic analyses during step-increments to and from various intensities of exercise, we were able to build a profile of $\dot{V}O_{2p}$ dynamics across a wide range of exercise intensities spanning the *moderate*-intensity domain (Chapter III) and beyond (Chapter IV). These results demonstrated that the rate of adjustment ($\tau\dot{V}O_{2p}$) and magnitude of change in $\dot{V}O_{2p}$ for a given WR (G) are slowed and increased, respectively, in a manner dependent on the baseline intensity; supporting non-linear response dynamics of $\dot{V}O_{2p}$.

It was reported previously that phase II $\dot{V}O_{2p}$ kinetics are invariant and exponential when initiated from a common (low) baseline intensity regardless of WR increment (Barstow & Mole 1991; Özyener *et al.* 2001; Scheuermann & Barstow 2003; Spencer *et al.* 2013); consistent with first-order kinetic control of $\dot{V}O_2$. However, slowed $\dot{V}O_2$ kinetics when initiating exercise from a raised metabolic intensity challenges this long held notion. Chapter III represents the first study to observe that phase II $\dot{V}O_{2p}$ kinetics get slower with transitions from increasing baseline intensity but remain unchanged with transitions of varying WR increments performed from a constant baseline within a single group of participants. Collectively, these findings appeared to implicate that instantaneous baseline metabolic rate is the primary mechanism by which $\dot{V}O_{2p}$ kinetics are controlled under these conditions (rather than the kinetic properties of the muscle fibres recruited to address the change in WR). However, modeling the summed influence of multiple theoretical muscle compartments revealed that $\tau\dot{V}O_{2p}$ could appear fast (e.g., 20 s), and similar to *in vivo* measurements, despite being derived from $\tau\dot{V}O_{2m}$ values ranging 15-40 s (mean = 27 s) and $\tau\dot{Q}_m$ ranging 20-45 s suggesting that within the *moderate*-intensity domain phase II

$\dot{V}O_{2p}$ kinetics are slowed dependent on the pre-transition WR (rather than baseline metabolic rate, *per se*) and transitions of increasing ΔWR may be strongly influenced by the heterogeneity of metabolic and circulatory dynamics amongst muscle fibre pools recruited to address the step-change.

One of the key findings in Chapter III, was the "linear" $\tau\dot{V}O_{2p}$ and G_P vs WR relationship that was established within the *moderate*-intensity domain. This finding refutes the notion that $\dot{V}O_2$ kinetics at the muscle level function as a linear system. However, the $\dot{V}O_{2p}$ response to ramp-incremental (RI) exercise has been shown to increase linearly with WR (Davis *et al.* 1982; Meyer *et al.* 1998; Boone & Bourgois 2012) and the dynamics of response have been well described by a mono-exponential function with a single time constant and gain (Whipp *et al.* 1981; Hughson & Inman 1986; Swanson & Hughson 1988) which is consistent with the action of a dynamically linear system. This implies that the dynamic responses of the underlying muscle fibre populations that vary with WR throughout a ramp protocol are metabolically and kinetically homogenous.

Therefore, the purpose of Chapter IV, was twofold: 1) to establish how WR influences $\tau\dot{V}O_{2p}$ and gain including WRs associated with intensities above the lactate threshold (i.e., those above *moderate*-intensities); and 2) to examine whether an apparently linear $\dot{V}O_{2p}$ vs WR relationship during RI could be reconciled by these observations. Using a series of step-transitions from various baseline intensities, ranging from *moderate* to *very heavy*, it was established that $\tau\dot{V}O_{2p}$ increases in a curvilinear manner and gain increases linearly as a function of WR. Based on these relationships, it was possible to examine whether the "linear" $\dot{V}O_{2p}$ response to RI exercise was best described by an exponential function with constant or variable time constant and gain parameters. Results demonstrated

that although the time constant and gain increase progressively with WR (and thus reflect a non-linear system), their changes could combine to produce a near linear $\dot{V}O_{2p}$ response to RI exercise.

An additional aim of the study in Chapter IV was to examine whether the established $\tau\dot{V}O_{2p}$ and G vs WR relationships could be used to explain the apparent non-linear system response dynamics during: 1) simulated RI protocols of varying ramp slopes; and 2) simulated step-transitions to *heavy*-intensity exercise. It had previously been demonstrated that the $\dot{V}O_{2p}$ response to slowly incrementing ramp protocols, increases in excess compared to increases observed at lower WRs (curvilinear upward above the LT) (Scheuermann & Kowalchuk 1998; Zoladz & Korzeniewski 2001). Our simulated $\dot{V}O_{2p}$ responses demonstrated how a progressively increasing time constant and gain that dynamically change as WR increases throughout ramp exercise could manifest as a slowly developing additional, or "excess", component of $\dot{V}O_{2p}$ (see Figure 4.5). Additionally, during *heavy*-intensity exercise, it is common to observe a second slowly rising component of $\dot{V}O_{2p}$ (that follows an early, fast, exponential rise in $\dot{V}O_{2p}$) which leads to a greater overall O_2 cost compared to that observed during moderate-*intensity* exercise (Barstow & Mole 1991). Modeling the summed influence of multiple theoretical muscle compartments derived from $\tau\dot{V}O_{2m}$ values ranging 25-120 s and G values ranging 9-13 $mL{\cdot}min^{-1}{\cdot}W^{-1}$ (based on the established phase II $\tau\dot{V}O_{2p}$ and G_P vs WR relationships) yielded a $\dot{V}O_{2p}$ response profile that projected beyond the "steady-state" $\dot{V}O_{2p}$ expected based on a "linear" $\dot{V}O_{2p}$ vs WR from RI exercise (see Figure 4.6). While these simulations were able to rectify (perhaps) the increased O_2 cost observed at supra-LT intensities, they were unable to resolve how the $\dot{V}O_{2p}$ response profile might exhibit a fast, early exponential phase

followed by a supplementary increase in $\dot{V}O_{2p}$ which acts to delay the time required to achieve a steady-state.

In summary, this series of studies examined the non-linear behavior of $\dot{V}O_{2p}$ with particular attention paid to the phenomenon that $\dot{V}O_{2p}$ are slowed as a function of baseline intensity. The data suggest that while this consistently observable phenomenon refutes the notion that $\dot{V}O_2$ kinetics at the muscle level operate as a linear system, modeling the integrated venous return of multiple metabolic units with diverse $\dot{V}O_{2m}$ and blood flow kinetics demonstrated how a muscle system comprised of compartments that behave with linear characteristics but also with varying response dynamics, can combine to a common pulmonary $\dot{V}O_{2p}$ signal that exhibits non-linear behavior. Additionally, it is demonstrated that in some situations, these diverse arrays of muscle compartments can combine to produce a linear $\dot{V}O_{2p}$ response (e.g., RI exercise) acting to obscure the underlying kinetic response characteristics of the system. Taken together, these data suggest that the intensity-dependent non-linear $\dot{V}O_{2p}$ responses may be attributable to "heterogeneity" within the range of muscle fibres recruited to address the exercise challenge. Importantly, each of these muscle fibres may independently behave as a linear, first-order system (each potentially with their own critical rate control modulator). Therefore, non-linear $\dot{V}O_{2p}$ responses to exercise may manifest from a "heterogeneity" of linear, first-order responses.

Assumptions and Limitations

The interpretation the data and their implication for $\dot{V}O_{2p}$ control were based on several assumptions:

First, the interpretation of many of the findings in this thesis relied on data that were simulated based on the multi-compartmental model of Benson *et al.* (2013) which was

adapted from the original computational model of Barstow *et al.* (1990). These models were originally developed to assess how $\dot{V}O_{2p}$ is modulated by the circulatory system on its way to the lungs, and how it eventually manifests as the three-phase $\dot{V}O_{2p}$ response profile (where phase II kinetics are assumed to represent $\dot{V}O_{2m}$ kinetics). Simulations based on this model mimic real laboratory-based experiments in human participants in that the input is a work rate profile (e.g. step-increase in WR), and the output is a $\dot{V}O_{2p}$ profile. However, the input parameters to this model rely on several assumed relationships that are based on actual human responses measured *in vivo*. For example, the change in steady-state $\dot{V}O_{2m}$ is determined by a functional gain of 9.5 $L \cdot min^{-1} \cdot W^{-1}$ and steady-state cardiac output is then determined by the $\dot{Q}$-to-$\dot{V}O_{2m}$ relationship (i.e., a linear relationship with a slope of 6.0 and an intercept of 3.6 $L \cdot min^{-1}$). Furthermore, the manner by which $\dot{V}O_{2m}$ and $\dot{Q}$ achieve the new "steady-state" is determined by their kinetics, which are also input parameters for the model. Given these model parameter inputs, the output can assess how closely phase II $\dot{V}O_{2p}$ kinetics match $\dot{V}O_{2m}$ kinetics, and how the circulatory systems modifies this relationship. However, the model can only predict the effects of the components it includes: in this case how the circulatory system (venous volume, blood mixing, blood flow etc.) modifies $\dot{V}O_{2m}$ on its way to the lungs. The model cannot predict outcomes related to other mechanisms that are not included as parameters in model, for example, the effects of a higher baseline WR on mitochondrial activity and how this affects $\dot{V}O_{2m}$.

Second, the blood flow kinetics ($\tau\dot{Q}_m$) for the multi-muscle compartment model (utilized to simulate the homogenized responses of multiple muscle compartments with heterogeneous $\dot{V}O_{2m}$ kinetics on transition to various intensities of exercise) were assumed to increase in a similar manner to those of $\tau\dot{V}O_{2m}$ (which were inferred based on measured

$\tau\dot{V}O_{2p}$) but by a fixed ratio of 1.09 ($\tau\dot{Q}_m/\tau\dot{V}O_{2m}$). This ratio was chosen *a priori* to avoid kinetic mismatches where changes in the dynamics of O_2 delivery are slower than $\dot{V}O_{2m}$ causing C_vO_{2m} to drop to zero during the initial portion of the on-transient. Given that (MacPhee *et al.* 2005) had previously shown that conduit (bulk) leg blood flow kinetics are slowed with transition from elevated baseline intensities and that peripheral blood flow dynamics have been shown to be slower in rat skeletal muscle predominately comprised of type II muscle fibres compared to muscle with greater proportions of type I fibres (Behnke *et al.* 2003; McDonough *et al.* 2005; Ferreira *et al.* 2006) (i.e., higher-order compared to lower-order), we reasoned that $\dot{Q}_m$ kinetics would slow as a function of WR and, by extension, with fibre populations located at higher positions within the recruitment hierarchy.

Third, the relationship between the kinetics and efficiency of $\dot{V}O_2$ amongst muscle compartments is based on the assumption that the baseline WR from which a transition is initiated can effectively isolate and reveal the response characteristics specific to the muscle fibres that reside within a particular position in the motor unit recruitment hierarchy. This assumption precludes the inclusion of previously active muscle fibre populations in contributing to the subsequent $\dot{V}O_{2p}$ response. This is not likely to be the case as previously active motor units may increase their rate coding (increased frequency of stimulation by the innervating axon) to address greater contractile requirements. That $\tau\dot{V}O_{2p}$ and G vs WR relationships were able to provide a reasonable prediction of the $\dot{V}O_{2p}$ response to RI exercise may suggest that previously active muscle fibre pools (i.e. those recruited at lower WR steps) were made to respond with dynamics similar to their higher-order counterparts (when they were recruited again at a higher WR step); possibly as a

consequence of an elevated intramuscular metabolic rate and reduced contractile and metabolic efficiency (Grassi *et al.* 2011).

Lastly, the proposition that in human skeletal muscle, there exists a continuum of muscle fibre pools recruited in a hierarchical fashion that respond to changes in metabolic demand with first-order $\dot{V}O_2$ kinetics that are progressively slower and progressively less efficient in their use of O_2 to synthesize energy is based on the consideration that each individual muscle fibre within human skeletal muscle is, itself, a unique system that responds to changes in metabolic demand with its own loci of control – dependent on its metabolic biochemical properties and oxidative capacitance. Thus, the assumption is that progression throughout the recruitment hierarchy spans muscle fibres with a continuum of $\dot{V}O_2$ response characteristics. Considerable evidence exists to suggest that fibres that reside at higher position within the recruitment hierarchy are less oxidative and less energetically efficient (He *et al.* 2000) and that considerable functional and biochemical diversity exists within fibres of the same MHC isoform (i.e., within fibre-type classes type I, IIA and IIX (Bottinelli, 2001; Schiaffino & Reggiani 2011). Furthermore, it has been suggested that all fibres within a single motor unit share similar oxidative capacity (Burke *et al.* 1971; Burke *et al.* 1973; Nemeth *et al.* 1981) and that muscle fibres belonging to motor units at greater positions within the recruitment hierarchy have greater total [PCr] content and slower PCr kinetics (Soderlund & Hultman 1991). Additionally, greater contributions of type II muscle fibres on transition to exercise has been linked to both slower and less efficient $\dot{V}O_{2p}$ kinetics in humans measured *in vivo* (Barstow *et al.* 1996; Pringle *et al.* 2003; Krustrup *et al.* 2004; Krustrup *et al.* 2008). Therefore, it is not unreasonable to surmise that the non-linear behavior of $\dot{V}O_{2p}$ may manifest from the simultaneous activation of a population of

heterogeneous motor units on transition to exercise reflecting a diversity of linear, first-order control.

Future Directions

The examination of $\dot{V}O_{2p}$ kinetic responses from a range of baseline WRs was instrumental in investigating how a linear $\dot{V}O_2$ muscle system may exhibit non-linear $\dot{V}O_{2p}$ responses to exercise. While the evidence provided does suggest that human muscle may consist of a range of muscle fibre pools that individually respond to changes in metabolic demand with exponential kinetics, these findings need to be substantiated. In Chapter IV, it was demonstrated that a system with time constant and gain parameters that change with WR can balance each other out to produce a linear response during ramp exercise. However, it could be argued that the mono-exponential model (one that was based on single time constant and gain parameters) fit the data equally as well. Future work should strive to replicate this study with the addition of slower incrementing ramp protocols. This should facilitate a $\dot{V}O_{2p}$ response that is non-linear and demonstrate how a mono-exponential model would fail to characterize the response. Furthermore, step-increments of varying WR could also be introduced into this type of study to determine whether the simulated output of muscle compartments (with the variable time constant and gain parameters) can predict a measured $\dot{V}O_{2p}$ response to *heavy*- or *very heavy*-intensity constant-load exercise. Importantly, it would also be useful to measure the relationships between blood flow kinetics and WR so that the influence of various circulatory dynamics amongst compartments, on the $\dot{V}O_{2p}$ profile, could be scrutinized further.

References

Barstow TJ, Jones AM, Nguyen PH & Casaburi R (1996). Influence of muscle fiber type and pedal frequency on oxygen uptake kinetics of heavy exercise. *J Appl Physiol* **81**, 1642-1650.

Barstow TJ & Mole PA (1991). Linear and nonlinear characteristics of oxygen uptake kinetics during heavy exercise. *J Appl Physiol* **71**, 2099-2106.

Behnke BJ, McDonough P, Padilla DJ, Musch TI & Poole DC (2003). Oxygen exchange profile in rat muscles of contrasting fibre types. *J Physiol* **549**, 597-605.

Boone J & Bourgois J (2012). The oxygen uptake response to incremental ramp exercise: methodological and physiological issues. *Sports Med* **42**, 511-526.

Bottinelli R (2001). Functional heterogeneity of mammalian single muscle fibres: do myosin isoforms tell the whole story? *Pflugers Arch* **443**, 6-17.

Burke RE, Levine DN, Tsairis P & Zajac FE,3rd (1973). Physiological types and histochemical profiles in motor units of the cat gastrocnemius. *J Physiol* **234**, 723-748.

Burke RE, Levine DN & Zajac FE,3rd (1971). Mammalian motor units: physiological-histochemical correlation in three types in cat gastrocnemius. *Science* **174**, 709-712.

Davis JA, Whipp BJ, Lamarra N, Huntsman DJ, Frank MH & Wasserman K, (1982). Effect of ramp slope on determination of aerobic parameters from the ramp exercise test. *Med Sci Sports Exerc* **14**, 339-343.

Ferreira LF, McDonough P, Behnke BJ, Musch TI & Poole DC (2006). Blood flow and O_2 extraction as a function of O_2 uptake in muscles composed of different fiber types. *Respir Physiol Neurobiol* **153**, 237-249.

Grassi B, Porcelli S, Salvadego D & Zoladz JA (2011). Slow VO_2 kinetics during moderate-intensity exercise as markers of lower metabolic stability and lower exercise tolerance. *Eur J Appl Physiol* **111**, 345-355.

He ZH, Bottinelli R, Pellegrino MA, Ferenczi MA & Reggiani C (2000). ATP consumption and efficiency of human single muscle fibers with different myosin isoform composition. *Biophys J* **79**, 945-961.

Hughson RL & Inman MD (1986). Oxygen uptake kinetics from ramp work tests: variability of single test values. *J Appl Physiol* **61**, 373-376.

Krustrup P, Secher NH, Relu MU, Hellsten Y, Soderlund K & Bangsbo J (2008). Neuromuscular blockade of slow twitch muscle fibres elevates muscle oxygen uptake and energy turnover during submaximal exercise in humans. *J Physiol* **586**, 6037-6048.

Krustrup P, Soderlund K, Mohr M & Bangsbo J (2004). Slow-twitch fiber glycogen depletion elevates moderate-exercise fast-twitch fiber activity and O2 uptake. *Med Sci Sports Exerc* **36**, 973-982.

MacPhee SL, Shoemaker JK, Paterson DH & Kowalchuk JM (2005). Kinetics of O_2 uptake, leg blood flow, and muscle deoxygenation are slowed in the upper compared with lower region of the moderate-intensity exercise domain. *J Appl Physiol* **99**, 1822-1834.

McDonough P, Behnke BJ, Padilla DJ, Musch TI & Poole DC (2005). Control of microvascular oxygen pressures in rat muscles comprised of different fibre types. *J Physiol* **563**, 903-913.

Meyer K, Schwaibold M, Hajric R, et al. (1998). Delayed VO_2 kinetics during ramp exercise: a criterion for cardiopulmonary exercise capacity in chronic heart failure. *Med Sci Sports Exerc* **30**, 643-648.

Meyer RA (1988). A linear model of muscle respiration explains monoexponential phosphocreatine changes. *Am J Physiol* **254**, C548-53.

Nemeth PM, Pette D & Vrbova G (1981). Comparison of enzyme activities among single muscle fibres within defined motor units. *J Physiol* **311**, 489-495.

Özyener F, Rossiter HB, Ward SA & Whipp BJ (2001). Influence of exercise intensity on the on- and off-transient kinetics of pulmonary oxygen uptake in humans. *J Physiol* **533**, 891-902.

Pringle JS, Doust JH, Carter H, et al. (2003). Oxygen uptake kinetics during moderate, heavy and severe intensity "submaximal" exercise in humans: the influence of muscle fibre type and capillarisation. *Eur J Appl Physiol* **89**, 289-300.

Scheuermann BW & Barstow TJ (2003). O_2 uptake kinetics during exercise at peak O_2 uptake. *J Appl Physiol* **95**, 2014-2022.

Scheuermann BW & Kowalchuk JM (1998). Attenuated respiratory compensation during rapidly incremented ramp exercise. *Respir Physiol* **114**, 227-238.

Schiaffino S & Reggiani C (2011). Fiber types in mammalian skeletal muscles. *Physiol Rev* **91**, 1447-1531.

Soderlund K & Hultman E (1991). ATP and phosphocreatine changes in single human muscle fibers after intense electrical stimulation. *Am J Physiol* **261**, E737-41.

Spencer MD, Murias JM, Kowalchuk JM & Paterson DH (2013). Effect of moderate-intensity work rate increment on phase II tauVO_2, functional gain and Delta[HHb]. *Eur J Appl Physiol* **113**, 545-557.

Swanson GD & Hughson RL (1988). On the modeling and interpretation of oxygen uptake kinetics from ramp work rate tests. *J Appl Physiol* **65**, 2453-2458.

Whipp BJ, Davis JA, Torres F & Wasserman K (1981). A test to determine parameters of aerobic function during exercise. *J Appl Physiol Respir Environ Exerc Physiol* **50**, 217-221.

Zoladz JA & Korzeniewski B (2001). Physiological background of the change point in VO_2 and the slow component of oxygen uptake kinetics. *J Physiol Pharmacol* **52**, 167-184.

APPENDIX I: Ethics approvals

Western Research

Use of Human Participants - Initial Ethics Approval Notice

Principal Investigator: Dr. John Kowalchuk
File Number: 104808
Review Level: Full Board
Protocol Title: The influence of an elevated baseline metabolic rate on the rate of adjustment of pulmonary O2 uptake during step-transitions within the moderate intensity domain
Department & Institution: Health Sciences\Kinesiology Western University
Sponsor: Natural Sciences and Engineering Research Council

Ethics Approval Date: February 18, 2014
Ethics Expiry Date: February 27, 2015

Documents Reviewed & Approved & Documents Received for Information:

Document Name	Comments	Version Date
Other	EMS contact	2013/12/17
Other	Physical Activity Readiness Questionnaire	2013/12/17
Recruitment Items	in-class script-Received Feb 3, 2014	
Western University Protocol		
Letter of Information & Consent	v2	2014/02/11

This is to notify you that the University of Western Ontario Health Sciences Research Ethics Board (HSREB) which is organized and operates according to the Tri-Council Policy Statement: Ethical Conduct of Research Involving Humans and the Health Canada/ICH Good Clinical Practice Practices: Consolidated Guidelines; and the applicable laws and regulations of Ontario has reviewed and granted approval to the above referenced study on the approval date noted above. The membership of this HSREB also complies with the membership requirements for REB's as defined in Division 5 of the Food and Drug Regulations.

The ethics approval for this study shall remain valid until the expiry date noted above assuming timely and acceptable responses to the HSREB's periodic requests for surveillance and monitoring information. If you require an updated approval notice prior to that time you must request it using the University of Western Ontario Updated Approval Request form.

Member of the HSREB that are named as investigators in research studies, or declare a conflict of interest, do not participate in discussions related to, nor vote on, such studies when they are presented to the HSREB.

The Chair of the HSREB is [redacted]. The HSREB is registered with the U.S. Department of Health & Human Services under the IRB registration number IRB 00000940

[redacted]

Signature

Ethics Officer to Contact for Further Information

[redacted]

This is an official document. Please retain the original in your files.

Western Research

Research Ethics

Western University Health Science Research Ethics Board
HSREB Full Board Initial Approval Notice

Principal Investigator: Dr. John Kowalchuk
Department & Institution: Health Sciences\Kinesiology,Western University

HSREB File Number: 106312
Study Title: Predicting the pulmonary oxygen uptake response to ramp-incremental exercise from O2 uptake kinetics
Sponsor: Natural Sciences and Engineering Research Council

HSREB Initial Approval Date: March 23, 2015
HSREB Expiry Date: March 23, 2016

Documents Approved and/or Received for Information:

Document Name	Comments	Version Date
Letter of Information & Consent		2015/02/17
Recruitment Items	In-class announcement script (received Feb.20/15)	
Other	EMS CONTACT (received Feb.20/15)	
Other	Figure 1: Schematic of Exercise Protocol (Received Feb.20/15)	
Western University Protocol	(received Feb.20/15)	2015/02/20
Other	PAR-Q. (received Feb.20/15)	

The Western University Health Science Research Ethics Board (HSREB) has reviewed and approved the above named study, as of the HSREB Initial Approval Date noted above.

HSREB approval for this study remains valid until the HSREB Expiry Date noted above, conditional to timely submission and acceptance of HSREB Continuing Ethics Review.

The Western University HSREB operates in compliance with the Tri-Council Policy Statement Ethical Conduct for Research Involving Humans (TCPS2), the International Conference on Harmonization of Technical Requirements for Registration of Pharmaceuticals for Human Use Guideline for Good Clinical Practice Practices (ICH E6 R1), the Ontario Personal Health Information Protection Act (PHIPA, 2004), Part 4 of the Natural Health Product Regulations, Health Canada Medical Device Regulations and Part C, Division 5, of the Food and Drug Regulations of Health Canada.

Members of the HSREB who are named as Investigators in research studies do not participate in discussions related to, nor vote on such studies when they are presented to the REB.

The HSREB is registered with the U.S. Department of Health & Human Services under the IRB registration number IRB 00000940.

[redacted]

Ethics Officer to Contact for Further Information

[redacted]

This is an official document. Please retain the original in your files.

Western University, Research, Support Services Bldg., Rm. 5150
London, ON, Canada N6A 3K7 t. 519.661.3036 f. 519.850.2466 www.uwo.ca/research/services/ethics

LETTER OF INFORMATION

The influence of an elevated baseline metabolic rate on the rate of adjustment of pulmonary O_2 uptake during step-transitions within the moderate intensity domain

Principle Investigator: John M. Kowalchuk, PhD

Purpose of the Study:

You are invited to participate in a research study examining how different levels of light-to-moderate exercise effect the way the human body uses oxygen (O_2) when going from lower to higher moderate-intensity work rates. Each exercise protocol will begin with a bout of very light/easy cycling after which you will be to perform two step-increases in work rate (for example: from "very light" to "light-exercise" and "light-" to "moderate-exercise"), with each bout lasting six minutes. The effect of progressively increasing "baseline" work rate on O_2 uptake kinetics during moderate-intensity exercise is not known. Therefore, in this study, pulmonary O_2 uptake and leg muscle deoxygenation will be examined during multiple moderate-intensity exercise bouts.

Participation in this study involves visits to the research laboratory at the Canadian Centre for Activity and Aging (Arthur and Sonia Labatt Health Science Centre, Room 313) on a maximum of 13 different occasions, with each visit taking approximately 60 minutes.

A total of 32 healthy (16 per group) young men will be invited to participate in this study. In order to participate you must be between 18-39 years of age and healthy. You will not be able to participate in the study if you have been diagnosed previously with any respiratory, cardiovascular, metabolic or musculoskeletal disease; or you are currently on medication; or you are a smoker; or you respond to the exercise protocol in an irregular manner or cannot tolerate the exercise protocol; or if you respond "YES" to any of the questions on the Physical Activity Readiness Questionnaire (PAR-Q). If you are participating in another study at this time, please inform the investigator to determine if it is appropriate for you to participate in this study.

Research Testing Protocol

Should you decide to participate in the study, initial testing will include an incremental exercise test to your limit of tolerance on a two-legged stationary cycle ergometer in the upright, seated position. The test will begin with the exercise intensity being very light and easy (very little resistance). After several minutes, the exercise intensity will increase gradually until you are unable to continue and have to stop because either you will be unable to turn the pedals and maintain a required cadence, because the intensity is too high, or you will perceive the exercise as being too uncomfortable. This visit should last no more than 30 minutes.

Following the initial incremental cycle exercise test, you will be randomly entered into one of two groups and asked to return to the laboratory to perform up to four repetitions of six different exercise protocols.

In Group one, each exercise protocol will be begin with a 6 minute period of 20 W cycling followed by an instantaneous increase in resistance to either 40, 60, 80, 100, or 120 W. You will exercise at this intensity for an additional 6 minutes, and then the work rate will instantaneously increase (again) by 40 watts and this intensity will be sustained for another 6 minutes (total = 18 minutes; see **Figure 1**). For this group, all exercise will be of "moderate-intensity" (exercise that can be performed for a prolonged period of time, e.g., fast walking, easy jogging or bicycling) and the maximal intensity will be approximately 40-50% of your peak work rate.

In Group two, each exercise protocol will begin with a 2 minute period of 20 W cycling followed by an instantaneous increase to a "heavy-intensity" work rate (exercise where it will be difficult to carry a conversation due to increased breathing rate, e.g., running uphill). You will exercise at this intensity for 6 minutes and then the resistance will be reduced to either 20, 40, 60, 80, or 120 W for an additional 6 minutes, after which the resistance will be increased again by 40 W for another 6 minutes (total = 20 minutes; **see Figure 2**). For this group, the "heavy-intensity" exercise bout will require you to sustain ~75% of your peak work rate for six minutes.

Repeat testing in each condition is required in order to reduce normal biological variability associated with such testing and increase the underlying signal-to-noise ratio which means the amount of accurate data points to the amount of errant data points from non-uniform breathing. Each visit will last approximately 60 minutes.

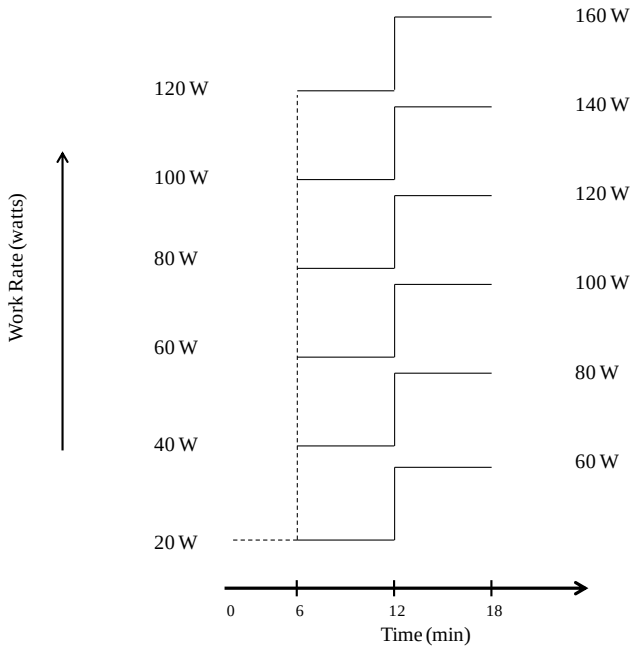

Figure 1: Schematic of Moderate (MOD) double-step protocol

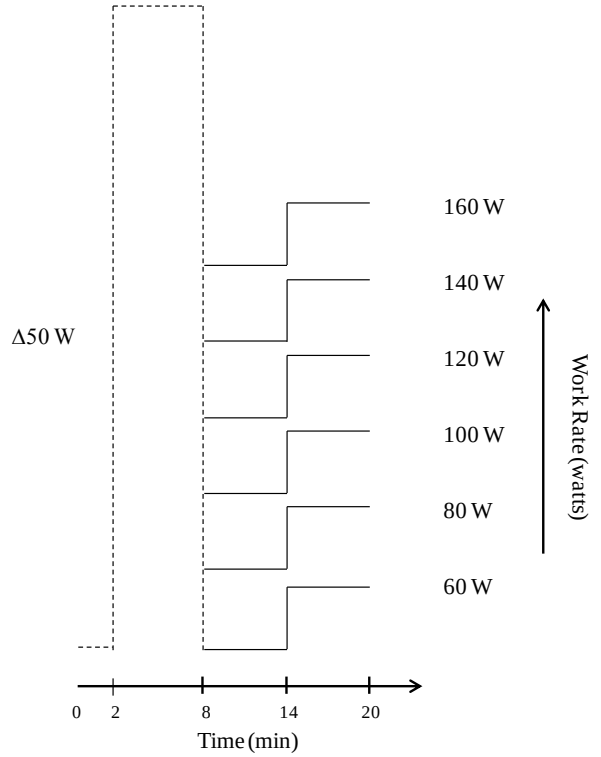

Figure 2: Schematic of Heavy-intensity priming with MOD step protocol

Research Procedures:

During each of the exercise tests you will be required to wear a nose-clip (to prevent you from breathing through your nose) and a rubber mouthpiece (similar to breathing through a snorkel or diving mask); nose-clips and mouthpieces are disinfected before each test. This will enable us to measure the volume of air that you breathe in and out, and measure the gas concentration in that air.

During each of the exercise tests, the oxygenation of your leg muscle will be measured using near-infrared spectroscopy which projects light into a specific location of your leg muscles and measures the amount of light coming out at another location. A small piece of equipment will be placed on your leg approximately midway between your hip and your knee. It will be secured with tape, covered to prevent light from entering or leaving the area, and bound with elastic bandage to minimize movement. You might experience a bit of discomfort by having this equipment secured to your leg during the exercise period; however, this is a non-invasive procedure which is not associated with any risks or discomfort.

Heart rate and rhythm will be continuously monitored by electrocardiogram. One electrode will be placed on each of the following areas: left chest, right chest, and left side under your ribs and connected to an electrocardiograph. The electrodes use adhesive tape to secure to the skin. There are no known risks or discomforts associated with this procedure.

Possible Risks and Discomforts:

You may experience some minor discomfort from wearing the nose-clip and rubber mouthpiece, and by having the NIRS probes secured to your leg during the exercise period. These sensations often become less noticeable with time during the exercise.

Any exercise carries a slight risk of a heart attack (less than approximately 6:10,000) or may be uncomfortable if you are unfit or not used to exercise. There may be some minor discomfort during the exercise testing. You may experience increased awareness of breathing, muscle fatigue and soreness, increased sweating, or a general feeling of fatigue or nausea, none of which are unexpected consequences of exercise. These feelings are expected to disappear shortly after exercise is stopped.

All testing procedures will only be conducted when a lab technician or research assistant that is certified in CPR is present. In the case of an emergency, 911 will be called using the telephone located in the testing laboratory. An automatic external defibrillator is also available within the testing building. If a heavy pressure sensation or pain develops in your chest or down your left arm it is important that you discontinue the exercise immediately and report these sensations to the exercise supervisor, or seek medical attention if you have left the exercise area.

Participation in this study requires a time commitment which may be inconvenient for you at some point during the study.

Benefits of Participation:

This is a basic physiology/biochemistry study and, as such, there will be no direct benefits received as a consequence of participating in the study. If you are interested, the rational for conducting the research and theory and significance of each of the tests will be explained, as will your individual results from each of the tests. You will also have the opportunity to learn about and better understand your physiological responses to an exercise situation.

Confidentiality:

Records from this study are confidential and will be stored securely at the Canadian Centre for Activity and Aging, Sonia Arthur Labatt Health Sciences Building. Your records will be identified by a number rather than your name. The data will be available for analysis within the research group. Published reports resulting from this study will not identify you by name. If you wish to withdrawal your data at any time you can do so by contacting the Principal Investigator, Dr. John Kowalchuk at [redacted]. Representatives of the University of Western Ontario Health Sciences Research Ethics Board may contact you or require access to your study-related records to monitor the conduct of the research.

Voluntary Participation:

Participation in this study is voluntary. You may refuse to participate, refuse to answer any questions or withdraw from the study at any time with no effect on your academic or employment status.

You will be given a copy of this letter of information and signed consent forms. You do not waive any legal rights by signing the consent form. If you have any questions regarding this study please contact Dr. John Kowalchuk [redacted], Daniel Keir [redacted] or Taylor Robertson [redacted] at the Canadian Centre for Activity and Aging, Sonia and Arthur Labatt Health Sciences Building, The University of Western Ontario, London. If you have any question about the conduct of this study or your rights as a research subject you may contact the Director of the Office of Research Ethics, The University of Western Ontario, [redacted].

LETTER OF INFORMED CONSENT

The influence of an elevated baseline metabolic rate on the rate of adjustment of pulmonary O_2 uptake during step-transitions within the moderate intensity domain

Principal investigator: John M. Kowalchuk, PhD

Records from this study are confidential and will be stored securely at the Canadian Centre for Activity and Aging, Sonia Arthur Labatt Health Sciences Building. Your records will be identified by a number rather than your name. The data will be available for analysis within the research group. Published reports resulting from this study will not identify you by name.

We would like to keep your contact information in order to contact you about participating in future studies. If you would like to be contacted about future studies please initial below.
□ ___ (initials)

I have read the Letter of Information, have had the nature of this study explained to me and I agree to participate. All questions have been answered to my satisfaction and I will receive a copy of the Letter of Information and signed consent form.

.

Participant:

_____ _____
Name (please print) Signature

_____
Date

Investigator (i.e. Person Responsible for Obtaining Informed Consent):

_____ _____
Name (please print) Signature

_____
Date

LETTER OF INFORMATION

Predicting the pulmonary O_2 uptake response to ramp-incremental exercise from pulmonary O_2 uptake kinetics

Principle Investigator: John M. Kowalchuk, PhD

Purpose of the Study:

You are invited to participate in a research study examining how different levels of light-to-heavy intensity exercise effect the way the human body uses oxygen (O_2) when going from lower to higher-intensity work rates. Each exercise protocol will begin with a bout of very light/easy cycling after which you will be to perform a series of step-increases in work rate (for example: from "light-" to "moderate-exercise" and from "moderate" to "heavy-exercise"), with each bout lasting six to eight minutes. The effect of progressively increasing "baseline" work rate from light-to-heavy intensity exercise on the speed at which O_2 uptake increases is unclear. Therefore, in this study, lung O_2 uptake and leg muscle oxygenation will be examined during multiple step-incrementing exercise tests spanning from "light" to "heavy-exercise".

Participation in this study involves visits to the research laboratory at the Canadian Centre for Activity and Aging (Arthur and Sonia Labatt Health Science Centre, Room 313) on a maximum of 12 different occasions, with each visit taking approximately 40 minutes.

A total of 17 healthy young men will be invited to participate in this study. In order to participate you must be between 18-39 years of age and healthy. You will not be able to participate in the study if you have been diagnosed previously with any respiratory, cardiovascular, metabolic or musculoskeletal disease; or you are currently on medication; or you are a smoker; or you respond to the exercise protocol in an irregular manner or cannot tolerate the exercise protocol; or if you respond "YES" to any of the questions on the Physical Activity Readiness Questionnaire (PAR-Q). If you are participating in another study at this time, please inform the investigator to determine if it is appropriate for you to participate in this study.

Research Testing Protocol

Should you decide to participate in the study, testing will include three ramp incremental exercise tests to your limit of tolerance on a two-legged stationary cycle ergometer in the upright, seated position. The test will begin with the exercise intensity being very light and easy (very little resistance). After several minutes, the exercise intensity will increase gradually until you are unable to continue and have to stop because either you will be unable to turn the pedals and maintain a required cadence, because the intensity is too high, or you will perceive the exercise as being too uncomfortable. These visits should last no more than 40 minutes.

In addition to the ramp incremental cycle exercise tests, you will be asked to perform up to four repetitions of two different step-incremental exercise protocols. Each exercise protocol will begin with a 6 minute period of either 20 W or 50 W cycling followed by an instantaneous increase in resistance by 60 W (to either 80W [from 20W baseline] or 110 W [from 50W baseline]. You will exercise at this intensity for an additional 6 minutes, and then the work rate will instantaneously increase (again) by 60 watts and this intensity will be sustained for another 6 minutes. This exercise intensity will be followed by two additional instantaneous 60 W increases in resistance lasting 8 minutes each (total = 34 minutes; see **Figure 1**). Half of the exercise (approximately 18 minutes) will be of "light-" to "moderate-intensity" (exercise that can be performed for a prolonged period of time, e.g., fast walking, easy jogging or bicycling) while the other half (approximately 16 minutes) will be of "heavy-intensity" (exercise where it will be difficult to carry a conversation due to increased breathing rate, e.g., running or bicycling uphill).

Repeat testing in each condition is required in order to get cleaner data associated with such testing and to increase the underlying signal-to-noise ratio which means the amount of good/accurate data points to the amount of bad data points that may result from breaths associated with coughs or swallowing. Each visit will last approximately 40 minutes.

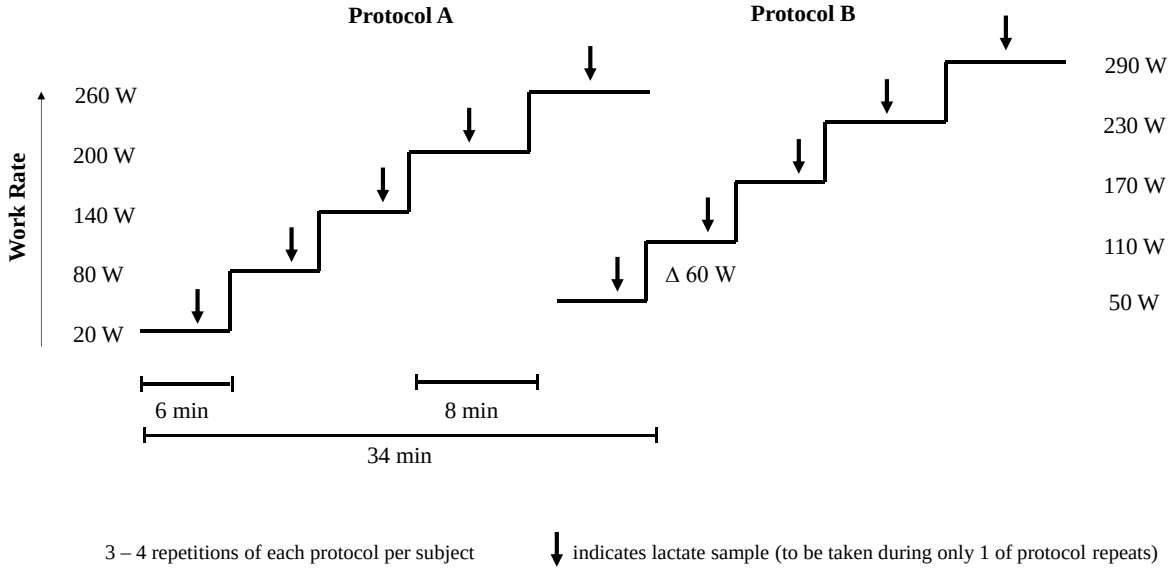

Figure 1: Schematic of Exercise Protocol

Research Procedures:

During each of the exercise tests you will be required to wear a nose-clip (to prevent you from breathing through your nose) and a rubber mouthpiece (similar to breathing through a snorkel or diving mask); nose-clips and mouthpieces are disinfected before each test. This will enable us to

measure the volume of air that you breathe in and out, and measure the gas concentration in that air.

During each of the exercise tests, the oxygenation of your leg muscle will be measured using near-infrared spectroscopy which projects light into a specific location of your leg muscles and measures the amount of light coming out at another location. A small piece of equipment will be placed on your leg approximately midway between your hip and your knee. It will be secured with tape, covered to prevent light from entering or leaving the area, and bound with elastic bandage to minimize movement. You might experience a bit of discomfort by having this equipment secured to your leg during the exercise period; however, this is a non-invasive procedure which is not associated with any risks or discomfort.

Heart rate and rhythm will be continuously monitored by electrocardiogram. One electrode will be placed on each of the following areas: left chest, right chest, and left side under your ribs and connected to an electrocardiograph. The electrodes use adhesive tape to secure to the skin. There are no known risks or discomforts associated with this procedure.

Blood lactate (or muscle acid) levels will be measured during two of the exercise tests (a total of five times) at select time points (see **Figure 1**). A small pin prick will be made to your earlobe in order to draw a droplet of blood. You may experience some pain or discomfort related to the earlobe prick

Possible Risks and Discomforts:

You may experience some minor discomfort from wearing the nose-clip and rubber mouthpiece, and by having the NIRS probes secured to your leg during the exercise period. These sensations often become less noticeable with time during the exercise.

Any exercise carries a slight risk of a heart attack (less than approximately six events in every ten thousand tests.) or may be uncomfortable if you are unfit or not used to exercise. There may be some minor discomfort during the exercise testing. You may experience increased awareness of breathing, muscle fatigue and soreness, increased sweating, or a general feeling of fatigue or nausea, none of which are unexpected consequences of exercise. These feelings are expected to disappear shortly after exercise is stopped.

All testing procedures will only be conducted when a lab technician or research assistant that is certified in CPR is present. In the case of an emergency, 911 will be called using the telephone located in the testing laboratory. An automatic external defibrillator is also available within the testing building. If a heavy pressure sensation or pain develops in your chest or down your left arm it is important that you discontinue the exercise immediately and report these sensations to the exercise supervisor, or seek medical attention if you have left the exercise area.

Participation in this study requires a time commitment which may be inconvenient for you at some point during the study.

Benefits of Participation:

This is a basic physiology/biochemistry study and, as such, there will be no direct benefits received as a consequence of participating in the study. If you are interested, the rational for conducting the research and theory and significance of each of the tests will be explained, as will your individual results from each of the tests. You will also have the opportunity to learn about and better understand your physiological responses to an exercise situation.

Confidentiality:

Records from this study are confidential and will be stored securely at the Canadian Centre for Activity and Aging, Sonia Arthur Labatt Health Sciences Building. Your records will be identified by a number rather than your name. Your de-identified data will be kept indefinitely so that it is available for analysis within the research group. Published reports resulting from this study will not identify you by name. If you wish to withdraw your data at any time you can do so by contacting the Principal Investigator, Dr. John Kowalchuk at [redacted]. Representatives of the University of Western Ontario Health Sciences Research Ethics Board may contact you or require access to your study-related records to monitor the conduct of the research.

Voluntary Participation:

Participation in this study is voluntary. You may refuse to participate, refuse to answer any questions or withdraw from the study at any time with no effect on your academic or employment status.

You will be given a copy of this letter of information and signed consent forms. You do not waive any legal rights by signing the consent form. If you have any questions regarding this study please contact Dr. John Kowalchuk [redacted], Daniel Keir [redacted] or Taylor Robertson [redacted] at the Canadian Centre for Activity and Aging, Sonia and Arthur Labatt Health Sciences Building, The University of Western Ontario, London. If you have any question about the conduct of this study or your rights as a research subject you may contact the Director of the Office of Research Ethics, The University of Western Ontario, [redacted].

LETTER OF INFORMED CONSENT

Predicting the pulmonary O_2 uptake response to ramp-incremental exercise from pulmonary O_2 uptake kinetics

Principal investigator: John M. Kowalchuk, PhD

Records from this study are confidential and will be stored securely at the Canadian Centre for Activity and Aging, Sonia Arthur Labatt Health Sciences Building. Your records will be identified by a number rather than your name. The data will be available for analysis within the research group. Published reports resulting from this study will not identify you by name.

We would like to keep your contact information in order to contact you about participating in future studies. If you would like to be contacted about future studies please initial below.
□ ___ (initials)

I have read the Letter of Information, have had the nature of this study explained to me and I agree to participate. All questions have been answered to my satisfaction and I will receive a copy of the Letter of Information and signed consent form.

.

Participant:

_____ _____
Name (please print) Signature

_____
Date

Investigator (i.e. Person Responsible for Obtaining Informed Consent):

_____ _____
Name (please print) Signature

_____
Date

PERMISSION TO REPRODUCE PREVIOUSLY PUBLISHED MATERIALS

Chapter II:

Prior permission from *Experimental Physiology* is not required if the purpose of the reproduction is for inclusion in a thesis dissertation.

CURRICULUM VITAE

Daniel A. Keir
School of Kinesiology, Faculty of Health Sciences
Canadian Centre for Activity and Aging
The University of Western Ontario
London, Ontario, Canada

Education

2011 - 2015 **Doctor of Philosophy (Ph.D.)**, Integrative Physiology of Exercise, *The University of Western Ontario, London, Ontario*

2008 - 2010 **Master of Human Kinetics (M.H.K.)**, *Laurentian University, Sudbury, Ontario*

2004 - 2008 **Honors Bachelor of Science (B.Sc.)**, Kinesiology, *Laurentian University, Sudbury Ontario*

Research

Peer-Reviewed Original Research Publications (10)

1. **Keir, D.A.,** Fontana, F.Y., Robertson, T.C., Murias, J.M., Paterson, D.H., Kowalchuk, J.M., & Pogliaghi, S. (2015) Exercise intensity thresholds: Identifying the boundaries of sustainable performance. *Medicine and Sciences in Sports and Exercise*. 47(9): 1932-40.

2. Fontana, F.Y., **Keir, D.A.**, Belotti, C., De Roia, G.F., Murias, J.M., & Pogliaghi S. (2015) Determination of RCP in healthy adults: can non-invasive NIRS help? *Journal of Science and Medicine in Sports*. 18(5): 590-5.

3. **Keir, D.A.,** Nederveen, J.P., Paterson, D.H., & Kowalchuk, J.M. (2014) Pulmonary O_2 uptake kinetics during moderate-intensity exercise transitions when initiated from low versus elevated metabolic rates: insights from manipulations in cadence. *European Journal of Applied Physiology* 114(12): 2655-65.

4. **Keir, D.A.,** Murias, J.M., Paterson, D.H., & Kowalchuk, J.M. (2014) Breath-by-breath $\dot{V}O_{2p}$ kinetics: effect of data processing on confidence in estimating model parameters. *Experimental Physiology.* 99(11): 1511-22.

5. Murias, J.M., Spencer, M.D., **Keir, D.A**., & Paterson, D.H. (2013) Systemic versus vastus lateralis muscle blood flow and oxygen extraction during ramp incremental exercise. *American Journal of Physiology. Regulatory, Integrative and Comparative Physiology.* 304(9): R720-5.

6. Murias, J.M., **Keir, D.A.**, Spencer, M.D., & Paterson, D.H. (2013) Sex-related differences in muscle deoxygenation during ramp incremental exercise. *Respiratory Physiology & Neurobiology*. 189(3): 530-6.

7. Spencer, M.D., **Keir, D.A.**, Nederveen, J.P., Murias, J.M., Kowalchuk, J.M., & Paterson, D.H. (2013) Prolonged moderate-intensity exercise $\dot{V}O_2$ response following heavy-intensity priming exercise with short and longer-term recovery. *Applied Physiology, Nutrition, & Metabolism.* 38(5): 566-73.

8. **Keir, D.A.**, Thériault, F., & Serresse, O. (2013) Evaluation of the running–based anaerobic sprint test as a measure of repeated sprint ability using collegiate level soccer players. *Journal of Strength and Conditioning Research*. 27(6): 1671-8.

9. Zöry, R., Aulbrook, W., **Keir, D.A.**, & Serresse, O. (2013) Occurrence of fatigue induced by a whole body vibration session is not frequency dependent. *Journal of Strength and Conditioning Research*. 27(9): 2552-61. Names indexed incorrectly: Raphael, Z., Wesley, A., Daniel, K.A., Olivier, S.

10. **Keir, D.A.**, Zöry, R., Boudreau-Larivière, C., & Serresse, O. (2012) Mechanical efficiency of treadmill running: effect of anaerobic energy contributions at various speeds. *International Journal of Sports Physiology and Performance.* 7(4): 382-9.

Manuscripts Under Review (1)

1. **Keir, D.A.**, Robertson, T.C., Benson, A.P., Rossiter, H.B., & Kowalchuk, J.M. The influence of metabolic and circulatory heterogeneity on the expression of pulmonary $\dot{V}O_2$ kinetics in humans. (*Experimental Physiology:* EP-RP-2015-085338)

Letters to the Editor/Commentaries (3)

1. **Keir, D.A.,** Fontana, F.Y., Robertson, T.C., Murias, J.M., Paterson, D.H., Kowalchuk, J.M., & Pogliaghi, S. Considerations for identifying the boundary of sustainable performance: Response to Craig et al. *Medicine and Sciences in Sports and Exercise.* 47(9): 1998-9

2. **Keir, D.A.,** Murias, J.M., Paterson, D.H., & Kowalchuk, J.M. (2015) Breath-by-breath VO_{2p} kinetics: effect of data processing on confidence in estimating model parameters: Response to Francescato et al. *Experimental Physiology.* 100:476.

3. Murias, J.M., **Keir, D.A**., Spencer, M.D., & Paterson, D.H. Sex-related differences in muscle deoxygenation during ramp incremental exercise: Response to Peltonen et al. *Respiratory Physiology & Neurobiology.* 195:61-2.

Refereed Abstracts (7)

1. **Keir, D.A.**, Robertson, T.C., Benson, A.P., Rossiter, H.B., & Kowalchuk, J.M. The influence of metabolic and circulatory heterogeneity on the expression of pulmonary $\dot{V}O_2$ kinetics in humans. *Appl. Physiol. Nutri. Metabol*

2. Fontana, F.Y., **Keir, D.A.**, Murias, J.M., Pogliaghi, S. (2015) A single sub-maximal 3-min test for Critical Power estimation. *Med. Sci. Sport & Exer. Suppl*

3. **Keir, D.A.,** Pollock, M., Thuraisingam, P., Paterson, D.H., Heigenhauser, G.J.F., Rossiter, H.B., & Kowalchuk, J.M. (2014) The effect of hyperventilation-induced hypocapnic alkalosis on the slowing of VO_{2p} kinetics in acute hypoxia. *Appl. Physiol. Nutri. Metabol. 39 Suppl. 1*:S24.

4. **Keir, D.A.,** Nederveen, J.P., Paterson, D.H., & Kowalchuk, J.M. (2014) The adjustment of pulmonary O_2 uptake during moderate-intensity exercise transitions may be regulated by different mechanisms when initiated from low versus elevated metabolic rates. *Med. Sci. Sport & Exer. Suppl.1:S.*

5. **Keir, D.A.,** Murias, J.M., Paterson, D.H., & Kowalchuk, J.M. (2013) Breath-by-breath pulmonary O_2 uptake data processing: improving confidence in model parameters. *Appl. Physiol. Nutri. Metabol. Suppl.*

6. **Keir, D.A.,** Murias, J.M., Spencer, M.D., & Paterson, D.H. (2013). Systemic versus peripheral blood flow and oxygen extraction during ramp incremental exercise. *Med. Sci. Sport & Exer. Suppl.1:S.*

7. Serresse, O., **Keir, D.A.,** & Thériault, F. (2008). Validity and reliability of the Running-based anaerobic sprint test (RAST) using elite level soccer players. *Appl. Physiol. Nutri. Metabol. 33 Suppl. 1:*S91.

Grants and Awards

Grants

2013 - 2015 **Natural Sciences and Engineering Research Council of Canada (NSERC),** Post-Graduate Doctoral Scholarship (PGSD) – funded for 6 terms ($42,000)

2011 - 2012 **Ontario Graduate Scholarship (OGS),** Ministry of Training, Colleges and Universities – funded for 3 terms ($15,000)

2011- 2015 **Western Graduate Research Scholarship**, University of Western Ontario Institutional Scholarship – 2011-14 academic year(s) ($15,000, annually)

2009 **NSERC,** Graduate Studies Scholarship, Research Capacity Development Grant – Laurentian ($5,000)

Travel Grants and Other Awards

2014 **International Mobility Grant (CooperInt) – Junior Visitor Program,** University of Verona Internationalization program – funded for 3 months (7,500 € ~ $11,250 CAD)

2014 **Northwater Capital Management Award in Aging,** Canadian Centre for Activity and Aging ($1000)

2013 **Non-invasive Neuromuscular Interest Group Award Winner,** American College of Sports Medicine Annual Meeting ($200)

2013 **Faculty of Health Sciences Graduate Student Conference Travel Award,** The University of Western Ontario ($650)

2013 **School of Kinesiology Travel Award,** The University of Western Ontario ($550)

2013 **Graduate Thesis Research Award,** The University of Western Ontario ($789)

2012 **Graduate Thesis Research Award,** The University of Western Ontario ($616)

2012 **CIHR–R2A 2012 Student Presenter Award,** Canadian Centre for Activity and Aging Annual Conference ($200)